Dendritic cells and $CD4^+$ T cells: dual roles in the clearance and pathogenesis of herpes simplex type 1 viral infection

by

Gregory Mettauer Frank

B.S., Biology, Virginia Tech, 2004

Submitted to the Graduate Faculty of

Medicine in partial fulfillment

of the requirements for the degree of

Doctor of Philosophy

University of Pittsburgh

2009

UNIVERSITY OF PITTSBURGH

SCHOOL OF MEDICINE

This dissertation was presented

by

Gregory Mettauer Frank

It was defended on

11-20-2009

and approved by

Olivera J. Finn, Ph.D.
Distinguished Professor and Chair, Department of Immunology

Pawel Kalinski, M.D. Ph.D.
Associate Professor, Department of Surgery

Paul R. Kinchington, Ph.D.
Associate Professor, Department of Ophthalmology

Angus W. Thomson, Ph.D. D.Sc.
Distinguished Professor, Department of Surgery

Dissertation Advisor:
Robert L. Hendricks, Ph.D.
Joseph F. Novak Professor and Vice Chair, Department of Ophthalmology

Copyright permission was granted for:

Frank GM**,** Lepisto AJ, Freeman ML, Sheridan, BS, Cherpes, TC, Hendricks RL (2010) $CD8^+$ T cell memory generated without $CD4^+$ help is transiently compromised in latent infection. Journal of Immunology.

Figure 4 – "Corneal stroma is avascular" adapted from Ambat, et al. (2006). Corneal avascularity is due to soluble VEGF receptor-1. Nature.

Figure 5 – "T helper subsets and the factors that drive their differentiation**"** adapted from Jetten AM. (2009). Retinoid-related orphan receptors (RORs): critical roles in development, immunity, circadian rhythm, and cellular metabolism. Nuclear Receptor Signaling.

Copyright permission letters are on file with Gregory Frank

DENDRITIC CELLS AND CD4 T CELLS: DUAL ROLES IN THE CLEARANCE AND PATHOGENESIS OF HERPES SIMPLEX VIRAL INFECTION

Gregory Frank, Ph.D.

University of Pittsburgh, 2009

Herpes Stromal Keratitis (HSK) is one of the leading causes of infectious blindness in the developed world. HSK is characterized by corneal damage and scarring that results from a Th1 cytokine-mediated immunopathology. It is triggered by reactivation of HSV-1 from latency in sensory neurons of the trigeminal ganglion (TG) and its subsequent transport to the eye through axons that innervate the cornea. My thesis work explored key components of both the HSV-specific $CD8^+$ T cell response that maintains HSV-1 latency in sensory neurons, and the opposing roles of the immune system in controlling HSV-1 replication in the cornea and promoting the immunopathology that results in corneal scarring and blindness. We hypothesized and provide strong supporting evidence that $CD4^+$ T cells act as a double-edged sword, on the one hand providing critical help to HSV-specific $CD8^+$ T cells that enables them to control viral latency through avoidance of exhaustion within the infected TG. On the other hand, we employed HSV-specific $CD4^+$ T cell clones to explore their role in orchestrating the immunopathology associated with HSK. We also explored the Ying and Yang of dendritic cell involvement in HSK. While our previous studies suggested a role for DC in promoting HSK, we now employ a unique localized DC depletion model to establish that "first responding" DCs are critical in mobilizing both the innate and adaptive immune response that clears virus from the cornea. Finally, we employed newly available recombinant mouse strains lacking IL-12p40, p35, or both p40 and p35 to explore the involvement of the IL-12 cytokine family in HSK. The

heterodimeric cytokines IL-12 (p40/p35) and IL-23 (40/p19) are thought to regulate HSK by promoting production of the requisite TH1 cytokine IFN-γ. However, we find that HSK development does not require IL-12p40 and is thus independent of IL-12 and IL-23. Instead, HSK late progression actually requires a previously unrecognized IL-12p40-independent, proinflammatory function of IL-12p35.

TABLE OF CONTENTS

LIST OF TABLES

LIST OF FIGURES

PREFACE

I would be remiss if I did not first thank Robert Hendricks, my thesis dissertation advisor, for his support, leadership, and unflinching optimism during my dissertation research. I consider him not only the guiding light of my development into a scientist, but also a dear friend. I look forward to many more years of his advocacy and guidance as I continue my career in scientific research.

My Thesis committee, Drs. Finn, Kalinski, Kinchington, and Thomson have all provided critical insights and guidance as well into the development of my research proposal. I would like to thank them for their time and efforts in ensuring that I chart the best course during my dissertation proposal.

I would also like to thank the members of the Hendricks lab past and present for their perspectives and discussions that never failed to further my development of a scientist. In particular I would like to thank Drs. Lepsito, Freeman, Sheridan, and Cherpes as well as Dawn Maker for directly contributing both data and concepts to my thesis research.

Lastly I would like to thank my Parents, Jerry and Claudia Frank, and my siblings Brian, Cathy, Kristy, Blake, and Andy for their unwavering support during my graduate career, as well as throughout entire my life.

1.0 INTRODUCTION

1.1 HERPES SIMPLEX VIRUS TYPE 1

1.1.1 Epidemiology

The human herpesvirus family represents a group of structurally similar viruses that incur a considerable burden on health care systems throughout the world. In the United States the seroprevalence of herpes simplex virus type-1 (HSV-1) has been estimated at 58% of the total population, while other developed nations report an incidence of HSV-1 infection as high as 75% (1,2). Although HSV-1 seropositivity varies by age and is influenced by a variety of risk factors, these studies nevertheless clearly demonstrate that HVS-1 is a ubiquitous infectious agent throughout the world (3-5).

HSV-1 predominately infects the orofacial region, where the primary infection tends to be asymptomatic; the most common manifestation is the cold sore. Of note is the ability of HSV-1 to infect the sensory nerve termini innervating the site of infection, travelling up to the neuron cell bodies, where it establishes latency. Latency is a quiescent state defined as the presence of viral genome within the host neuron in the absence of infectious virions (6). Within certain host neurons HSV-1 may reactivate and shed virus back down to the original site of infection. While often asymptomatic, shed virus can lead to a broad range of clinical entities, such as herpes

labialis, gingivostomatitis, endophthalmitis, and the potentially fatal encephalitis. Of greater interest to our lab is the complication of recurrent HSV-1 corneal infection called herpes stromal keratitis (HSK), which is the leading infectious cause of blindness in the United States, as well and a leading indicator for penetrating keratoplasty (7-9).

Therapeutic approaches to HSV-1 are compounded by the ability of the virus to establish latency, which in turn renders the virus difficult to eradicate once latent infection has been established. At this time there are no effective vaccines which can prevent HSV-1 infection, or its subsequent reactivation from latency (4). Current treatments now consist of antiviral drugs, such as acyclovir, which are capable of selectively inhibiting viral DNA synthesis (10).

1.1.2 Viral Structure

HSV-1 is a double stranded DNA virus comprised of 4 distinct components. The innermost component is the viral genome, which is approximately 152 kilobases in size, and encodes 84 viral proteins (11). The second component, the capsid, is an icosadeltahedral structure of viral proteins that encase the viral genome. The third element is the tegument, an amorphous layer of various proteins that are needed for wresting control of host transcriptional machinery and initiation of viral transcription upon host cell infection. The final component is the lipid bilayer envelope, which is acquired from host cell membrane during viral egress. The envelope is also studded with a number of viral glycoproteins with established functions in both viral egress and entry (12), (Figure 1).

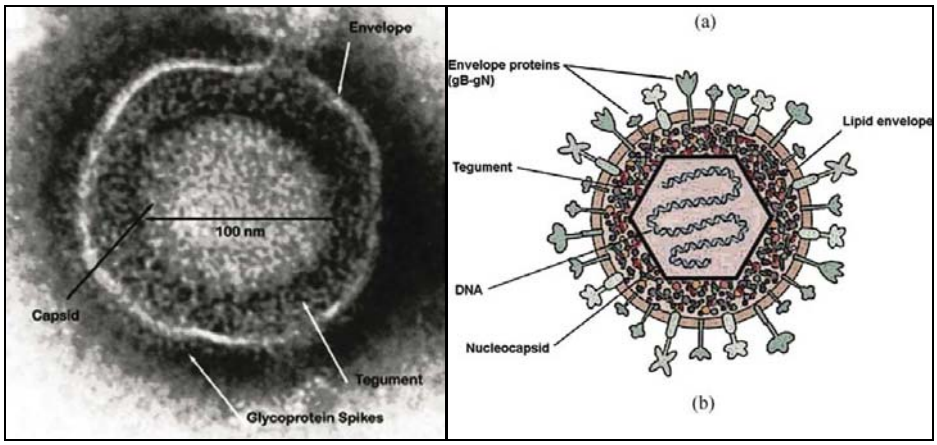

Figure 1 - Depiction of viral structure and morphology.

On the left is an electron micrograph of an intact viral particle. The right illustration depicts a schematic of the viral components in relation to the electron micrograph. Adapted from Todar, K. 2009. Online Lecture.

1.1.3 HSV-1 life cycle: Lytic Infection and Latency

Upon primary lytic infection, HSV-1 genes are expressed in a highly regulated sequential fashion (figure 2). These genes fall into three classifications, each group contributing a unique function towards the formation of new infectious virions (table 1).

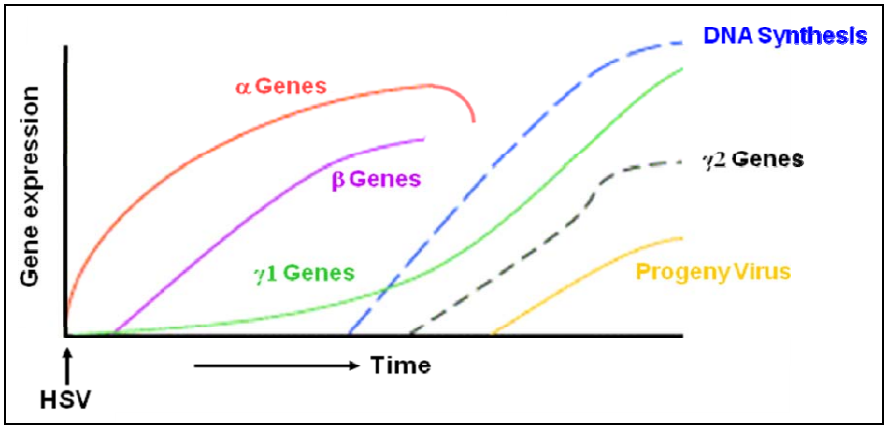

Figure 2 – Depiction of sequential activation of HSV-1 gene products

This figure illustrates the sequential activation of genes upon HSV-1 infection of a host cell. Courtesy of Brian Sheridan, Ph.D.

Table 1 – Brief classifications of the sequential HSV-1 genes

Class	Kinetics of transcription	Functions
Immediate Early (α)	Without host *de novo* protein synthesis	Transactivate β and γ gene transcription; repress host and α gene transcription; immune evasion
Early (β)	After *de novo* protein synthesis, prior to DNA replication	DNA replication machinery
Leaky-Late (γ1)	Initiated prior to DNA replication, majority transcribed after	Virus attachment and assembly; tegument proteins
True-Late (γ2)	Requires DNA replication for transcription	Capsid assembly; virus attachment; tegument proteins

As depicted in the table above, the first gene products expressed by HSV-1 upon lytic infection are the immediate early (IE), or α-genes. These genes are expressed within one to two hours of initial infection, and do not require *de novo* viral protein synthesis. The IE genes encode six proteins: ICP0, ICP4, ICP22, ICP27, ICP47, and $U_s1.5$. All IE proteins except ICP47 play a role in the transactivation of viral transcription, with ICP0, ICP4, and ICP24 being the most critical to this process.

The IE proteins transactivate the second group of viral genes, the early (E) or β-genes. These genes, normally expressed between four and eight hours after infection, function to initiate viral DNA replication, a process which is needed to activate the Late, or γ genes. The γ-genes are further subdivided into two groups, the "leaky-late" γ1 genes and the "true-late" γ2 genes. The γ1 genes, such as glycoprotein B (gB) are expressed at low levels prior to DNA replication, after which they increase exponentially in expression. The γ2 genes only expressed following viral DNA synthesis. Collectively, these γ-genes primarily encode the structural proteins required for final viral assembly. The newly formed virions upon assembly egress from the cell,

thus completing what is described as the lytic infection pathway, so called as it inexorably leads to host cell death.

HSV-1 can also assume a latent lifestyle in which viral genome can persist for prolonged periods without virion formation or destruction of the host cell. Latency is established *in vivo* when the neurotropic HSV-1 infects a sensory neuron innervating the site of primary infection. The exact processes that drive HSV-1 from a lytic path to latency are not well understood. Some research suggests the quiescent nature of the neuron as well as certain neuron specific proteins may play a role in divergence into this dormant state (13,14). This is a relatively stable process, as individuals retain latent HSV-1 within their sensory neurons for life. While no viral proteins are detected during HSV-1 latency, latency associated transcripts (LAT) were discovered in latently infected neurons (15-17). Much research has been expended establishing the function of these unique transcripts. However a large body of work has found that LATs are not absolutely critical for the establishment of, or reactivation from latency (18-20). Other studies have established a role of LATs in promoting neuron survival by protecting the neurons from apoptosis (21,22). Recent evidence has also found LATs help determine the propensity of how HSV-1 establishes in certain neuronal subsets (23). A final group of studies found microRNAs are encoded by the LAT gene, and these function to impair ICPO protein expression, providing a level of control of reactivation under certain conditions (24).

The underpinnings of how HSV-1 transitions from latency back to a productive lytic infection are poorly understood at best. The process of reactivation ultimately leads to the release of transmissible viral particles back down to the primary site of infection. Certain conditions, such as immunocompromise, UV-B irradiation, physical stressors such as hypothermia and invasive surgery, and psychological stress have all been associated with an

increase in reactivation from latency (25-31). While the dogma previously forwarded that these insults lead to reactivation solely by directly changing the neuron's physiology, recent work by this lab and others have actively promoted an additional role for the immune response in retaining HSV-1 in latency, and that many of these stressors impact the immune system.

1.2 THE CORNEA

1.2.1 Structure of the cornea

As our lab and this research focuses on ocular HSV-1 infection and its subsequent transition into HSK, a brief overview of the structure of both the eye and cornea are required. The cornea is a critical component of the eye whose function, in conjunction with the lens, refracts light to the retina. The cornea consists of three sections, as described in figure 3. The outermost layer, the epithelium, consists of seven to nine actively dividing cells. Its primary function is to provide a mechanical barrier that protects the eye from foreign objects as well as to water and to create a surface with promotes the retention and absorption of tear film (32). Immediately below the epithelium is the bowman's layer, a thin but dense layer of collagen which both protects and retains the shape of the underlying corneal stroma (33,34). The third and largest layer is that of the corneal stroma, the main refractive element of the cornea. The stroma contains an extremely organized system of collagen fibers which are bundled into structures called

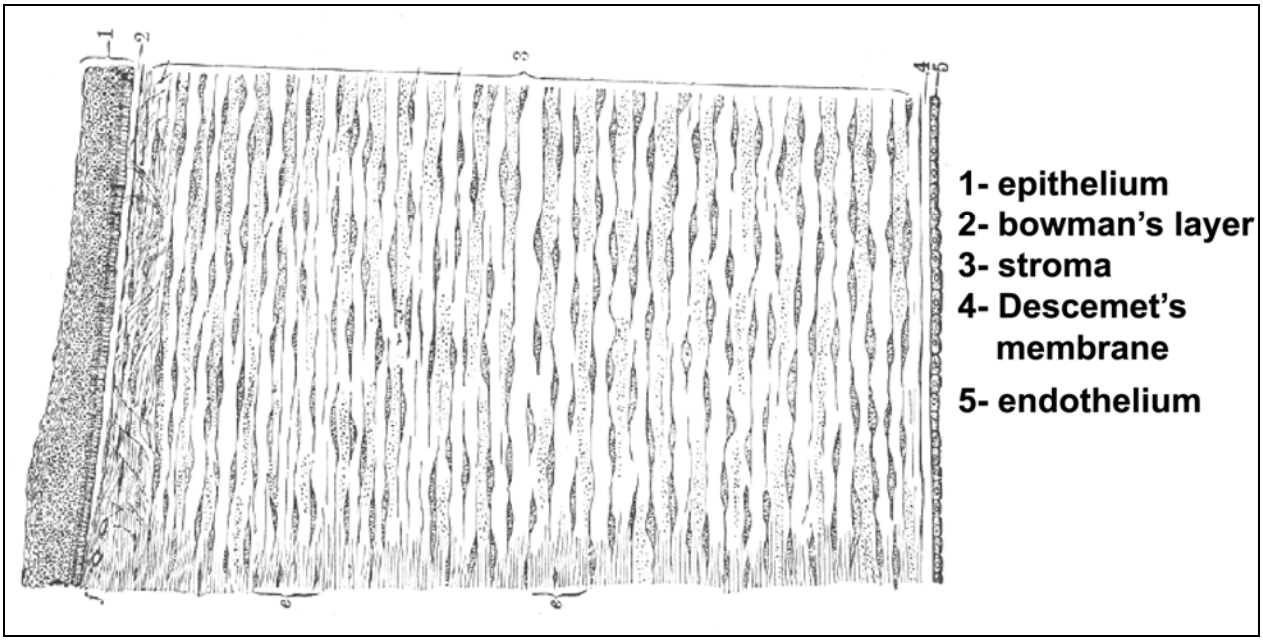

Figure 3 – basic anatomy of the cornea

Illustration depicting the five distinct layers of the cornea strata. Moving anterior to the posterior as follows: epithelium, bowman's layer, stroma, Descemet's membrane, and endothelium. Adapted from Gray's Anatomy (public domain image).

Lamellae (35,36). The lamellae are organized in a parallel fashion to the corneal epithelium, running from the one side of the cornea to another. These fibers run in superior to inferior or nasal to temporal fashion, and can interweave over each other. This organization of the lamellae provides the unique transparent nature and refractive power of the cornea. Interspersed between the lamellae are keratocytes, which function to maintain the organization to the corneal matrix. Following injury, these cells have been implicated in scar formation as they turn into corneal fibroblasts (37). Below the stroma lies Descemet's membrane, which functionally is closely associated with the endothelial layer. It consists of a thin layer collagen, though a different type from the lamellae within the cornea. This collagen layer is secreted by the underlying endothelial cells. The endothelial layer is a monolayer of non-dividing cells bathed in the

aqueous humor of the anterior chamber. The endothelium within the eyes serves to pump waste and excess water from the overlying corneal cells into the aqueous humor as well as actively transport vital nutrients to maintain these cells (38,39).

As one views the cornea face on, one can see the corneal stromal bed interfaces with the conjunctiva around the periphery of the cornea (figure 4). The conjunctiva is a highly vascularized bed of tissue, but blood vessels terminate abruptly at the stromal interface.

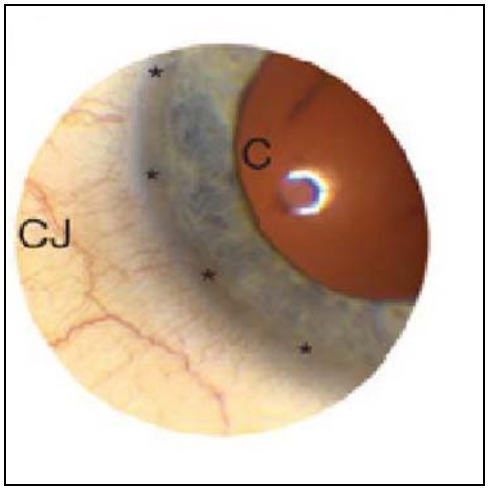

Figure 4 – Corneal Stroma is Asvascular

Photograph of a human cornea. C represents the cornea stroma, while CJ represents the conjunctiva. The stars mark the abrupt end of blood vessel infiltration at the interface between the two tissues. Adapted from Ambat et al. 2006. Nature

As the endothelial cells provide the necessary mechanism to remove waste and provide nutrients to the corneal bed, it is not reliant on vasculature for tissue survival. This is allows the cornea to remain devoid of vessels, thus allowing the tissue to remain perfectly transparent. Until recently, it was not well understand how the cornea was capable of retaining its avascular nature when surrounded by the heavy vascularized conjunctiva, and even more so as vascular endothelial growth factor (VEGF, a potent inducer of neovascularization) is found within the

cornea. However a recent study observed this VEGF is bound by soluble VEGF-receptor, produced constitutively within the cornea bed (40). This sequesters VEGF from exerting its function, thus retaining the avascularity of the cornea.

1.2.2 The immune privilege of the cornea

While the unique ability of the cornea to remain avascular helps maintain its organized structure for visual acuity, it also provides an important advantage by allowing the cornea to remain immune privileged. Immune privilege is historically defined as a site that can tolerate an introduction of a foreign antigen without generating an inflammatory response. This allows the corneal architecture so important for vision to remain organized. Much of the knowledge of the cornea's immune privilege comes from corneal transplantation studies, where grafts placed into the avascular bed enjoy a very high acceptance rate (41,42). Indeed, a number of anti-inflammatory mechanisms, such as transforming growth factor β (TGF-β), Fas Ligand, and α-melanocyte-stimulating hormone (α-MSH) have been discovered to operate within the anterior chamber of the eye (43-46).

Previously, it was thought that avascular nature of the cornea corresponded to a lack of immune cells, such as antigen presenting cells (APCs) within the cornea. While some studies had reported $CD11c^+$ dendritic cells (DCs) within the corneal stroma, others have observed conflicting results (47-49). Recent work by our lab and others has discovered that immune populations are in fact present within the cornea (our unpublished observations), (49,50). These populations of APCs are sparse, and appear to be closely interfaced with the epithelium, actually residing in the basement membrane, not the corneal stroma. It is unknown at this time whether these cells within the cornea function identically to their counterparts elsewhere in the body (i.e.

promote an inflammatory response), or if they have specialized functions within the cornea. Additional research on the role of these resident cells is needed to further our understanding of the complex immune privilege qualities of the eye.

1.3 THE IMMUNE RESPONSE: CONTROL OF OCULAR HSV-1 INFECTION

1.3.1 The Innate Immune Response

1.3.1.1 First responders of the innate Immune response

Upon initial encounter with a pathogen, the body's innate immune system mobilizes rapidly to control the primary infection. In the model of ocular HSV-1 infection, virus begins lytic replication within the epithelium of the cornea. This elicits the first line of intrinsic defense mechanisms within the cornea, Type I interferons (51). These soluble factors play a role in mobilizing both the infected cells as well as its neighbors to resist viral replication, upregulate MHC class I machinery, as well as invoke the infiltration of innate responders. Studies observing the innate immune response to ocular HSV-1 infection identified polymorphonuclear (PMN) neutrophils, natural killer (NK) cells, and γδ TCR cells important in initial control of virus (52-55). In the face of the innate immune system's efforts, HSV-1 nevertheless gains access to the nerve termini at the corneal epithelium, and travel by retrograde axonal transport to the trigeminal ganglion (TG), the common sensory nerve trunk that innervates the orofacial region. This process normally occurs very rapidly after primary infection, with virus reaching the TG within 24-48 hours (56).

The innate immune response also plays a critical role within the TG before the adaptive immune system is sufficiently mobilized. Macrophages and γδ TCR cells infiltrate the TG soon after viral access. The infiltrating macrophages play an antiviral role through nitric oxide (NO) and tumor necrosis factor (TNF) while the γδ T cells help limit viral spread through type II interferons (IFN-γ) (52,57-59). Thus the innate immune response effectively limits viral spread within the ganglion. However the innate immune system is unable to completely eradicate HSV-1 from either the cornea or the TG, only containing viral replication while the adaptive immune response is marshaled within the lymphoid tissues draining the site of infection.

1.3.1.2 Dendritic cells

Arguably one of the most important cells within the innate immune response is the dendritic cell (DC). These cells are present throughout the body, and serve as sentinels, surveying foreign particles that body comes into contact with. They play integral roles in helping both the innate and adaptive immune response mobilize properly to infection. DCs are a very heterogeneous population, greatly complicating classification. However recent attempts have broadly classified DCs into two groups: classical DCs (myeloid lineage DCs) and plasmacytoid DCs (lymphoid lineage). Further subdivisions can be made of these groups for the purposes of HSV-1 infection as described in table 2. Plasmacytoid DCs (pDCs) are characterized by their non-myeloid lineage as well as being potent producers of type one interferons (60). Classical DCs (cDCs) are phenotypically identified $CD11c^{+}CD11b^{+}$ and, and largely comprise of two sets ($CD8\alpha^{+}$ and $CD8\alpha^{-}$) and are thought to be the primary lymphoid antigen presenting cells to T and B cells. Langerhans cells are a subset of cDCs that are located within the epidermis of the skin (61).

These cells are thought to be important peripheral sentinels that acquire and transport viral antigen for presentation in the lymphoid tissues.

Table 2 – Selected dendritic cell subsets – phenotypic markers and basic functions

Class	Phenotypic markers	Functions
Plasmacytoid DCs (pDC)	CD317, GR-1, $CD11c^{low}$, $CD11b^{low}$	Potent producers of IFN-α/β: antiviral functions
Classical DCs (cDC)	CD11c, CD11b, $CD8\alpha^{+\text{ OR }-}$	Presentation of antigen within the DLN to T cells and B cells Can infiltrate peripheral sites for local costimulation
Langerhans cells (LC) (Epidermal DCs)	Langerin, Birbeck granules, $CD11c^{low}$	Peripheral acquisition of antigen – indirect transportation to DLN Potential immunomodulatory role

While the role of DCs within the cornea has not been completely elucidated, studies abound concerning the function of these cells in response to HSV-1 infection in other peripheral sites. The classic dogma of DCs during the steady state is that of an actively phagocytic stance, constantly sampling potential antigens from their surroundings. However when a DC comes into contact with a pathogen, it is able to recognized pathogen associated molecular patterns (PAMPS), which are unique bacterial and viral components not shared with any cells within the body (62,63). This drives the DC to undergo a maturation process, which upregulates the MHC-II and costimulatory molecules on the DC, and also promotes its egress out of the peripheral tissue. DCs exit peripheral tissue via the lymphatic system, which drains into the lymph nodes (DLN) where they are the lynchpin of generating an adaptive immune response.

Work by Carbone et al examined DCs in response to flank infections of HSV-1 and have found more complex relationships exist in how DCs transport and present antigens to the adaptive arm of the response. Studies have found that LCs do not actually present antigen to T cells, but "hand off" antigen to $CD8\alpha^+$ cDCs which go on to present the antigen (64). A further example is the observations of distinct functional roles of Langerhans cells that reside in different layers of the skin. Epidermal resident LCs tend to play an immunomodulatory role, while dermal resident LCs play the more classical role in mobilizing the immune response (65,66). This raises the possibility that local resident DCs may play a different role in the immune response to HSV-1 versus those that may migrate into the infected cornea in response to danger signals. Further studies have also observed differential migratory and presentation of DC subsets in response to HSV-1, suggesting a more complex interplay of the heterogeneous DC population in activating the adaptive arm then previous considered (67,68).

DCs also play key roles in the innate immune response to viral infection. As stated above, the specialized pDC subset plays a key role in anti-viral cytokine production in response to virus associated PAMPS. cDCs have also been identified to play a role in helping to mobilizing the innate immune response. A large body of work observed a critical function of DC produced IL-15 in helping to activate NK cell cytotoxic functionality (69-71). Thus dendritic cells play important roles in bringing both the innate and adaptive arms of the immune response to bear on vial pathogens such as HSV-1.

1.3.2 Initiation of the Adaptive Response

In order to completely control HSV-1 infection, the adaptive arm must be marshaled. The adaptive immune system can be broadly defined into both B and T cells. B cells, upon activation

with their cognate antigen produce HSV-1 neutralizing antibodies, which play a role in combating viral spread. T cells can be further broken into two major sub-groups based on the coreceptor CD4 and CD8.

1.3.2.1 $CD4^+$ T cells

$CD4^+$ T cells often referred to as T helper cells, play a role in activating and promoting the survival of other immune cells. $CD4^+$ T cells play a vital role in activating B cell antibody isotype switching, and also activate macrophages, increasing their phagocytic and anti-viral functions (72,73). $CD4^+$ T cells can be further broken up into four functionally distinct groups based on the milieu of cytokines present at the time of TCR engagement (Figure 5).

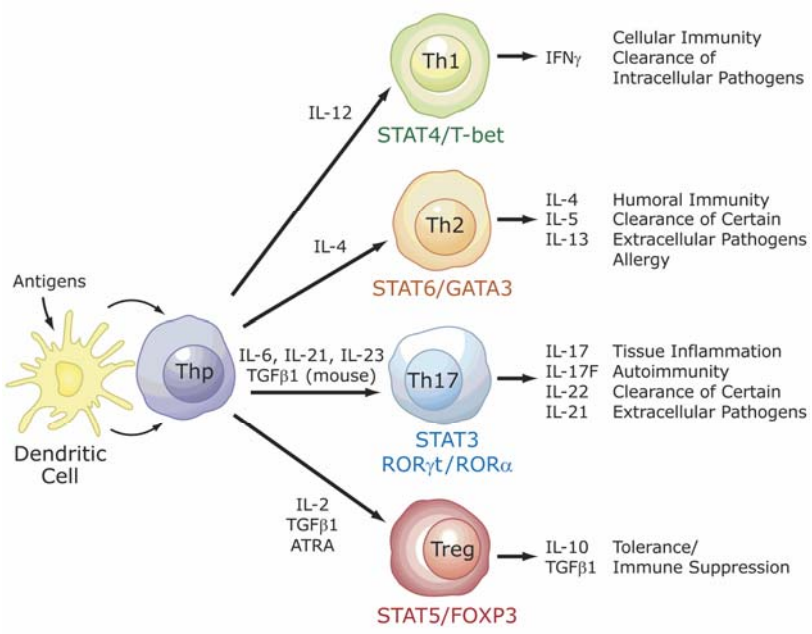

Figure 5 – T helper subsets and the factors that drive their differentiation

Illustration of the factors that drive a naïve T cell into its lineage. IL4 drives T_H2 differentiation, IL-12 drives TH1 differentiation, TGF-β and IL-6 drive TH17 differentiation, and TGF-β alone can convert a $CD4^+$ T cell into a T-reg. Please note how cytokines produced by certain helper

subsets suppress the differentiation of naïve T cells into competing lineages. Adapted from Jetton AM. 2009. Nuclear Receptor Signaling.

TH1 cells produce IFN-γ and IL-2 and orient the immune response to fight intracellular pathogens. This is the predominant T helper subset generated in response to ocular HSV-1 infection. T_H2 cells produce IL-4, IL-5, and IL-13 and play a role in mobilizing the immune system to combat extracellular pathogens (74). TH17 cells are characterized by IL-17 production, and have potent inflammatory functions, and are implicated in a number of immunopathologies such as rheumatoid arthritis and colitis (75). The final subset, T-regulatory cells, suppresses immune responses through a variety of cytokines and surface receptors such as TFG-β, IL-10, galectin, and CTLA-4 (76-78). These cells are defined phenotypically by the receptor CD25 and the transcription factor FoxP3.

1.3.2.2 $CD8^+$ T cells

$CD8^+$ T cells are one of the main tools in the immune system's arsenal against intracellular infections such as HSV-1, and correspondingly the most important component of the adaptive immune response to HSV-1 ocular infection. Indeed, in murine models deficient in $CD8^+$ T cells, HSV-1 replication is not fully controlled within the TG, often leading to fatal encephalitis (79,80). The hallmark of the $CD8^+$ T cell is its ability to kill virally infected cells; due to this designation, $CD8^+$ T cells are sometimes referred to as cytotoxic T lymphocytes (CTLs) (81). The most well established method of CTL function is lytic granules such as granzymes, which are delivered to the target cell with perforin, and function to initiate apoptotic machinery within the cell forcing it to undergo programmed cell death. In addition to their cytotoxic effector mechanisms, $CD8^+$ T cells also secrete IFN-γ and TNF, both potent anti-viral cytokines.

1.3.2.3 Initiation of the T cell response

As stated above, DCs within the DLNs that acquired HSV-1 antigens present them to CD8 and $CD4^+$ T cells in the context of MHC class I and II, respectively. Naïve T cells traffic through the DLNs and can come into contact with these DCs. When a T cell that recognizes its cognate antigen comes into contact, they require three distinct signals to initiate commitment to effector T cell lineage. The first signal is that of the antigen presented in the context of MHC, which is recognized by the T-cell receptor. The second signals are mediated by costimulatory molecules. These molecules are only unregulated on a DC when it has received maturation signals, such as activation of TLRs to viral associated elements. In the absence of these interactions such as B71.1/1.2:CD28 and CD40:CD154 T cells will be tolerized to the antigen (82,83). The final and third signal are cytokines such as IL-4 or IL-12, which not only allows proper activation of naïve T cells but also promotes differentiation into effector T-subset. As seen in figure 5 IL-12, a cytokine produced normally by APCs, promotes the differentiation of a naïve T cell into one that is equipped to combat intracellular pathogens such as HSV-1 (84,85).

When a naïve T cell obtains the proper signals to differentiate into an effector T cell, the process of clonal expansion begins. In most cases, T cells initiate a massive expansion (up to 50,000 fold increases), acquiring an activated phenotype and exiting the lymphoid organ (86). During this stage T cells enter into circulation and travel throughout the body, notably to sites of infection, which is the cornea and TG in the case of ocular HSV-1 infection. From initiation of clonal expansion, T cells peak in number within 5-7 days. After this phase, T cells undergo an organized process of cell death called contraction where the vast majority of effector cells are lost. The small population that survives is the memory pool; these cells are characterized by long term survival and rapid response upon encounter with antigen (87).

1.3.3 T cell memory

1.3.3.1 Memory precursors

Much work has been expended in understanding how T cell memory is formed and maintained. As much more is understood concerning $CD8^+$ T cell memory, this section will largely discuss how CTL memory is formed. During the effector stage, certain events take place that pave the way for memory development. One study found that when effector T cells engage an APC and undergo clonal expansion, they divide asymmetrically; they observed that the daughter cell distal to the APC retained less CD3,CD8 and LFA-1, but higher levels of the protein PKC-ξ (88). Furthermore they found that these distal daughter cells had a phenotype that was similar to that of memory, while the proximal cells had an effector cell phenotype. Another group of studies identified memory precursors, effector cells phenotypically distinct from the effector pool that tended to survive contraction to go on and form memory. Memory precursors tended to retain expression of IL-7R, which is downregulated on effector expansion), and lacked the expression of killer cell lectin-like receptor G1 (KRLG1) seen on short lived effector cells (89-91).

1.3.3.2 Central and Effector Memory

Mirroring the phenotypic wrinkles of the effector pool, memory cells also retain certain phenotypic differences. Two major subgroups of memory exist: central memory and effector memory. These two groups have distinguishing characteristics and functionality. Central memory, as the name implies, are largely found within the lymphoid organs. They tend to express CD44, CD127, CD62L, and CCR7, but are capable of expanding rapidly in response to antigen (92). Effector memory cells tend to be found in the periphery, and lack the lymphoid organ homing receptors CD62L and CCR7, but also retain high levels of CD44 and CD127. The

most striking differences of effector memory T cells is their ability to rapidly produce IFN-γ and TNF-α when compared to central memory (93). It is thought that effector memory cells exist to rapidly respond to their corresponding antigen, playing a delaying action while central memory cells rapidly expand into new effector cells to eradicate the pathogen. The mechanism by how effector and central memory form remain a mystery, but certain groups have observed memory precursors formed earlier in clonal expansion tend to form central memory, while those forming later go on to form effector memory (94,95).

1.3.3.3 $CD4^+$ T cell help of $CD8^+$ T cell memory

Illustrating the complex interplay in the immune response, $CD4^+$ T cells have been implicated in aiding $CD8^+$ T cell memory formation. A large number of early studies employing noninfectious immunizations observed $CD4^+$ T cell interaction with DCs via CD40:CD40L were necessary for the formation of both CTL effector populations and their subsequent functional long-lived memory (96,97). However, in models of acute infectious disease, it became apparent that ubiquitous components of pathogens, called PAMPs (pathogen associated molecular patterns) could induce DC maturation independent of $CD4^+$ T cells, resulting in a normal $CD8^+$ T cell effector response, but a defective $CD8^+$ T cell memory pool. These findings suggested a "programming" model in which signals from $CD4^+$ T cells during the priming and expansion phase programs $CD8^+$ T cells for functional memory (98,99). Recent studies forward a scenario where $CD4^+$ T cells augment programming of $CD8^+$ T cells through the production of IL-2 (100,101). A second study has identified a role where $CD4^+$ T cells enhance IL-15 production from DCs, which in turn helps form fully functional $CD8^+$ T cell memory (96,97,102).

A smaller body of work suggests a completely different role for CD4 help. Bevan et al observed $CD8^+$ T cell memory diminished over time when transferred into CD4 deficient hosts.

They concluded $CD4^+$ T cells are helping to maintain memory in non-antigen specific fashion (103). The mechanisms by how $CD4^+$ T cells effect this maintenance is unclear; It is well established that $CD8^+$ T cell memory does not require regular antigen engagement, but the homeostatic maintaining signals via IL-7 and IL-15 (87,104). So far no evidence has linked $CD4^+$ T cells to the production of these cytokines. It does appear in light of all these data that the requirements for CD4 help in the formation of $CD8^+$ T cell memory warrants further experimental elucidation.

1.3.4 The immune response and HSV-1 Latency

1.3.4.1 $CD8^+$ T cell Immunosurveillance of latently infected neurons

Strong evidence demonstrates that macrophages and γδ T cells play an integral role in keeping viral replication in check within the ganglion while the adaptive immune system is marshaled. Studies have also established the critical role for $CD8^+$ T cells in bring viral replication under control early within the trigeminal ganglion. How does the immune response continue as the virus achieves latency in the neurons?

$CD8^+$ T cells enter into the TG and peak in numbers at 8 days post infection (dpi), concurrent with the initial establishment of latency of HSV-1. In the B6 murine model of infection, the majority of the infiltrating $CD8^+$ T cells (50%) are specific for an immunodominant epitope on the glycoprotein B protein ($gB_{498-505}$) (105,106). These cells, from here on described as gB-CD8, undergo contraction that stabilizes and forms a pool of cells which are retained for the life of the animal. The majority of these memory gB-CD8 maintain an activated phenotype by CD69 and granzyme B expression, suggesting that these cells are receiving antigenic stimulation within the TG well after viral latency has been established (107).

Complementing these observations is the continued expression of a number of inflammatory cytokine and chemokine transcripts (108-110). Histological analysis of latent TGs have found $CD8^+$ T cells are found within close apposition of neurons, and their TCR is polarized to the neuron cell body, illustrating a scenario where gB-CD8s are regularly recognizing their antigen on neurons (106). As seen in Figure 6, histology of mice infected with a HSV-1 virus that express EGFP off the gB promoter reveal neuronal expression of EGFP during viral latency. This strongly suggests that neurons latently infected with neurons may be producing viral proteins in the absence of detectable infectious virus.

When TGs are cultured in *ex vivo* explants, HSV-1 spontaneously reactivates from a small number of latently infected neurons. gB-CD8s are able to protect these neuron cultures from reactivation (106,111). This growing body of data presents a paradigm shift in how we think neuron latency is maintained: not only does HSV-1 appear to be reactivating with much higher frequency than previously thought, HSV-specific $CD8^+$ T cells are immunosurveying latently infected neurons and actively pushing the virus back into a latent state.

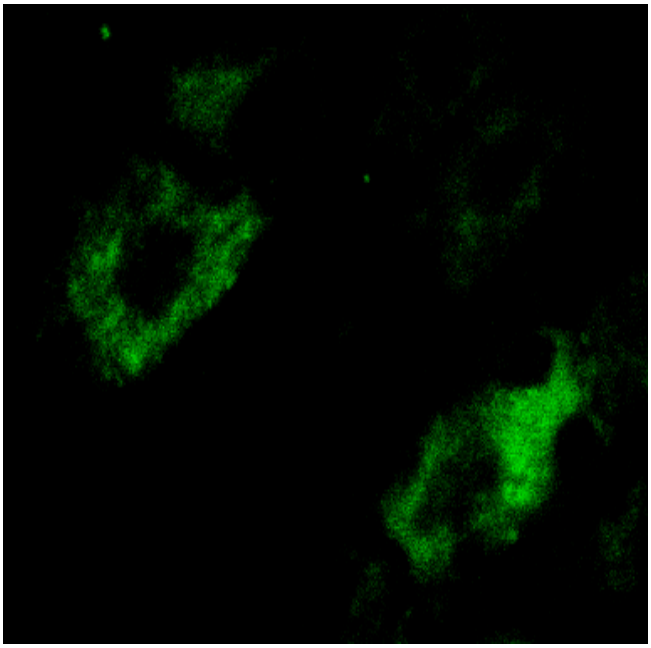

Figure 6 – Neurons within the latently infected ganglia are expressing glycoprotein B

Histology of whole TGs infected with HSV-1 promoter gB-EFGP. TGs were harvested during HSV-1 latency (35 dpi). Image courtesy of Brian Sheridan, Ph.D.

A number of subsequent studies have dissected the effector mechanisms by which $CD8^+$ T cells maintain latency. An important observation found when $CD8^+$ T cells are added to a culture and protection is established, an anti-CD8 antibody can neutralize CD8 function, and subsequently neuron reactivation occurs (106). This instructive observation informs us $CD8^+$ T cells, normally a cytotoxic killer, is using non-lytic mechanisms to maintain neuronal latency. This protection from neuronal activation is at least partially mediated by IFN-γ (112,113). More recent studies have found lytic granules are capable of protecting the remaining neurons in non-cytolytic fashion; granzyme B actually cleaves IE viral proteins, thus interfering with viral reactivation (114).

1.3.4.2 Long term antigen exposure and exhaustion – latent vs. chronic infections

These studies forward a long-term role for gB-$CD8^+$ T cells, constantly immunosurveying latently infected neurons, and when necessary, using their effector mechanisms to maintain latency. This is in stark contrast to what is observed during persistent infections with viruses such as LCMV, HCV, and HIV, where long term antigenic stimulation is detrimental to $CD8^+$ T cell functionality (115-117). In persistent infections induced by LCMV clone 13, functional exhaustion of virus-specific memory $CD8^+$ T cells is characterized by the serial loss of production of IL-2, TNF, IFN-γ, and granzyme B (115,118). This $CD8^+$ T cell exhaustion appears a result in part from their acquisition of inhibitory receptors (119,120).

One of the most well studied inhibitory receptors is program death-1 (PD-1). This molecule can be expressed on a large number of cells within the immune system, ranging from T cells, NK cells, to activated monocytes (121-123). Its primary ligand, PD-L1 is widely expressed through the body by a large number of immune and parenchymal cells. It is believed that PD-1 plays a role in control of effector expansion during normal immune responses. There is evidence that expression of PD-L1 may be induced by inflammatory mediators (124-127). Interestingly, mice that are deficient in $CD4^+$ T cells at the time of clone 13 LCMV infection exhibit a more profound $CD8^+$ T cell functional exhaustion and never clear the virus (115,128,129).

$CD8^+$ T cells isolated from latently infected neurons however remain fully functional even months into viral latency (130). A number of potential explanations for this lack of exhaustion exist. It might reflect the fact that replicating virus is rapidly eradicated during acute infection, preventing prolonged antigen exposure during the programming of $CD8^+$ T cells. Once programming is complete, persistent exposure to low levels of antigen does not appear to

have an adverse effect on the virus-specific memory T cell population. Also, the frequency of antigen encounters within the TG appears to be periodic, not constant as seen in classic chronic infection models. Few studies have looked in depth at functional exhaustion in the context of a latent infection, and did not observe role of CD4 help of $CD8^+$ T cell memory formation. One such study did observe $CD4^+$ T cell deficiency during the acute phase of murine gammaherpesvirus 68 infection renders virus-specific memory $CD8^+$ T cells incapable of maintaining viral latency, suggesting that non-helped $CD8^+$ T cells might be susceptible to functional exhaustion in the context of a latent viral infection (131,132).

1.4 THE IMMUNE RESPONSE: IMMUNOPATHOGOLOGY OF OCULAR HSV-1 INFECTION

1.4.1 Herpes Stromal Keratitis Pathogenesis

As stated above, a serious complication of ocular HSV-1 infection is the blinding disease herpes stromal keratitis, one of the leading causes of infectious blindness in the United States. The prevalence of the disease within the United States is estimated to be approximately a half million cases (8). In the clinic HSK is defined as either necrotizing keratitis or immune keratitis, which is non-necrotizing. Necrotizing keratitis is considered the more severe of the two diseases, being characterized by necrosis, epithelial defects, and heavy leukocytic infiltration into the corneal stroma; if left untreated, it can develop on to perforate the cornea. The second subtype, immune keratitis is more frequently seen in the clinic, and is considered a less severe in risk to the cornea.

It is defined by heavy leukocytic infiltration, neovascularization, and can persist for weeks. Necrosis and epithelial defects do not normally develop in immune keratitis.

Mouse models of HSK have been developed in efforts to understand the pathogenesis of this disease. Murine HSK has some stark differences with human keratitis. While HSK in the clinic is the result of viral reactivation down to the cornea, HSK in mice develops one week following primary infection. Also, viral replication is often seen in human keratitis, while in mice HSK develops following viral clearance from the cornea. Murine HSK appears to more closely resemble immune keratitis, with dense leukocytic infiltrate, neovascularization, and persistence of disease over time. It can also present epithelial defects as disease severity peaks, a characteristic of necrotizing keratitis. Despite these differences, the murine model of HSK has shed much light on how disease progresses.

As stated above, HSK in the mouse begins to develop at 7 dpi. It is important to note that infectious virus is usually not detected in the cornea, suggesting HSK develops in the absence of viral replication. Disease normally peaks in severity between 14-21 dpi, as illustrated in Figure 7. This disease is characterized by increasing stromal opacity as well as neovascularization from the periphery into the avascular cornea. HSK lesions in the mouse are characterized by a dense infiltration of PMN neutrophils, $CD4^+$ T cells, dendritic cells, and few $CD8^+$ T cells (133-135). It appears that a large number inflammatory and angiogenic factors work in concert to overwhelm the corneal immune privilege. It appears the proximal mediators of stromal damage is neutrophil directed matrix metalloprotease 9 (MMP-9), which leads to the corneal scarring and damage that lead to blindness (136). However to understand the pathogenesis of HSK, the ultimate mediators of disease must be identified.

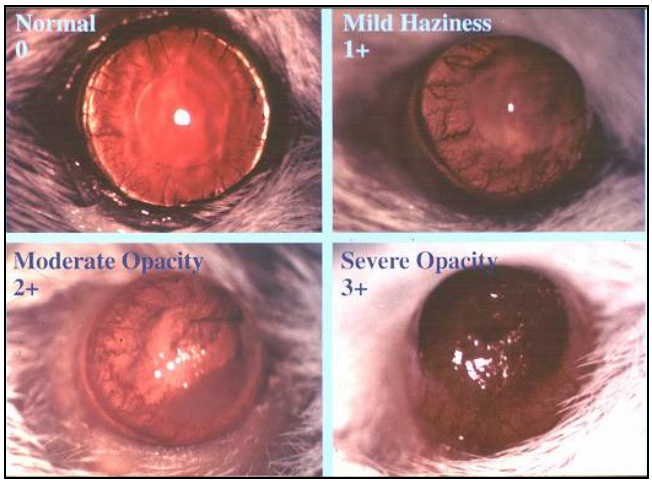

Figure 7 - Photographs of HSK development in BALB/C mice

4 slit lamp photographs depicting the four main severity scores of HSK. A non-infected normal eye has no vessel in growth and is clear. Mild haziness of the cornea characterizes a severity score of 1. Scores of 2, 3 depict increasing opacity of the corneal stroma, and also increasing ingrowth of new blood vessels. By a disease score of 3, the cornea is very opaque and completely neovascularized, and is indicative of blindness. Image courtesy of Robert Hendricks, Ph.D.

1.4.2 The role of $CD4^+$ T cells in HSK

Early studies in athymic nude mice, which lack T cells, found HSK did not develop (137). HSK could be induced in nude mice by an adoptive transfer of T cells, providing strong evidence HSK is a T cell driven immunopathology (138). Studies subsequently tested which T cell subset contributed more to HSK, and found that $CD4^+$ T cells were the subset responsible for HSK development in mice (139-141). Furthermore, HSK was established as a TH1 mediated disease. TH1 cytokines, notably IL-2 and IFN-γ were identified to be critical in HSK progression; IL-2 providing chemotactic and survival signals to PMN neutrophils, and IFN-γ upregulating PCAM-1 on blood endothelial cells, promoting PMN extravasation into the cornea (142,143). Taken

collectively, strong evidence exists that HSK is a TH1 mediated disease, orchestrated by $CD4^+$ T cells. This leads to the next question, how and why are $CD4^+$ T cells mediating such a destructive immune response within the cornea?

A large body of work has attempted to resolve these questions, and the answer remains contentious. These studies have forwarded three models of how $CD4^+$ T cells are initiating HSK: molecular mimicry, bystander activation, and HSV-1 specificity. The model of molecular mimicry states autoaggressive $CD4^+$ T cells falsely recognize host antigens that bear similarities to the viral protein UL6 are mediating HSK (144-147). However, these findings are complicated by observations that this auto-immune response occurs only in corneal infection with the KOS strain of HSV-1, not the RE strain. Moreover, a study by another group failed to confirm cross-reactivity between the UL6 protein and corneal proteins, or the capacity of UL6-specific $CD4^+$ T cells to induce HSK (148). Additionally, analysis of the specificity of T cell clones isolated from human corneas with HSK has not revealed reactivity to either UL6 or corneal antigens (149). These conflicting studies call into to doubt the validity that molecular mimicry is a wide-spread mechanism for how $CD4^+$ T cells induce HSK.

The model of bystander activation induced HSK states large amount of inflammatory cytokines produced in the cornea during HSV-1 ocular infection may drive normally non-aggressive "bystander" T cells into activating their effector functions, creating a "cytokine storm" that further drives bystander activation, inducing HSK. This model is supported by data obtained from early studies using mice that are transgenic CD4 TCR specific for ovalbumin (ova). Although the $CD4^+$ T cells of these mice were incapable of recognizing viral antigens, the mice developed severe corneal inflammation following HSV-1 infection. $CD4^+$ T cells expressing the ova-specific TCR were recovered from the HSK lesions, and $CD4^+$ T cell

depletion abrogated inflammation (150). These studies provided proof of principle that HSK-like disease can develop in the absence of HSV-1 reactive $CD4^+$ T cells. However, the model contained serious flaws that complicate interpretation. Lacking a HSV-1 specific adaptive immune response, virus was never cleared from the corneas, and mice showed high morbidity at the time of HSK evaluations. In fact, when HSV-1 replication was controlled with anti-viral drugs, little inflammation developed (151). Thus, while these models showed the uncontrolled viral replication can lead to bystander activation of $CD4^+$ T cells, this is not the case in immunocompetent mice that control HSV-1 replication. While it seems likely that bystander activation may play a role in HSK once inflammation is well developed, the evidence strongly suggests another force is needed to initiate HSK.

A view favored by our group and others is that HSV-1 specific $CD4^+$ T cells play a requisite role in the induction and progression of HSK. HSV-1 specific $CD4^+$ T cell clones have been isolated from human and mouse (our unpublished observation) corneas at various stages of HSK (149). Perhaps the best evidence for an involvement of HSV-1 specific T cells in HSK came from studies where mice were tolerized to HSV-1 antigens. Injection of HSV-1 into the ocular anterior chamber induces a deviant form of immunity referred to as anterior chamber-associated immune deviation (ACAID) (152). Preferential inhibition of $CD4^+$ T cell functions such as delayed-type hypersensitivity and production of TH1 cytokines characterize ACAID (153). Induction of ACAID to HSV-1 antigens at the time of HSV-1 corneal infection protected the cornea from HSK (154). Furthermore, in human patients with active HSK, HSV-1 specific T cells have been isolated from corneal buttons, suggesting that viral specificity is important for HSK progression (149,155).

Realistically, HSK is probably driven by a combination of HSV-1 specific cells and bystander activated cells. As HSK is a chronic disease and also occurs in the absence of live virus (in our murine model of HSK), it is rational to hypothesize that HSV-1 specific $CD4^+$ T cells initiate HSK in response to HSV-1 antigens, after which the "cytokine storm" leads to bystander activation, which contributes to the chronicity of the disease. Further experimentation is needed to definitively identify the role of HSV-1 specific $CD4^+$ T cells in the initiation of HSK.

1.4.3 The role of APCs in HSK

In previous sections we have detailed how important dendritic cells and other APCs are in generating the protective adaptive immune response to HSV-1. Given the immune component of HSK, the question arises: do APCs also play a role in the immunopathogenesis of HSK? Within the cornea there are a small number of APCs present within the corneal epithelium basement membrane. The limbal regions of the cornea and the conjunctiva are densely populated by dendritic cells, thought to be Langerhans cells (156). Studies have observed that these peripheral DCs move into the central cornea very rapidly upon corneal insult, and presumably directly or indirectly transport antigens for presentation for the immune response. Studies looking at the role of APCs in ocular HSV-1 infection suggest that APCs may be playing a pathogenic role in HSK as well.

Studies from several laboratories have established an important role for corneal DCs in HSK. When the surface of one mouse eye is exposed to ultra violet light, LCs are depleted from the epithelium When one eye is UV irradiated and the mouse is bilaterally corneally infected, a role for DCs is observed not only in the inductive phase of the T cell response in lymphoid

organs, but also in the effector phase of the response within the infected cornea (157). The latter conclusion was based on the observation that HSK developed normally in the eye with DCs, but failed to develop in the LC-depleted cornea. This raises an interesting concept that DCs within the cornea are playing a direct role in destroying the immune privilege that is combating the initiation of HSK. Another study used two different strains of HSV-1 to study APC roles in HSK (140). The KOS strain of HSV-1 gives rise to a low incidence of HSK, which tends to be mild in severity when compared to the HSV-1 RE, which gives rise to severe HSK in high incidences. It was identified KOS was a poor inducer for the peripheral migration of DCs into the central cornea following initial infection; when this migration was induced, HSK that developed following KOS infection was similar to that of RE.

Subsequent studies observed a large secondary influx of DCs into corneas that went on to develop HSK. Furthermore they identified that local blockade of the costimulatory molecule B7.1 within the cornea hindered HSK development (158). Other studies found local OX40:OX40L and CD40:CD40L costimulatory interactions were dispensable to HSK development (159,160). Regardless, this strongly suggests that local antigen presentation and costimulation by APCS is necessary for the initiation of HSK.

Other studies have looked at factors normally produced by APCs and how they influence HSK development. The IL-12 cytokine family, consisting of the heterodimers IL-12, IL-23, IL-27, and IL-35, has received attention due to its diverse and complex functions in immunity. IL-12 consists of a p40 and a p35 subunit(161) and stimulates the differentiation and activation of naïve $CD4^+$ T cells toward a TH1 phenotype, promoting IFN-γ production (162). The role of IL-12 in disease has been confounded by the discovery of IL-23, which consists of the same p40 subunit coupled to a unique p19 subunit (163). IL-23 promotes both proliferation of

effector/memory TH1 cells and also the maintenance of TH17 cells whose signature cytokine is IL-17 (164). Interestingly, homodimerization of p40 yields a unique molecule capable of anti-inflammatory function through blockade of the IL-12Rβ1 (165,166) but also of pro-inflammatory function as a chemoattractant for DC and macrophages (167,168). Muddying the waters further, p35 can also interact with a second binding partner, Esptein-Barr virus-induced gene-3 (EBI3), forming the inhibitory cytokine IL-35 (169,170). IL-35 promotes the proliferation of and IL-10 production by $CD4^+CD25^+$ $FoxP3^+$ natural Tregs, inhibits proliferation of $CD4^+$ $CD25^-$ effector cells, and inhibits differentiation of TH17 cells. Thus, IL-35 is considered to be an anti-inflammatory cytokine. The final member of the family, IL-27 consists of EBI3 and p28 (IL-30) and enhances TH1 polarization of naïve $CD4^+$ T cells (171).

The role of the primary TH1 driving cytokine IL-12 in HSK has been investigated previously with conflicting results. IL-12p40 mRNA and protein increases in response to HSV-1 corneal infection (172) and the protein is released by inflammatory cells rather than by infected epithelial cells (173). However, during the period of HSK development (7-22 dpi) IL-12p40 mRNA levels decrease in the cornea, and to our knowledge IL-12p70 protein levels have not been measured. Transgenic expression of IL-12p35/p40 fusion protein under the glial fibrillary acidic protein promoter (GFAP, expressed by nervous tissue) following ocular infection with the highly neurovirulent HSV-1 strain McKrae resulted in reduced viral titers in eyes and trigeminal ganglia and increased survival in mice (174). However, another study in which the corneas of IL-$12p35^{-/-}$ and IL-$12p40^{-/-}$ mice were infected with HSV-1 McKrae found no difference in corneal viral load but reduced HSK severity among IL-$12p35^{-/-}$ mice and no HSK among IL-$12p40^{-/-}$ mice, that had survived lethal infection at 28 dpi (175). The use of the highly neurovirulent McKrae strain of HSV-1, coupled with the study of HSK at a single time point only in animals

that had survived lethal infection limits the interpretation of these studies and their translation to human infection.

IL-23 has also recently been studied in the context of HSK. Mice deficient in p19 developed more severe lesions with higher incidence than their WT counterparts (176). This study concluded that the lack of IL-23 resulted in a drastically increased IL-12 driven TH1 $CD4^+$ T cell response, though no direct evidence implicating IL-12 in the enhanced HSK was provided.

When these studies are observed collectively, it becomes apparent that the exact role of DCs early in HSV-1 infection, and how this alters immune privilege to HSK need more elucidation. The studies looking at the IL-12 cytokine family also point to a potential role of this classically APC produced cytokine in ocular disease, and also requires further experimentation to clarify how it contributes to HSK.

2.0 SPECIFIC AIMS

Previously published studies, when taken collectively, suggest that $CD4^+$ T cells play dual roles in HSV-1 ocular infection, not only providing key signals to aid the formation of $CD8^+$ T cell memory that will remain functional within the ganglia, but also a pathogenic role in initiating HSK. We also see that dendritic cells that both reside and infiltrate into the cornea can have dual roles in directing the immune responses that control HSV-1 as well as playing a part in the immunopathology of HSK. To further study these diametrically opposed actions of $CD4^+$ T cells and dendritic cells the aims of this thesis were as follows:

Determine the role $CD4^+$ T cells in the generation and maintenance of virus specific $CD8^+$ T cells during HSV-1 infection and latency

Hypothesis: $CD4^+$ T cells are necessary for optimal generation of $CD8^+$ T cell memory, but are dispensable for maintaining the memory pool. Defective memory residing in the latently infected TG will be rescued by periodic encounter with antigen, while memory pools residing in non-infected tissue will remain compromised.

Identify the contributions of HSV-1 specific and bystander activated $CD4^+$ T cells in the development of HSK

Hypothesis: Following HSV-1 infection, HSK is triggered by HSV-1 specific $CD4^+$ T cells, while progression of disease requires HSV-1 specific $CD4^+$ T cells with a supplemental contribution from bystander activated cells.

Define the role of IL-12p35 and IL-12p40 in the progression of herpes stromal keratitis

Hypothesis: IL-12p70 is necessary for both the initiation and progression of herpes stromal keratitis. IL-12p40 homodimer and IL-23 both are not necessary for the inflammation that drives herpes stromal keratitis.

Identify the role local $CD11c^+$ dendritic cells in the innate driven control of HSV-1 ocular infection

Hypothesis: Local or early responding DCs within the cornea provide in situ signals that both direct the innate immune response to areas of viral infection within the cornea as well as initiate the adaptive immune response to HSV-1.

3.0 MATERIALS AND METHODS

3.1 REAGENTS

$gB_{498-505}$ (SSIEFARL) peptide was purchased from Invitrogen. Phycoerythrin (PE)-conjugated H-$2K^b$ tetramers complexed with the $gB_{498-505}$ peptide were kindly provided by the NIAID Tetramer Core Facility (Emory University Vaccine Center). Fluorochrome labeled antibodies against CD3 (clone 17A-2), CD4 (RM4-5), CD11a (2D7), CD25 (PC61), CD43 (1B11), CD45 (30-F11), CD49b (DX-5), VLA-4 (R1-2), CD69 (H1.2F3), CD107α (1d45), IFN-γ (XMG1.2), TNF (MP6-XT22), V-beta 8.1/8.2 (MR5-2), and I-A/I-E (M5/114.15.2) were purchased from BD Pharmingen (San Diego, CA). Fluorochrome labeled antibodies against CD8α (53-6.7), CD11b (M1/70), CD11c (N418), GR-1 (RB6-8CA), FoxP3 (FJK-1GS), and PDCA-1 (ebio927) were purchased from eBiosciences (San Diego, CA). Fluorochrome labeled antibodies against PD-1 (RMP1-30) and VLA-4 (R1-2) were purchased from Biolegend (San Diego, CA). Fluorochrome labeled α-langerin antibody (929F3.01) was purchased from Dendritics (Lyon, France). The appropriate isotype control antibodies were purchased their respective vendors.

3.2 MICE

3.2.1 Mice strains used in these studies

Six- to 8-week-old female wild type (WT) C57BL/6, BALB/cJ, IL-12p35$^{-/-}$ BALB/c, and IL-12p40$^{-/-}$ BALB/c and CD11c-DTR (C.FVB-Tg(Itgax-DTR/EGFP)57Lan/J) mice were purchased from Jackson laboratories (Bar Harbor, ME). The IL-12p35$^{-/-}$ and IL-12p40$^{-/-}$mice were bred through 4 generations to produce IL-12p35$^{-/-}$p40$^{-/-}$double knockout mice. IL-12p35 and IL-12p40 genes were individually genotyped to confirm knockout status using the following primers: IL-12p35 (forward 5'-CTGAATGAACTGCAGGACGA-3', reverse . 5'-ATACTTTCTCGGCAGGAGCA -3', expected size 172 base pairs) and IL-12p40 (forward 5'-CTTGGGTGGAGAGGCTAT TC -3', reverse 5'- AGGTGAGATGACAGGAGATC -3', expected size 280 base pairs). All experimental animal procedures were reviewed and approved by the University of Pittsburgh Institutional Animal Care and Use Committee and adhered to the ARVO Statement for the Use of Animals in Ophthalmic and Vision Research.

3.2.2 Murine Bone Marrow Chimera Generation

ChimeraCD11c-DTR mice required the generation of bone marrow chimeras for these studies, as intact CD11c-DTR mice can succumb to repeat treatments of diphtheria toxin. Briefly, BALB/cJ hosts underwent two treatments of 500 rads in an animal γ-irradiator, four hours apart. At the end of the irradiation regimen, 2.5x10^5 bone marrow cells from a CD11c-DTR donor were transferred intravenously (iv). Mice were housed under immunocompromised mouse conditions

and treated regularly with 2mg/mL neomycin from Sigma (St. Louis, MO) in their drinking water. Mice were considered fully reconstituted and ready for experimental use after 6 weeks.

3.2.3 *In vivo* antibody treatment

Mice were treated with an i.p injection of 0.15mg of rat anti-mouse CD4 antibody clone GK1.5 (BioXcell, Weston, FL) for *in vivo* depletion of $CD4^+$ T cells. For depletions prior to infection, injections were given 2 days before infection, followed by $^+1$, $^+3$, $^+8$, $^+15$, $^+22$, $^+29$, $^+36$, $^+43$, and $^+50$ dpi. For depletions during contraction, treatments were given at $^+8$, $^+15$, $^+22$, and $^+29$ dpi. For PDL1 blockade, mice were treated with 0.2mg of rat anti-mouse PDL1 antibody clone 10F.9G2 (BioXcell) every 3 days for 2 weeks prior to desired observation point.

3.2.4 *In vivo Diphtheria* toxin treatment

Diphtheria toxin (DT) purchased from Sigma Laboratories was prepared in a sterile solution of PBS at a concentration of 1mg/mL. For local treatment in the cornea, 50ng of DT in a 10uL volume was subconjunctivally injected. For systemic treatment, mice were injected i.p. with 150ng DT. For continuous treatment, injections were repeated every three days, with a lower dose (20ng for local treatment, and 100ng for systemic treatment).

3.2.5 Herpes Stromal Keratitis Scoring

Mice were monitored for HSK on alternate days between 7 and 21 days post-infection (dpi) by slit lamp examination. A standard scale ranging from 1 – 4 based on corneal opacity was used: 1^+

mild corneal haze, 2^+ moderate opacity, 3^+ complete opacity, 4^+ corneal perforation. Disease incidence was defined as HSK score greater or equal to 2 by 15 dpi. The extent of neovascularization and peri-ocular skin disease was also recorded.

3.3 VIRUS PROTOCOLS

3.3.1 Virus preparation and ocular HSV-1 infection

HSV-1 strain RE was grown in Vero cells, and intact virions were isolated on Optiprep gradients according to manufacturer's instructions (Accurate Chemical and Scientific Corp, Westbury, NY). Viral titer described as plaque forming units per mL (pfu/ML) was established by standard plaque assay infections of vero cell monolayers. For ocular HSV-1 infection, mice were anesthetized by intraperitoneal (i.p.) injection of 2.0 mg ketamine hydrochloride and 0.04 mg of xylazine (Phoenix Scientific) in 0.2 mL of Hanks balanced salt solution (Biowhittaker). The abraded central corneas of anesthetized mice were infected by topical application of 3μL of RPMI (Biowhittaker) containing 1 x 10^5 plaque-forming units (PFU) of HSV-1. All animal experiments were conducted in accordance with guidelines established by the University of Pittsburgh Institutional Animal Care and Use Committee.

3.3.2 Generation of 10 hour HSV-1 infected target lysates

HSV-1 antigens were extracted from Vero cells (3.5 x 10^6/mL) at 10 hours after HSV-1 RE infection (multiplicity of infection of 4). Confluent flasks of Vero cells were infected at an MOI of 4 for one hour, washed twice with Vero growth media (DMEM supplemented with: 10% FCS, 1% HEPES (Cambrex Bioscience, Charles City, IL), 0.1 mM nonessential amino acids (Invitrogen, Carlsbrad, CA), 1mM sodium pyruvate (Invitrogen), L-glutamine (2mM) 100U/ml penicillin and 100ug/ml streptomycin) and then incubated for 9 hours to generate the 10 hour lysates. To extract viral antigens, vero cells were subject to two 2 min homogenization cycles using the Retsch MM 300 Mixer Mill homogenizer, followed by three freeze/thaw cycles. The cell lysates was then UV inactivated for 10 minutes at 5cm.

3.4 PHENOTYPIC ANALYSIS OF CELLS

3.4.1 Tissue Preparation for Flow Cytometry

At indicated time post infection, mice were sedated and euthanized by cardiac perfusion with sterile PBS. Prior to perfusion draining lymph nodes (DLN), spleens, and corneas were harvested. DLN, Spleens, and Lungs were minced, and then incubated with 500uL (spleen, DLN), or 1mL (lungs) of DMEM (Biowhittaker, Walkersville, MD) containing 10% FCS (Atlanta Biologicals, Atlanta, GA) and 400U/mL collagenase type I (Sigma) for 1 hr at 37°C. Trigeminal Ganglions (TG) were digested in 100µL (TG) of collagenase or 1 hour at 37°C.

Corneas were treated with PBS 2mM EDTA for 15 minutes, and then the pigment epithelium, conjunctiva, and epithelium were dissected away from the cornea stroma. The cornea was cut into quarters, and incubated in 100ul of collagenase at a concentration of 800U/mL for 1 hour. Tissues were then dispersed into single cell suspensions (TGs and corneas via trituration with a micropipette) by and if necessary, treated with red blood cell lysis buffer prior to staining with the designated antibodies. Data were collected on a FACSAria cytometer and analyzed by FACSDiva software (BD Biosciences).

3.4.2 Phenotypic analysis

For all phenotypic analyses, cells were stained for CD45 to permit gating exclusively on bone marrow-derived cells. For analysis of CD8 and $CD4^+$ T cell populations and their phenotype, cells were stained with anti-CD8α and anti-CD4. For analysis of HSV-1 specific $CD8^+$ T cells (gB-CD8), cells were additionally co-stained with anti-CD8α and $gB_{498\text{-}505}$ H-$2K^b$ tetramers.

3.4.3 Fluorescently assisted cell sorting

At indicated time points, lungs and draining lymph nodes were dispersed into single cell suspension and stained with anti-CD8 and $gB_{498\text{-}505}$ H-$2K^b$ tetramers. Cells were sorted at high purity (purity-32) for $CD8^+$ gB $tetramer^+$ cells on a FACSAria cytometer (BD Biosciences).

3.5 T CELL FUNCTIONALITY

3.5.1 $CD8^+$ T cell stimulation for Intracellular cytokine staining and lytic granule exocytosis

Dispersed TG cells or post-gB tetramer sorted cells were stimulated directly with either 10^{-6} M (optimal) or 10^{-11} M (sub-optimal) $gB_{498-505}$ peptide pulsed B6WT350 fibroblast targets in the presence of FITC-conjugated anti-CD107a mAb and Golgi-plug (BD Biosciences) for 6 hr at 37°C/5% CO_2. The optimal and suboptimal peptide concentrations are based on previous studies (130). Following stimulation, cells were stained for surface expression of CD8α, followed by intracellular staining for IFN-γ and TNF-α after permeablization and fixation via Cytofix/Cytoperm (BD Biosciences). CD107a capture on the cell surface during stimulation provides sensitive detection of lytic granule exocytosis as previously described (177,178)

3.5.2 $CD4^+$ T cell stimulation

At indicated time points, DLNs were excised and dispersed into a single cell suspension. $CD4^+$ T cells were isolated via negative selection using the $CD4^+$ T cell isolation MACS bead kit (Miltenyi Biotech, San Diego, CA). T cells were then incubated at a 1:4 ratio with T cell depleted splenocytes that had been loaded with HSV-1 10 hour lysate overnight. The cells were cultured at 37°C for 72 hours, after which supernatant was collected for ELISA. Alternatively, for the last 12 hours of culture, golgi plug was added to arrest secretion of cytokines, followed by intracellular staining as described above.

3.5.3 Tetramer release assay

This assay was performed as described (179). Briefly, single-cell TG suspensions were stained with $gB_{498-505}$ tetramer for one hour at 37°C, the cells were then washed and then incubated with anti-H-$2D^b/K^b$ antibody to halt tetramer re-binding (28-8-6; BD Pharm) at 37°C for the designated times. Cells were then stained with anti-CD8α and anti-CD45 mAb, and analyzed via flow cytometry to observe loss of tetramer over time. Data expressed as $CD8^+$ $tetramer^+$ cells as a percentage mean fluorescence intensity (MFI)± SEM of the maximum binding observed at time zero. (n=10 mice/group)

3.6 DETECTION OF SOLUBLE FACTORS

3.6.1 ELISA for secreted IFN-γ

Immulon Microtiter plates (Thermo Labsystems) were coated overnight with primary anti-IFN-γ capture antibody (R4-6A2, ATCC). The plates were washed and blocked with 1% BSA in PBS. The supernatant fluids and standards were added and incubated at room temperature for 2 h. The plates were washed again, secondary biotinylated anti-cytokine detection Ab (polyclonal goat anti-mouse IFN-γ, R&D Systems) was added and incubated at room temperature for 1 h. The plates were then washed and developed with strepavidin-horseradish peroxidase (BD Pharmingen) and its substrate ((3,3' 5,5'-Tetramethylbenzidine Base, GIBCO BRL). Using standards as guides, the development was halted by the addition of 1N sulfuric acid. The colored

reaction product was measured with an enzyme immunoassay plate reader at 450 nm. The amount of cytokine in each supernatant was extrapolated from a standard curve. The detection sensitivity was 5.6 pg/ml for IFN-γ.

3.6.2 Detection of chemokine and cytokine production *in vivo* by bead assay

Individual corneas were excised at 17 dpi, quartered in sterile PBS, and pieces were transferred to tubes containing 300 μl PBS $^{+}$ complete protease inhibitor (Complex Mini Protease Inhibitor, Roche Applied Science, Indianapolis, IN) and sonicated (Fisher Model 100 Sonic Dismembrator, Fisher Scientific) 4 times for 15 seconds each. The sonicator tip was rinsed with 75 μl PBS $^{+}$ protease inhibitor, yielding a final volume of 600 μl/sample. To remove cellular debris, samples were microcentrifuged twice. 23-plex mouse cytokine/chemokine Bio-Plex assay (BioRad) was performed according to manufacturer's instructions.

3.7 DETECTION OF VIRAL LOAD *IN VIVO*

3.7.1 Detection of infectious virus on corneas

The corneal surfaces of mice were swabbed with sterile Weck-Cel surgical spears (Medtronic Solan, Jacksonville, FA) on days $^{+}$2, $^{+}$4, $^{+}$6, $^{+}$8 after HSV-1 infection, spears were placed in 0.5 ml RPMI, and frozen at -80° C until assayed. Samples were added to confluent Vero cells, incubated for 1 hour at 37° C, and overlayed with 0.5% methylcellulose. The cultures were

incubated for 72 hours, fixed with formalin, stained with crystal violet and viral cytopathic effect was detected with the aid of a dissecting microscope.

3.7.2 Quantitative real-time PCR for single viral genome copies

Total DNA was isolated from single-cell TG suspensions using DNeasy columns according to manufacturer's instructions (Qiagen, Valencia, CA). DNA was quantified by spectrophotometry and diluted to 1 ng/µl in nuclease-free dH_2O. 25 ng DNA or water control was mixed in duplicate with 25 µl mixture of TaqMan Universal PCR Master Mix (Roche) and an HSV-1 glycoprotein H (gH)-specific primer-probe set, custom designed and synthesized by ABI Assays-by-Design service. Samples (50µl/well) were assayed in 96-well plates with an ABI Prism 7700 sequence detector. ABI Primer Express v1.5a software default settings were used for instrument control and data analysis. The gH sequences were: forward primer (5'-CGACCACCAGAAAACCCTCTTT-3'), reverse primer (5'ACGCTCTCGTCTAGATCAAAGC-3'), and probe [5'-(FAM)TCCGGACCATTTTC(NFQ)-3'].

3.8 WHOLE MOUNT FLUOROSECENT MICROSCOPY

Whole corneas were excised from mice. The pigment epithelium was dissected away carefully, with special attention given to avoiding damage to the epithelium and conjunctiva. Corneas were cut in a cloverleaf fashion, washed in PBS 4% FBS, before stained with indicated antibodies in 4% FBS overnight at 4°C. Corneas were washed with PBS 4%FBS, fixed in 1%

paraformaldehyde (PFA) for 2 hours, washed once more in PBS 4% FBS, and mounted. For intracellular staining, following the primary antibody, corneas were washed with PBS 4% FBS, fixed and permeabilized in Cytofix/Cytoperm (BD), washed in Perm/wash (BD), and stained with intracellular antibodies overnight. Corneas were then washed in Perm/wash the following day and mounted. Images were acquired on an Olympus Fluoview 1000X confocal microscope with a 1.4NA 60X oil objective. Images were acquired by sequential scanning to avoid fluorescence crossover, and Z stacks were acquired at Nyquist sampling frequency through the tissue. All image reconstructions were made using Metamorph.

3.9 STATISTICAL ANALYSIS

All statistical analyses were computed with GraphPad Prism software using unpaired t-tests. P values <0.05 were considered statistically significant.

4.0 THE ROLE OF $CD4^+$ T CELLS IN THE GENERATION OF HSV-$CD8^+$ T CELLS

$CD4^+$ T cells have long been implicated a critical role in the formation of long-lived functional $CD8^+$ T cell memory. The requirements for $CD8^+$ T cell memory in context of viral infection diverge from acute models of infection, as latent virus can influence functional properties of CD8 memory T cells. Here we examined the role of $CD4^+$ T cell help in the generation of HSV-1 specific $CD8^+$ T cells, and how the unique properties of viral latency impact this process.

4.1 CD4$^+$ T CELL ABLATION INFLUENCES HSV-1 LATENCY

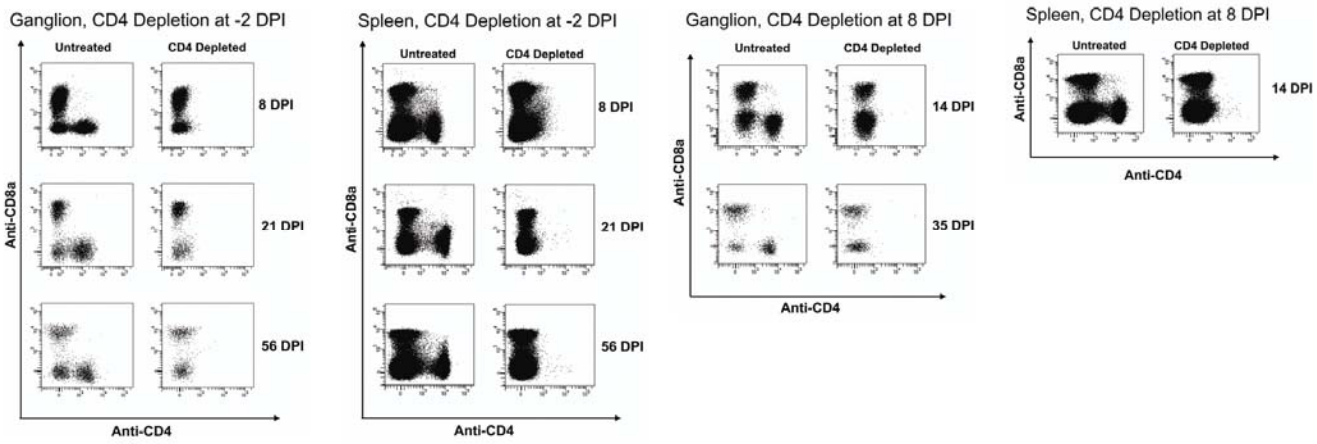

Figure 8 – Anti-CD4 antibody effectively ablates CD4$^+$ T cells from mice

Representative dot plots depicting CD8$^+$ and CD4$^+$ T cell populations within the infected ganglion and spleen of mice. At indicated time points dispersed ganglion and spleens were stained with antibodies and analyzed via flow cytometry. Panels A and B depict Tx starting at -2dpi. Panels C, D represent Tx started at 8 dpi. Flow plots were gated on CD45$^+$ cells.

Initial studies tested the effect of CD4$^+$ T cell ablation starting before HSV-1 corneal infection on the clearance of virus from the cornea, the establishment of viral latency in the trigeminal ganglion (TG), and on the maintenance of latency. Our studies employed an antibody treatment protocol that effectively ablated CD4$^+$ T cells from mice beginning 2 days before HSV-1 corneal infection and continuing through 60 dpi (Figure 8). Here we show that depletion of CD4$^+$ T cells through 8 dpi did not influence the clearance of HSV-1 from the cornea (Fig. 9A), the kinetics of latency establishment within the TG (not shown), or the load of latent viral genome at 8 dpi (Fig. 9B).

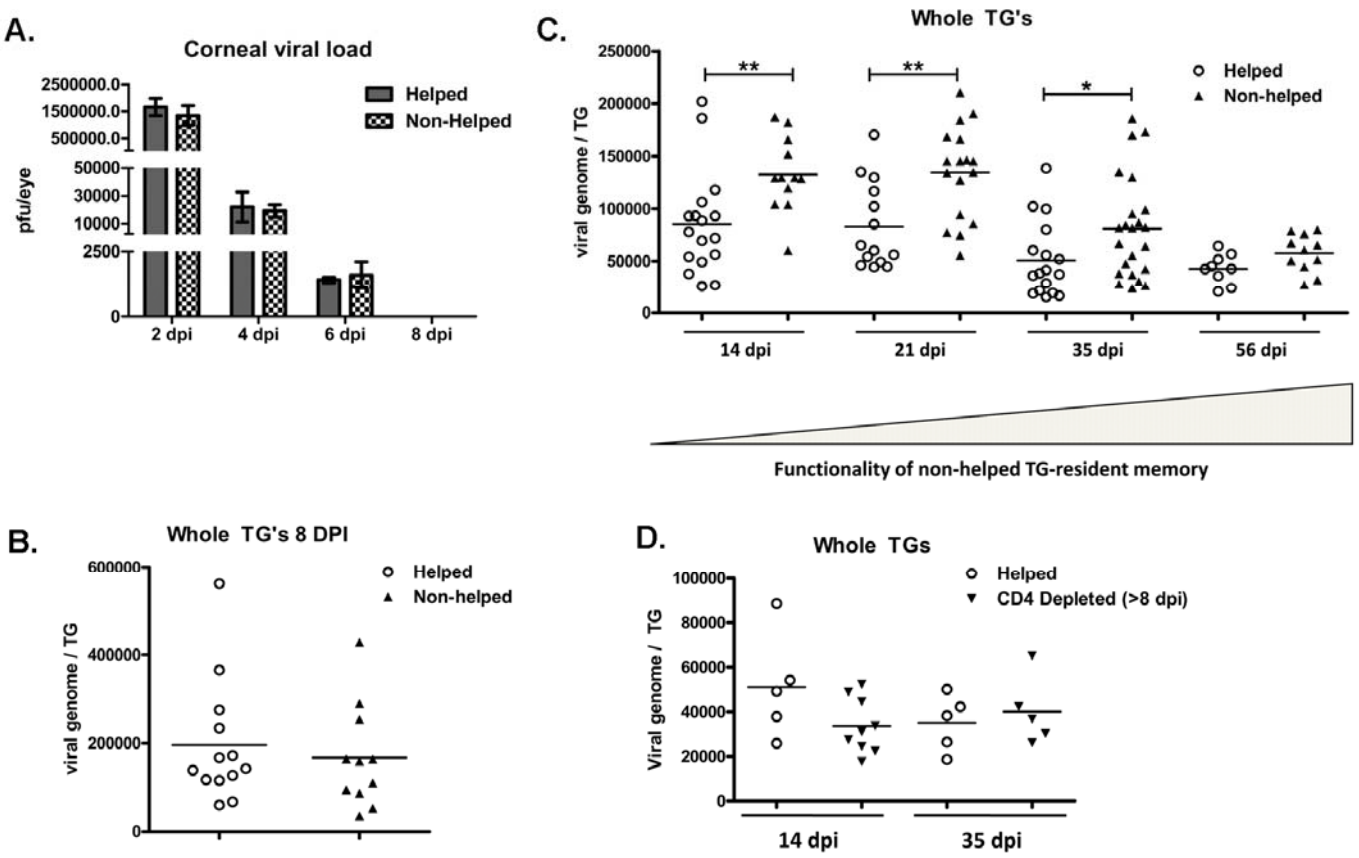

Figure 9 - CD4$^+$ T cell ablation influences the maintenance of HSV-1 latency

B6 mice that received HSV-1 corneal infections were continuously depleted of CD4$^+$ T cells beginning 2 days before (A-C) or 8 days after (D) infection. **A)** At indicated days post infection (dpi), eyes were swabbed with a sterile surgical spear and assayed for live virus by standard plaque assay. The data are presented as the mean ± SEM viral plaque forming units (pfu) per cornea of non-depleted (helped) mice and those continuously CD4-depleted starting at -2 dpi (non-helped). **B-D)** At the indicated dpi, DNA was extracted from trigeminal ganglia (TG) of and the number of copies of HSV-1 genome harbored in each TG was determined by quantitative real time PCR for the gH gene. Data from individual TG are presented (B&C) viral genomes /TG of helped and non-helped mice**. D)** Viral genomes /TG of non-depleted (helped) mice and those CD4-depleted starting 8 dpi (CD4-depleted > 8 dpi). ** $p<0.01$, * $p<0.05$), n=5-23 mice per group as indicated in scatter plots)

However, the $CD4^+$ T cell ablated mice failed to maintain the virus in a latent state between 8 and 35 dpi as indicated by a significant increase in the viral genome copy number in the TG (Fig. 9C). The latent viral load did return to normal levels by 56 dpi in $CD4^+$ T cell ablated mice. The failure of $CD4^+$ T cell ablated mice to control the early stages of HSV-1 latency did not reflect a direct requirement for $CD4^+$ T cells in control of viral latency because initiating CD4-depletion at 8 dpi did not result in a similar increase in the latent viral load (Fig. 9D).

4.2 $CD4^+$ T CELL HELP DOES NOT INFLUENCE THE SIZE OF THE HSV-SPECIFIC $CD8^+$ T CELL EFFECTOR OR MEMORY POOL

We previously demonstrated that diminished function of memory HSV-specific $CD8^+$ T cells within latently infected TG was associated with failure to maintain latency as indicated by an increase in viral genome copy number (29,180). Therefore, we hypothesized that the absence of $CD4^+$ T help during the first 8 days after HSV-1 infection may have resulted in an HSV-specific $CD8^+$ effector and/or memory T cell population within the TG that was incapable of maintaining HSV-1 latency. We used an HSV-1 corneal infection model in C57BL/6 (B6) mice in which tetramers containing an immunodominant glycoprotein B ($gB_{498-505}$) epitope were used to identify and quantify a majority of HSV-specific $CD8^+$ T cells (here referred to as gB-CD8).

The number of $CD4^+$ T cell-helped (helped) and $CD4^+$ T cell non-helped (non-helped) gB-CD8 peaked at similar levels in the draining lymph nodes (DLN, data not shown) and the infected TG (Fig. 10) at 8 dpi. In the infected TG, the non-helped gB-CD8 underwent a more rapid contraction between 8 and 14 dpi (Fig. 10A), but ultimately established a stable and numerically normal memory population (Fig. 10A). $CD4^+$ T cell ablation starting after the peak

of the effector response (8 dpi) resulted in accelerated contraction similar to that seen when $CD4^+$ T cells were ablated from the time of infection, suggesting a direct role for $CD4^+$ T cells in gB-$CD8^+$ T cell contraction (Fig. 10B).

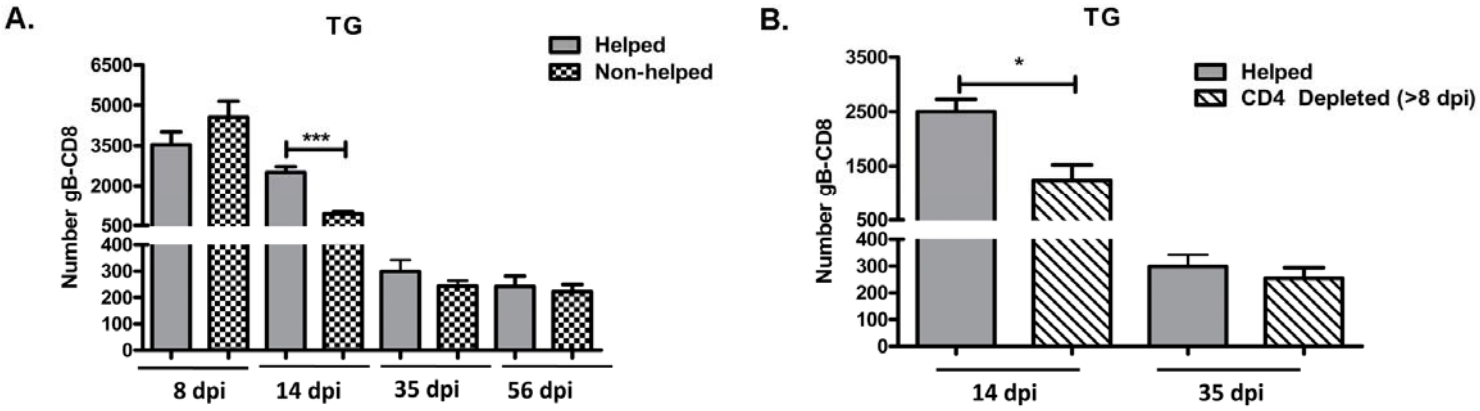

Figure 10 – $CD4^+$ T cell help does not influence the size of the gB-$CD8^+$ T cell effector or memory population.

B6 mice that received HSV-1 corneal infections were continuously depleted of $CD4^+$ T cells beginning 2 days before (A) or 8 days after (B) infection. At indicated days post infection (dpi), TG were excised and HSV-1 gB-specific $CD8^+$ T cells (gB-CD8) were quantified by simultaneous staining with anti-CD8α mAb and tetramers containing the immunodominant HSV-1 $gB_{498–505}$ epitope ($gB_{498–505}$ H2-K^b). **A)** Mean ± SEM of the absolute number of gB-CD8 per TG in non-depleted (helped) and continuously CD4-depleted starting -2 dpi (non-helped) mice. **B)** Mean ± SEM of the absolute number of gB-CD8 per TG in non-depleted (helped) and continuously CD4-depleted starting $^+$8 dpi (CD4-depleted > 8 dpi) mice. (*** $p<0.001$, * $p<0.05$) (n=10-15 mice/group)

4.3 NON-HELPED GB-CD8 EXHIBIT FUNCTIONAL ALTERATIONS UPON INFILTRATING THE INFECTED TG.

In this study we quantified four separate populations of gB-CD8. As we previously reported (130), one population of low functional avidity gB-CD8 produces effector cytokines only in

response to an optimal epitope density ($1x10^{-6}$M $gB_{498-505}$ peptide loaded fibroblasts); while a second high functional avidity population responds to both optimal and suboptimal ($1x10^{-11}$M $gB_{498-505}$ peptide loaded fibroblasts) epitope densities. Both the high and low functional avidity gB-CD8 populations contain subpopulations that express different functional programs: all responding gB-Cd8 produce IFN-γ and release lytic granules (IFN-γ/LG) when stimulated, but a subpopulation here referred to as polyfunctional also produces TNF-α (IFN-γ/TNF/LG). No gB-CD8 were single producers of TNF-α. These four subpopulations are illustrated in Figure 3B.

We sorted for gB-CD8 in the DLN at 8 dpi to test their functionality (Fig. 11A). Within the DLN, approximately 75 % of both helped and non-helped gB-CD8 responded to optimal gB peptide stimulation, and of these approximately 50% showed high functional avidity by responding to a suboptimal gB peptide dose (Fig. 11C). In the TG at 8 dpi, the mean frequency of helped gB-$CD8^+$ T hat responded to optimal gB peptide stimulation (67%) was not significantly different from their counterparts in the DLN (Fig. 11C). The frequency of non-helped gB-CD8 in the TG at 8 dpi that responded to optimal gB peptide stimulation (55%) was significantly reduced relative to their counterparts in the DLN ($p<0.05$) and to the helped gB-CD8 in the TG ($p<0.05$). The frequencies of high functional avidity helped and non-helped gB-CD8 in the TG at 8 dpi were not significantly different from each other or from their counterparts in the DLN (Fig. 11C).

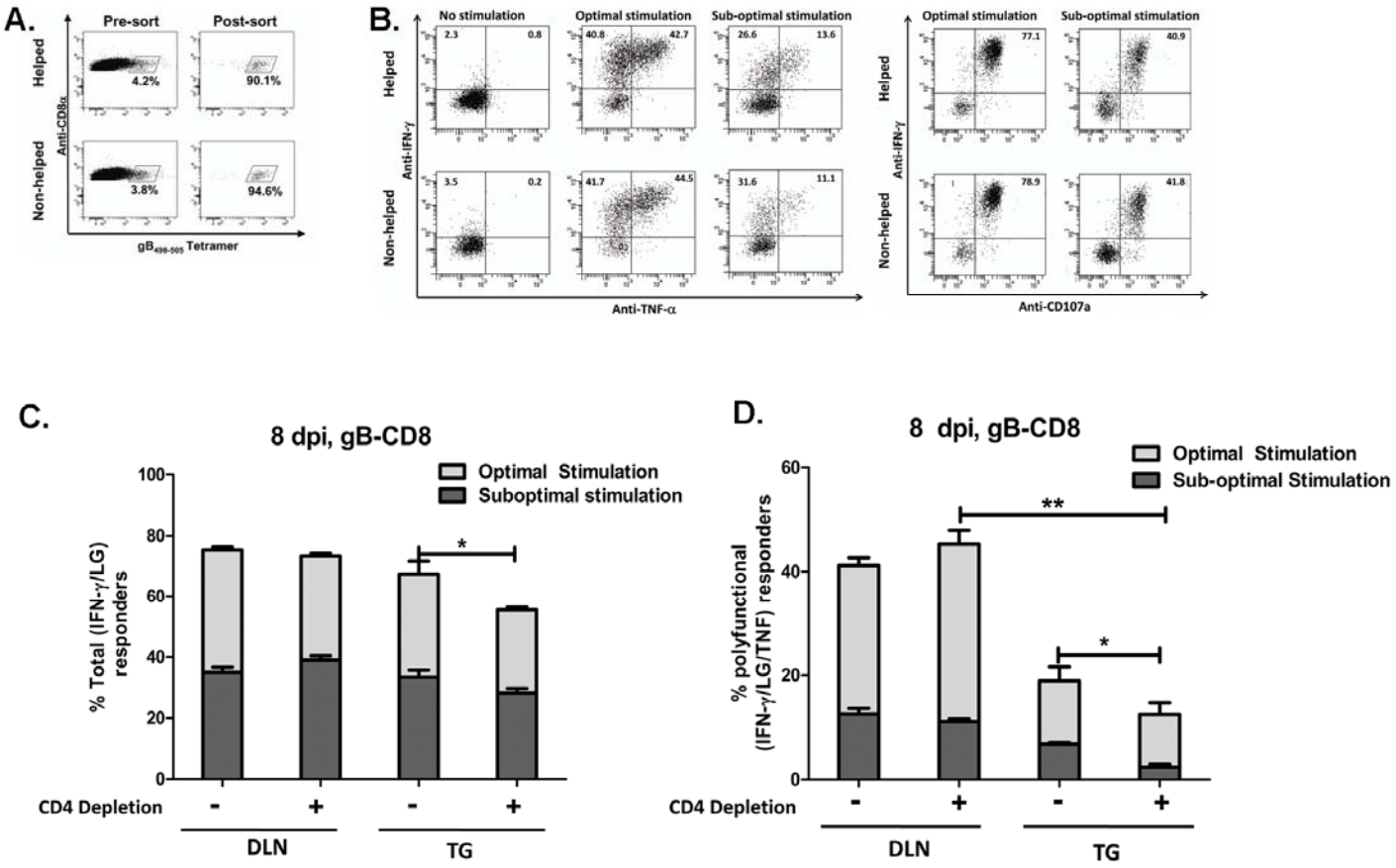

Figure 11 - Non-helped gB-CD8 exhibit functional alterations upon infiltrating the infected TG

B6 mice that received HSV-1 corneal infections were not depleted or continuously depleted of $CD4^+$ T cells beginning 2 days before infection. **A)** DLN were excised at 8 DPI, dispersed into single cell suspensions, and stained simultaneously with CD8α mAb and $gB_{498\text{-}505}$ tetramer. Tetramer positive $CD8^+$ T cells were sorted via FACS with a purity of greater than 90% as illustrated in representative dot plots. **B-D)** Sorted DLN cells or dispersed TG cells were stimulated for 6 hours with the B6WT350 fibroblast cell line loaded with $gB_{498\text{-}505}$ peptide at optimal ($1x10^{-6}$M) or sub-optimal ($1x10^{-11}$M) density, in the presence of the Golgi transport inhibitor brefelden-A and FITC-conjugated anti-CD107a antibody, followed by intracellular staining for cytokines IFN-γ and TNFα. **B)** Data are representative flow plots depicting background activation from tetramer binding, as well as IFN-γ and TNF-α production and lytic granule (LG) release ($CD107a^+$) following optimal and suboptimal gB peptide stimulation. **C&D)** Bars represent mean ± SEM total responder cells (IFN-γ/LG) or polyfunctional responder (IFN-

γ/LG/TNF) cells from both the DLN and TG at 8 DPI. The total bar represents response to optimal antigen, while the bar in bar graph represents response to sub-optimal antigen. (**$p<0.01$ * $p<0.05$) (n=8-10 mice/group).

The most dramatic difference between the gB-CD8 effector cells in the DLN and TG at 8 dpi was in the low frequency of polyfunctional (IFN-γ/LG/TNF) cells in the TG (Fig. 11D). While both the helped and non-helped gB-CD8 in the TG showed a marked reduction in the frequency of polyfunctional cells in response to optimal gB peptide stimulation relative to their counterparts in the DLN, high functional avidity polyfunctional cells were nearly undetectable in the non-helped gB-CD8 in the TG.

4.4 EARLY $CD4^+$ T CELL HELP IS REQUIRED TO AVERT GB-CD8 FUNCTIONAL COMPROMISE.

The frequency of helped gB-CD8 in the TG that responded to an optimal gB peptide stimulation remained quite constant from 8 through 56 dpi (Fig. 12A). Interestingly, the frequency of those cells that exhibited a high functional avidity by responding to a suboptimal gB peptide dose increased dramatically over the same period (Fig. 12A). In contrast, the non-helped gB-CD8 showed a sharp decline in functionality from 8 dpi to 14 dpi, when only 14% exhibited a high functional avidity. From 14-35 dpi the frequency of non-helped gB-$CD8^+$ T hat responded to an optimal dose of gB peptide declined further, but the frequency of high functional avidity cells increased. The frequency of both populations remained significantly reduced ($p<0.05$) relative to the helped gB-CD8 at 35 dpi. By 56 dpi the non-helped and the helped gB-CD8 showed the same frequency of cells capable of responding to an optimal and suboptimal dose of gB peptide.

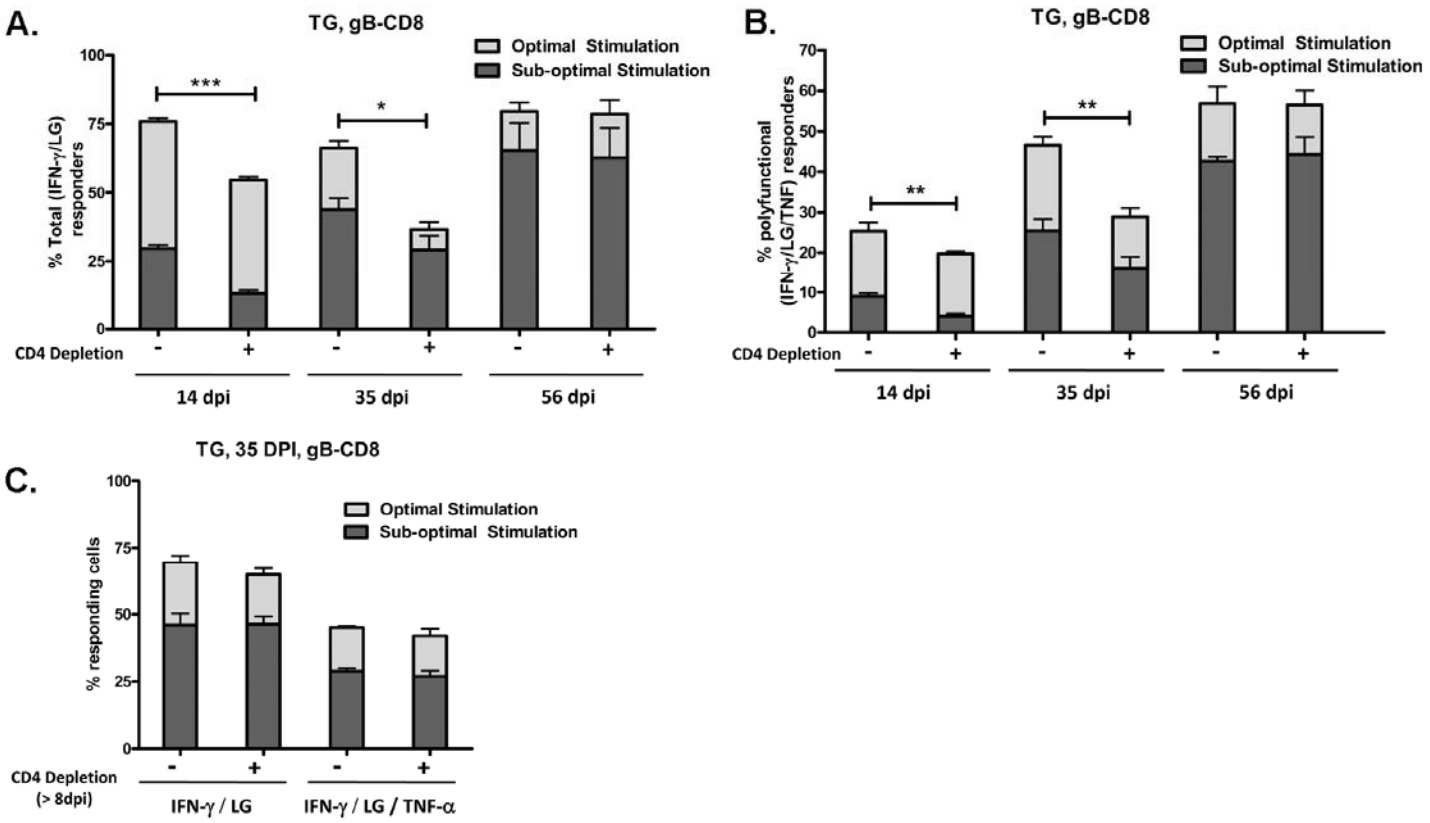

Figure 12 - Early CD4$^+$ T cell help is required to avert gB-CD8 functional compromise.

B6 mice that received HSV-1 corneal infections were not depleted or continuously depleted of CD4$^+$ T cells beginning 2 days before infection (non-helped, A&B), or beginning at 8 dpi (C). At the indicated dpi dispersed TG cells were stimulated with an optimal or sub-optimal dose of gB peptide and IFN-γ and TNFα production and lytic granule (LG) release were quantified as in Fig. 2. Data are presented as **A**) mean % ± SEM of gB-tetramer$^+$ CD8$^+$ T cells (gB-CD8) from CD4-depleted and non-depleted mice that responded (IFN-γ/LG) to optimal or suboptimal gB peptide stimulation, **B**) mean % ± SEM of polyfunctional (IFN-γ/LG/TNF) gB-CD8 in response to optimal or suboptimal gB peptide stimulation. **C)** mean % ± SEM of total (IFN-γ/LG) or polyfunctional (IFN-γ/LG/TNF) gB-CD8 in response to optimal or suboptimal gB peptide stimulation at 35 dpi. (*** $p<0.001$, **$p<0.01$ * $p<0.05$) (n=8-10 mice/group).

It is noteworthy that in addition to an increased frequency of high functional avidity cells within the overall gB-CD8 responding population in the TG from 8-56 dpi (IFN-γ/LG, Fig. 12A), the helped gB-CD8 also exhibited a gradual increase in the polyfunctional (IFN-γ/LG/TNF) subpopulation (Fig. 12B), and most of these cells exhibited high functional avidity by 56 dpi. Thus, in the helped gB-CD8 population in the TG there was a marked enrichment of polyfunctional and high functional avidity cells over time within the latently infected TG. In contrast, from 8-14 dpi the non-helped gB-CD8 exhibited a further decline in polyfunctional cells, which was particularly prominent among the high functional avidity cells that represented only 4% of the non-helped gB-CD8 at 14 dpi (Fig. 12B). This reduced functionality combines with a reduced number of non-helped gB-CD8 in the TG at 14 dpi (Fig. 10A) to define a highly compromised gB-CD8 population at this time. The frequency of polyfunctional cells within the non-helped gB-CD8 population increased from 14-35 dpi, but remained significantly reduced ($p<0.01$) relative to their helped counterparts following both optimal and sub-optimal gB peptide stimulation. By 56 dpi, the non-helped gB-CD8 regained full functionality. The augmentation of gB-CD8 functionality was imprinted by $CD4^+$ T cells during the first 8 days after infection because depletion of $CD4^+$ T cells beginning at 8 dpi had no effect on gB-CD8 function at 35 dpi (Fig. 12C).

4.5 LATENTLY INFECTED TG SELECTIVELY PROMOTE THE ENRICHMENT OF HIGH FUNCTIONAL AVIDITY GB-CD8 DURING ESTABLISHMENT OF MEMORY.

We have previously demonstrated that the microenvironment of the latently infected TG can influence functional properties of the resident gB-CD8 memory population, presumably due to persistent low-level exposure to viral antigens (130). To determine if the increased frequency of polyfunctional and high functional avidity gB-CD8 was unique to latently infected TG, we analyzed the functionality of gB-CD8 in the non-infected lungs of the same mice at 35 and 56 dpi (Figure 5A). As shown in Figure 5B&C, the gB-CD8 population in the lungs already showed a high frequency of polyfunctional cells by 35 dpi, and these remained high at 56 dpi. Thus, the acquisition of polyfunctional cells over time appeared to be inherent to the transition of gB-CD8 into memory. In contrast, the frequency of high functional avidity cells within both the overall responding gB-CD8 population (IFN-γ/LG) and within the polyfunctional (IFN-γ/LG/TNF) population declined significantly ($p<0.01$) between 35 and 56 dpi, when they constituted only 22% of the gB-CD8 population. The selective increase (total response $p<0.01$, polyfunctional $p<0.001$) in high functional avidity cells in the TG relative to the lungs is illustrated in Figures 5D&E. Thus, while acquisition of polyfunctionality appears to occur normally in gB-CD8 during the transition from an effector to memory population, latently infected tissue appear to provide a selective pressure for accumulation of high functional avidity gB-CD8.

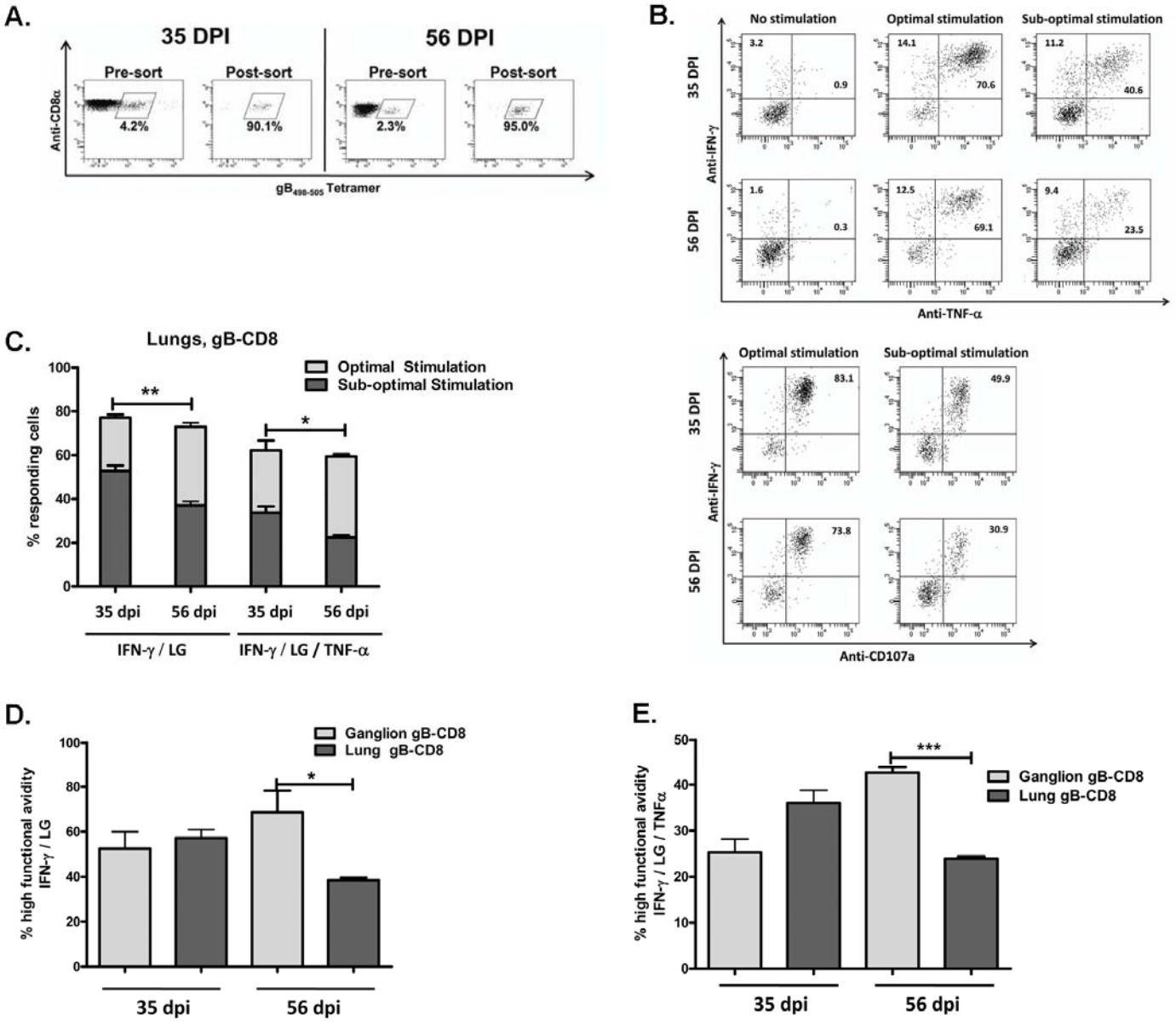

Figure 13- Latent virus influences some of the functional changes that occur in gB-CD8 during the establishment of memory.

A) Lungs were harvested at 35 or 56 dpi, dispersed cells were stained with $gB_{498-505}$ tetramers, and sorted gB-CD8 were ≥ 90% gB-tetramer$^+$ as illustrated in a representative dot plot. Sorted gB-CD8 were stimulated with an optimal or suboptimal dose of gB peptide and IFN-γ and TNFα production and lytic granule (LG) release were quantified as in Fig. 2. **B)** Representative flow plots depicting background activation from tetramer binding, as well IFN-γ, TNFα and LG responses to optimal and suboptimal gB peptide stimulation. **C)** bars represent mean ± SEM

of total (IFN-γ/LG) responders or polyfunctional (IFN-γ/LG/TNF) responders. The total bar represents the frequency of cells responding to optimal gB peptide stimulation, while the bar in bar graph represents the frequency of high functional avidity cells responding to a sub-optimal gB peptide dose. **D)** bars represent the frequency of high functional avidity total (IFN-γ/LG) and polyfunctional (IFN-γ/LG/TNF) gB-CD8 responders in the TG and lungs. (***p<0.001, **p<0.01, * p<0.05) (n=8-10 mice/group).

4.6 TCR AFFINITY DOES NOT CORRELATE WITH FUNCTIONAL AVIDITY IN NON-HELPED GB-CD8

The reduced functionality of non-helped gB-CD8 in the TG at 35 dpi could be due to low TCR affinity or exposure to a variety of immunomodulatory signals *in vivo* (179,181,182). To differentiate these two types of influences, we employed a tetramer release assay to compare the TCR affinity of helped and non-helped gB-CD8 obtained from TG at 35 dpi. As illustrated in Figure 14, the non-helped gB-CD8 exhibited an average TCR affinity that was essentially identical to that of helped gB-CD8, suggesting that the reduced functionality of the non-helped gB-CD8 detected directly ex vivo resulted from *in vivo* exposure to immunoregulatory influences.

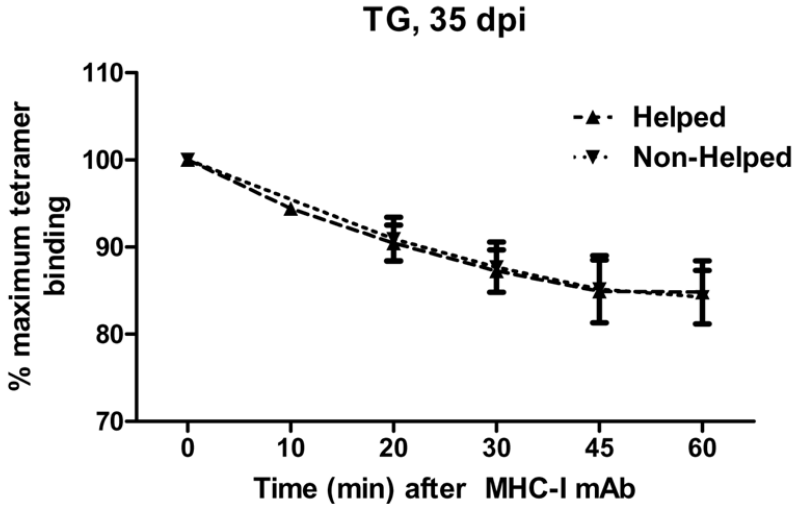

Figure 14 - TCR affinity does not correlate with functional compromise in non-helped memory.

TGs were harvested and dispersed at 35 dpi. TG suspensions were stained with $gB_{498-505}$ tetramer, and then incubated with anti-H-$2D^b/K^b$ antibody at 37°C for the designated times to observe tetramer dissociation. Cells were then stained with anti-CD8α and anti-CD45 mAb, and analyzed via flow cytometry. Data represent the mean fluorescence intensity (MFI) of $CD8^+$ $tetramer^+$ cells as a percentage ± SEM of the maximum MFI observed at time zero. (n=10 mice/group)

4.7 THE REDUCED FUNCTIONALITY OF NON-HELPED GB-CD8 IS ASSOCIATED WITH INCREASED PD-1 EXPRESSION.

We next determined if the functional compromise observed in non-helped gB-CD8 in TG between 8 and 35 dpi was associated with enhanced expression of the inhibitory receptor PD-1. At 8 dpi $PD\text{-}1^+$ expression was significantly elevated on non-helped gB-CD8 in both the DLN (Fig. 15A) and TG (Fig. 15B&C). Increased PD-1 expression was manifest as both an increased frequency and increased level (MFI) of PD-1 expression. The frequency of $PD\text{-}1^+$ non-helped

gB-CD8 gradually declined in the TG, but remained significantly elevated through 35 dpi. The increased PD-1 expression during this time was associated with reduced functionality (Fig. 13A, B). By 56 dpi, PD-1 expression on non-helped gB-CD8 in the TG was further reduced and no longer significantly different from that on helped gB-CD8; concurrent with complete functional recovery.

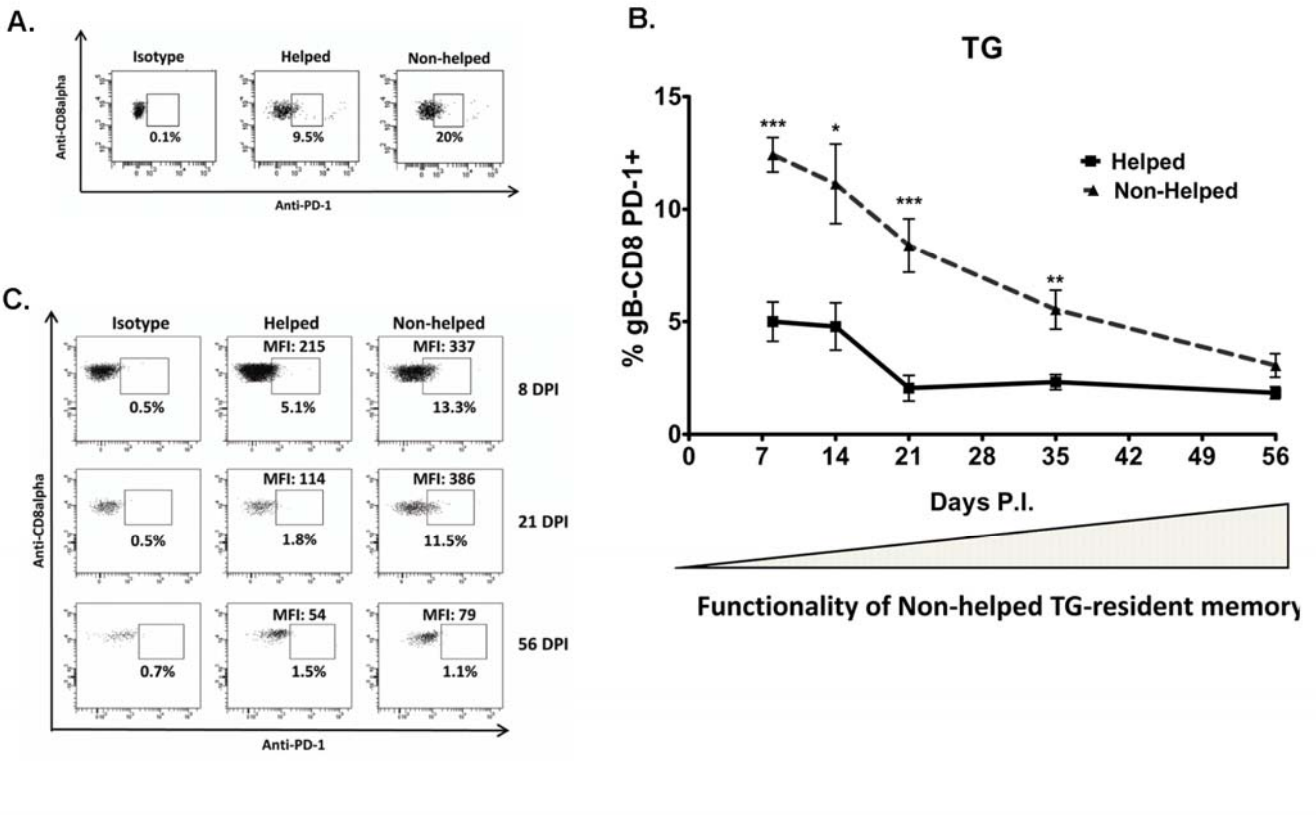

Figure 15 - The disregulated function of non-helped gB-CD8 is associated with increased PD-1 expression.

B6 mice that received HSV-1 corneal infections were not depleted or continuously depleted of $CD4^+$ T cells beginning 2 days before infection. DLN were excised at 8 dpi and TG were excised at the designated dpi, and dispersed cells were stained simultaneously with anti-CD8α, anti-CD45, anti-PD1, and $gB_{498\text{-}505}$ tetramer and analyzed via flow cytometry. Representative dot plots illustrate PD1 expression (based on isotype control) by **A**) non-CD4-depleted (helped) gB-CD8 in DLN at 8 dpi; and **B**) helped and CD4-depleted (non-helped) gB-CD8 in the TG at 8, 21, and 56 dpi. The mean fluorescence intensity (MFI) and frequency of the $PD1^+$ cells is indicated in each

plot **C)** symbols represent the mean ± SEM frequency of $PD1^+$ helped and non-helped gB-CD8 in the TG at the designated dpi. The wedge under the graph represents the corresponding change in functionality. *** $p<0.001$, **$p<0.01$ * $p<0.05$) (n=8-10 mice/group)

4.8 BLOCKADE OF PD-L1 RESTORES FUNCTION TO NON-HELPED GB-CD8 IN THE TG

Since transient functional dysregulation of non-helped gB-CD8 in TG was associated with elevated PD-1 expression, we predicted that blocking PD-1/PD-L1 interaction would restore normal function to these cells. TG were obtained from mice at 35 or 56 dpi following 2 weeks of systemic treatment with anti-PD-L1 or control mAb. At 35 dpi the non-helped gB-CD8 in the TG of mice that were treated with control mAb exhibited the anticipated reduction in the frequency of total gB-CD8 (Fig. 16A) and polyfunctional (Fig. 16C) capable of responding to gB peptide-pulsed targets. However, functionality was completely restored to the non-helped gB-CD8 following 2 weeks of anti-PD-L1 mAb treatment (Fig. 16A&C). In contrast, anti-PD-L1 treatment did not influence the function of helped gB-CD8 in TG at 35 dpi, or the function of helped or non-helped gB-CD8 in the TG at 56 dpi (Fig. 16B&D).

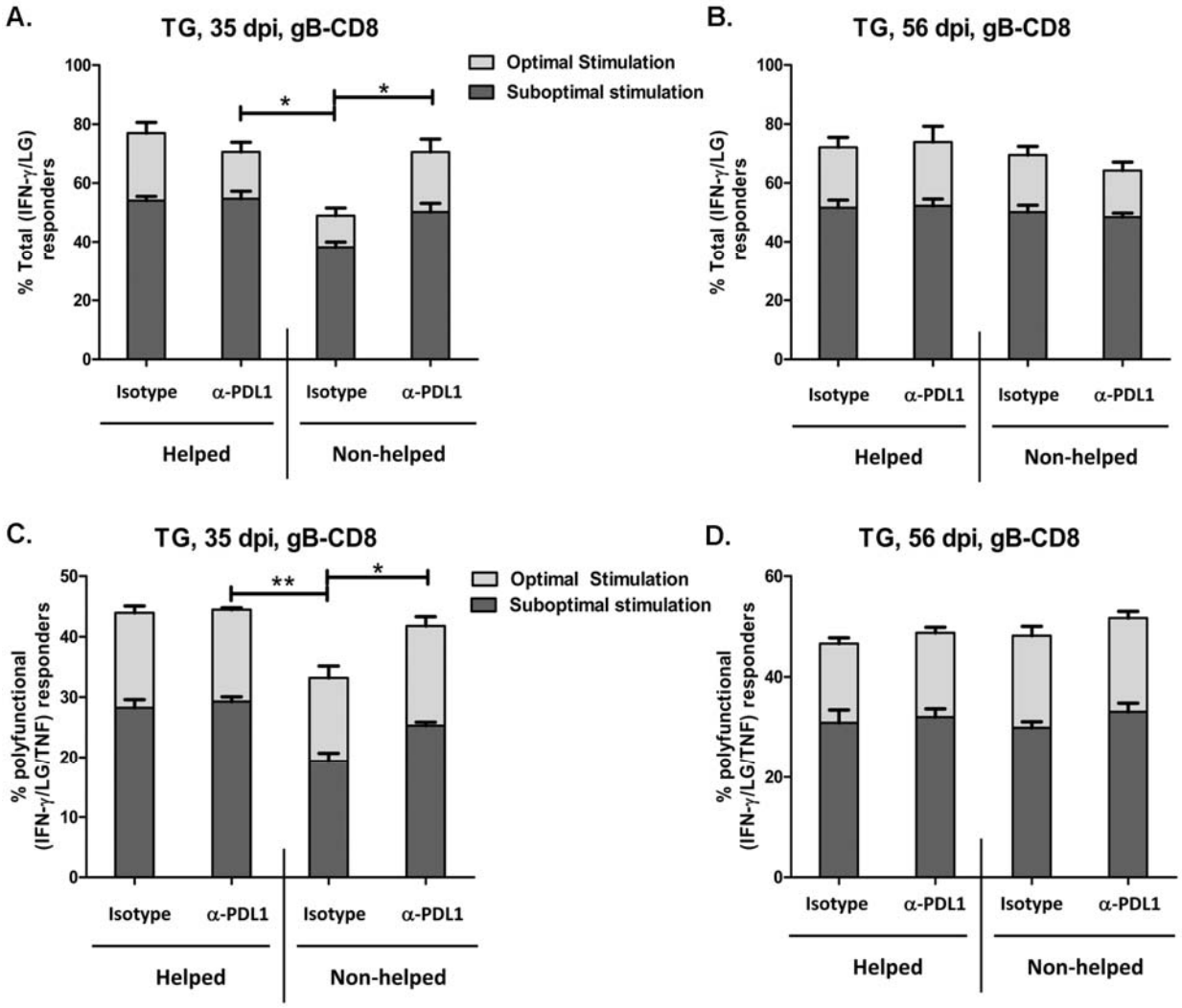

Figure 16 - Blockade of PD-1L restores function to non-helped gB-CD8 in the TG.

Untreated and CD4 ablated mice were treated via i.p. injection of 200ug of anti-PDL1 blocking or isotype control mAb for 2 weeks prior to **A,C)** 35 dpi, and **B,D)** 56 dpi. dispersed TG were stimulated with an optimal or suboptimal dose of gB peptide and IFN-γ and TNFα production and lytic granule (LG) release were quantified as in Fig. 2. Bars represent the mean ± SEM frequency of total (IFN-γ/LG) or polyfunctional (IFN-γ/LG/TNF) helped (from non-depleted mice) and non-helped (from CD4-depleted mice) gB-CD8 in control (isotype) and anti-PD-L1 (αPDL1)-treated mice. The total bar represents response to optimal antigen, while the bar in graph represents response to sub-optimal antigen. (** $p<0.01$, * $p<0.05$,) (n=10 mice/group).

4.9 DISCUSSION CHAPTER 4

The involvement of $CD4^+$ T cell help in $CD8^+$ T cell responses is complex and likely influenced by factors such as the nature of the immunogen, the activation status of APCs, and the microenvironment in which the effector and memory $CD8^+$ T cells reside. Here we employ a unique model system in which $CD8^+$ T cell priming occurs in the context of an acute HSV-1 infection, but the functional properties of the resulting HSV-specific $CD8^+$ T cell memory population can then be examined within disparate tissue microenvironments with or without persistent antigenic exposure (130). Moreover, in this model persistent low dose antigenic exposure in latently infected ganglia does not lead to $CD8^+$ T cell functional exhaustion as is seen with chronic viral infections that are characterized by extended exposure to high levels of viral antigens following initial infection. Indeed, in this model long-term functionality of the ganglionic gB-$CD8^+$ T cell population is required to maintain the virus in a latent state (29,114,180). We employ this model system to explore the influence of $CD4^+$ T cells on the gB-CD8 response.

We demonstrate that $CD4^+$ T cells influence the gB-CD8 response in two ways. First, the gB-CD8 effector population in the TG undergoes a more rapid contraction in the absence of $CD4^+$ T cells. This effect is exerted at the time of contraction as opposed to during the initial programming of the naïve gB-CD8, since contraction is accelerated when $CD4^+$ T cell ablation is initiated before infection or after the peak accumulation of effector gB-CD8 in the TG at 8 dpi. The mechanism by which $CD4^+$ T cells influence $CD8^+$ T cell contraction is currently unclear.

Accelerated contraction alone did not influence the functional characteristics, immunosurveillance capability, or size of the gB-CD8 memory pool established in the TG. Mice that were depleted of $CD4^+$ T cells beginning at 8 dpi showed an approximate 50% reduction in gB-CD8 at 14 dpi, but the capacity of the remaining $CD8^+$ T cells to maintain HSV-1 latency was not compromised as indicated by a similar latent HSV-1 genome copy number in TG. This is probably a reflection of the fact that the remaining gB-CD8 were functionally normal, and that at any given time only a small number of latently infected neurons appear to require $CD8^+$ T cell protection from reactivation (183). These findings do establish that $CD4^+$ T cells are not required for either the establishment or maintenance of HSV-1 latency in the TG following corneal infection.

Of greater consequence was the influence of $CD4^+$ T cells on the initial programming of gB-CD8. Depriving mice of $CD4^+$ T cell help during the initial programming and expansion phase of the $CD8^+$ T cell response to HSV-1 had no effect on the size of the gB-CD8 effector population in the TG at 8 dpi. This contrasts with findings from a flank HSV-1 infection model, where $CD4^+$ T cell deprivation resulted in reduced gB-CD8 effector expansion (184). Important differences in the two studies include the strain of HSV-1 used and the route of infection, both of which might influence the amount of $CD4^+$ T cell help required for the expansion of HSV-specific CD8 effector cells. We also saw no functional differences between the helped and non-helped gB-CD8 effector cells in the DLN at 8 dpi. However, the non-helped gB-CD8 did exhibit a progressive functional compromise following infiltration of the TG at 8 dpi through 35 dpi. The compromise was initially most pronounced among the high functional avidity polyfunctional (IFN-γ/LG/TNF) cells at 8 dpi, but progressive loss of the capacity to produce IFN-γ and release

lytic granules was observed at 14 and 35 dpi. The concurrent nature of the functional compromise in the non-helped gB-CD8 population in the TG and escape of HSV-1 from latency, as indicated by elevated HSV-1 genome copy number, underlines the importance of gB-CD8 functionality in maintaining HSV-1 in a latent state.

We previously demonstrated that gB-CD8 are maintained in the latently infected TG of IL-15 KO mice, but lost in their non-infected lungs (130). Those findings were consistent with the notion that exposure to viral antigens within the TG supplants the need for homeostatic signals in maintaining proliferation and survival of memory gB-CD8. Latently infected neurons express low levels of both MHC class I and viral proteins (106,114). Based on these observations, one might predict that high functional avidity gB-CD8$^+$ that are capable of detecting the low epitope densities likely present on latently infected neurons would be best suited to provide immunosurveillance and survive within latently infected ganglia. Our findings are consistent with this prediction since high functional avidity gB-CD8 are highly enriched in the latently infected TG, but not in the non-infected lungs, and transient compromise in the non-helped high functional avidity gB-CD8 was associated with failure to maintain HSV-1 latency. These findings are also consistent with the recent demonstration that CD8$^+$ T cells in latently infected TG represent a tissue-resident subpopulation of memory CD8$^+$ T cell that possess unique properties (185).

In a chronic LCMV infection model, intermediate levels of PD-1 expression on LCMV-specific CD8$^+$ T cells was associated with partial exhaustion that could be reversed by *in vivo* PD-L1 blockade (115). In our model, intermediate PD-1 expression (based on both frequency of positive cells and level of expression per cell) on non-helped gB-CD8 from 8-35 dpi was associated with partial functional exhaustion. This exhaustion was similar to that seen in the

LCMV infection model, with TNF-α being more severely affected before other effector mechanisms as exhaustion progressed (186). Moreover, *in vivo* blockade of PD-1/PD-L1 interaction effectively reversed the exhaustion in non-helped gB-CD8. This is in agreement with a recent study that observed that cells that were PD-1^{int} but not PD-1^{hi} were capable of functional recovery (187).

The source of PD-L1 that engages PD-1 on gB-CD8 in latently infected ganglia is not clear, but several observations point to latently infected neurons as likely candidates. First, it appears that PD-1 inhibits TCR signaling when the TCR and PD-1 ligands are expressed on the same cell (188). Second, extended PD-1/PD-L1 exposure is required for $CD8^+$ T cell functional exhaustion and gB-CD8 closely associate and form immunologic synapses with latently infected neurons (106,114,115). Finally we have observed PD-L1 expression on neurons in latently infected TG (our unpublished observation).

This of course, begs the question of why non-helped gB-CD8 express higher levels of PD-1 than their CD4-helped counterparts. We cannot formally rule out the possibility that non-helped gB-CD8 up-regulate PD-1 expression due to encounter with higher levels of viral antigen in the DLN or TG. However, we consider this unlikely because CD4-sufficient and CD4-deficient mice eliminate replicating virus from the cornea and TG with similar kinetics and establish latency with a similar load of viral DNA at 8 dpi. Instead we favor the hypothesis that the threshold level of TCR signaling required for PD-1 expression is set at a lower level when gB-CD8 are programmed in the absence of $CD4^+$ T cell help. The threshold level of TCR signaling required to induce PD-1 expression might then be met by non-helped, but not helped gB-$CD8^+$ T through encounter with antigen. Of interest is how the non-helped gB-CD8 pool still retained functionality despite elevated PD-1 expression within the DLN at 8 DPI. We

hypothesize concordant expression of costimulatory molecules with PD-L1 on APCs within the DLN may slow or prevent the onset of exhaustion. As these cells enter the TG and undergo prolonged interactions with neurons, they undergo progressive functional exhaustion. Elucidating the mechanism(s) leading to reduced PD-1 expression and functional recovery of non-helped gB-CD8 in HSV-1 latently infected TG between 35 and 56 dpi will require further study.

Several recent reports emphasize the importance of $CD8^+$ T cells in maintaining HSV-1 in a latent state within the TG. Effective immunosurveillance of latently infected neurons requires $CD8^+$ T cells with the capacity to respond to low levels of viral epitopes that likely exist on infected neurons. Our current findings demonstrate that $CD4^+$ T cell help during initial programming is important in generating a memory $CD8^+$ T cell population with sufficient sensitivity to provide this surveillance. Since HSV-1 reactivation from latency is the primary cause of recurrent herpetic disease, any vaccine designed to prevent reactivation will need to incorporate both CD4 and CD8 epitopes.

5.0 THE ROLE OF HSV-1 SPECIFIC CELLS IN HERPES STROMAL KERATITIS

While $CD4^+$ T cells have been implicated in orchestrating HSK, it remains highly contentious exactly how these cells mediate this inflammatory disease. Much debated exists on whether HSV-1 specificity is necessary for HSK pathogenesis to occur. We have isolated and cloned HSV-1 specific $CD4^+$ T cells from HSK inflamed corneas in BALB/C mice. We characterized these clones and identified what HSV-1 protein they recognize, and used adoptive transfer models to test that hypothesis that these cells can initiate HSK in host mice.

5.1 HSV-1 SPECIFIC CD4$^+$ T CELLS ARE PRESENT WITHIN THE INFECTED CORNEA

Previous research by Lepisto et al (unpublished) isolated HSV-1 specific CD4$^+$ T cells from HSK inflamed corneas. These corneas were cultured for several weeks to generate a cell line, which was then cloned. Initial characterizations identified these cell lines were HSV-1 reactive by IFN-γ production (Figure 17). This reactivity clearly establishes the presence of HSV-1 specific CD4$^+$ T cells cornea at the time of HSK progression.

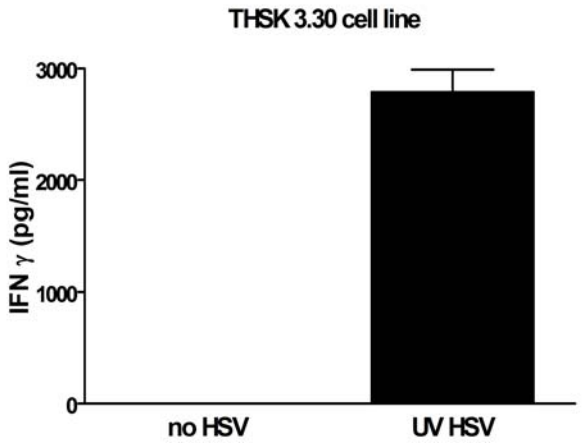

Figure 17 – HSV-1 specific cells isolated from HSK inflamed cornea are reactive to HSV-1

BALB/c mice were infected with 10^5 PFU of HSV-1 RE. CD4$^+$ T cells were purified from corneas of mice with HSK at D$^+$11 P.I. (as described in the Material and Methods) and were cultured until a stable cell line was established. This cell line was stimulated with UV-inactivated HSV pulsed DC (UV HSV) or unpulsed DC (no HSV) for 72 hrs and supernatants were collected and assayed for IFN-y by standard ELISA. Data represented as mean ± SEM pg/mL IFN-γ, data from 2 replicate experiments.

5.2 HSV-1 SPECIFIC CLONES RESPOND DIFFERENTIALLY TO HSV-1

This isolated cell line was cloned by limiting dilution and the isolated clones were tested for their HSV-1 reactivity. When stimulated with HSV-1 antigen loaded APCs, these clones responded differentially as measured by the output of IFN-γ. All clones appeared to be specific for HSV-1, but certain clones exhibited to lower reactivity via IFN-γ when compared to others. This is similar to observations in the clinic, where differential HSV-1 reactivity via cytokine production is observed from $CD4^+$ T cells isolated from the HSK inflamed cornea. (149,155,189).

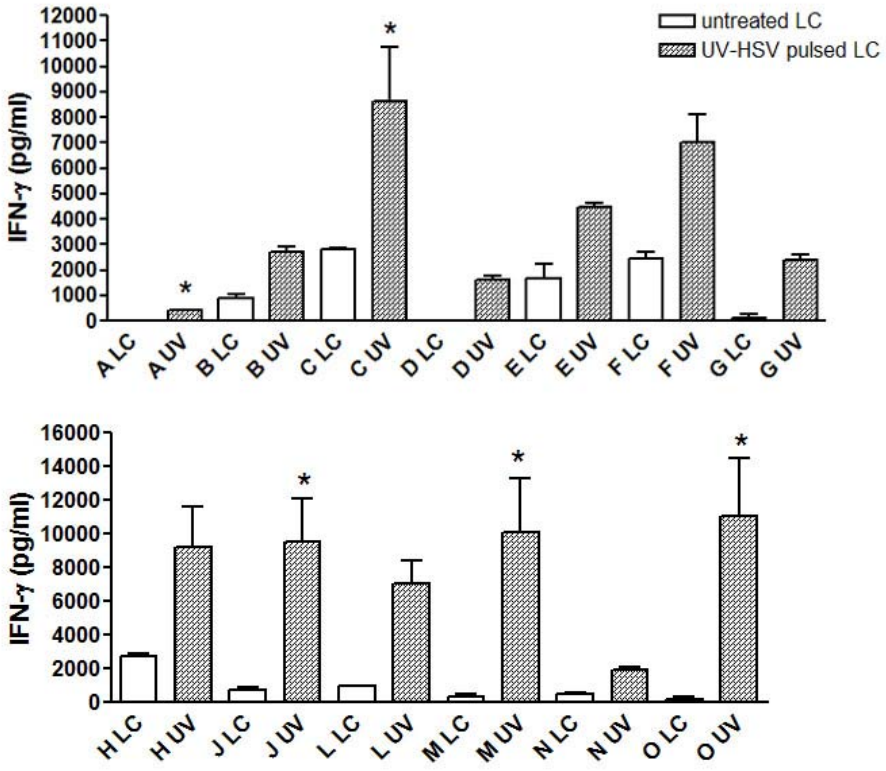

Figure 18 – Clones respond differentially to HSV-1 with IFN-γ

A cross section of clones (A-O) were stimulated with UV inactivated HSV pulsed APCs or unpulsed controls for 72 hours. Cells were stimulated at a 1:5 effector to target ratio. Supernatants were collected and assayed for IFN-γ by standard ELISA. Data represented as mean ± SEM pg/mL IFN-γ. (* $p<0.05$,). Data from 2 replicate experiments.

5.3 THE HSV-1 SPECIFIC CLONES ARE ALL SPECIFIC FOR GLYCOPROTEIN B OF HSV-1

Next we endeavored to identify the specific HSV-1 antigens that were recognized. We tested a cross section of these clones (both high and low IFN-γ reactive clones) with APCs loaded with the lysate of 293 T cells transfected with full length glycoprotein B, D, F, and G. Surprisingly, all clones assayed responded to APCs loaded glycoprotein B with levels similar to that of HSV-1 antigen loaded APCs (Figure 19), providing strong evidence that the HSV-1 component recognized by these clones was located on glycoprotein B.

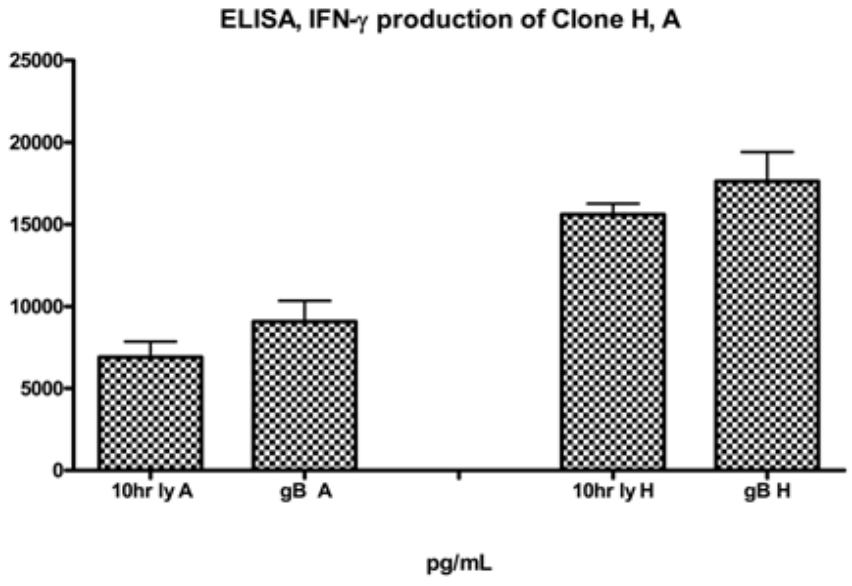

Figure 19 – HSV-1 specific clones are all specific for HSV-1 glycoprotein B.

Representative ELISA data from a "high reactive" and "low reactive" HSV-specific clones. Cells were stimulated with UV inactivated HSV pulsed APCs or APCs pulsed with gB-transfected 293 T cell lysate for 72 hours. Supernatants were collected and assayed for IFN-γ by standard ELISA. Data represented as mean ± SEM pg/mL IFN-γ. Data indicative of two independent experiments.

5.4 HSV-1 CLONES ARE OF A TH1 OR TH17 PHENOTYPE

Further characterization was performed on these clones to identify mechanisms behind the differential response of IFN-γ to gB. We hypothesized that the low IFN-γ reactive cells may be of a different helper subset than the high IFN-γ producers. A number of immunopathologies have recently identified a TH17 $CD4^+$ T cell component, such as rheumatoid arthritis, colitis, and experimental autoimmune encephalomyelitis (190,191). A study looking at human corneal fibroblasts in culture observed that IL-17 can induce heavy production of granulocyte macrophage colony-stimulating factor (GMCS-F), a potent chemoattractant for PMN neutrophils (192). This leads us to hypothesize that these low IFN-γ reactive cells may be TH17 cells. When high and low IFN-γ reactive cells were stimulated with HSV-1 antigen, and their supernatants were analyzed by luminex bead analysis, we observed that the low IFN-γ reactive cells did, in fact, produce IL-17 in response to HSV-1 (Figure 20). This strongly suggests that both TH1 and TH17 HSV-1 specific $CD4^+$ T cell subsets are present within the cornea at the time of HSK, raising the possibility that there is in fact an IL-17 driven component to HSK progression.

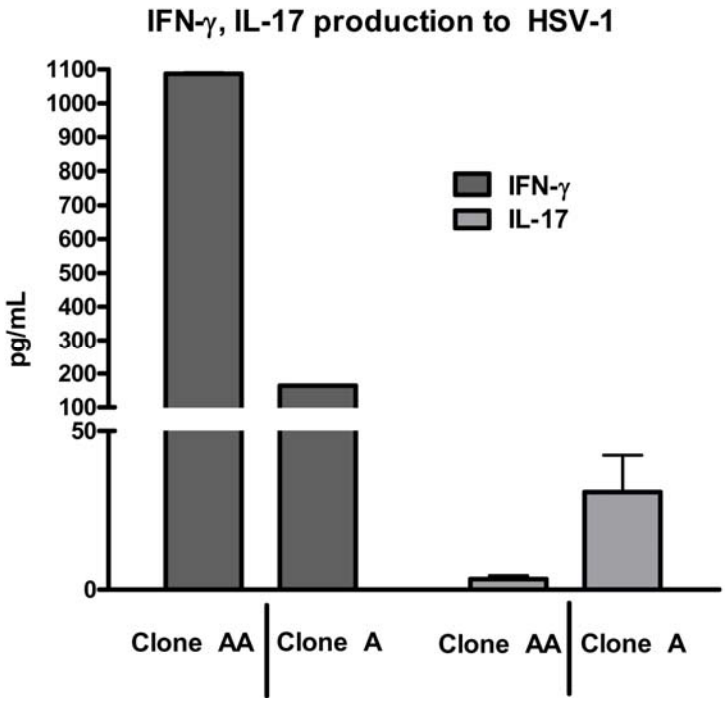

Figure 20 – HSV-1 clones respond to HSV-1 with either a T-helper 1 or 17 cytokine phenotype

Luninex bead analysis of HSV-1 stimulated high and low IFN-γ reactive cells. Cells were stimulated with UV inactivated HSV pulsed APCs for 72 hours. Supernatants were collected and assayed for IFN-γ and IL-17 via luminex cytokine bead array. Data represented as mean ± SEM pg/mL IFN-γ or IL-17. N=2 independent stimulations per group.

5.5 CD4 HSV-SPECIFIC CLONES ARE UNABLE TO ENTER THE INFLAMMED CORNEA

Armed with our identification of IFN-γ and IL-17 producing clones, we moved to *in vivo* studies utilizing adoptive transfer of clones into host mice. We initially used T cell-deficient hosts as hosts for the adoptive transfer of our clones. We hypothesized that both IFN-γ and IL-17

producing clones are needed to initiate productive HSK. Following an established method of transfer for $CD4^+$ T cells in the context of HSK, we adoptively transferred a TH1 and/or TH17 clone into severe combined immunodeficiency (SCID) mice (151). Surprisingly, we did not see any HSK develop in our host mice, regardless of whether they got either a TH1 (Clone AA), TH17 (Clone A), or both clones; mice receiving $CD4^+$ T cells from the draining lymph nodes of an acutely infected WT mouse did develop HSK normally (Figure 21). SCID mice receiving clones also did not control viral skin disease effectively, impeding HSK severity evaluations.

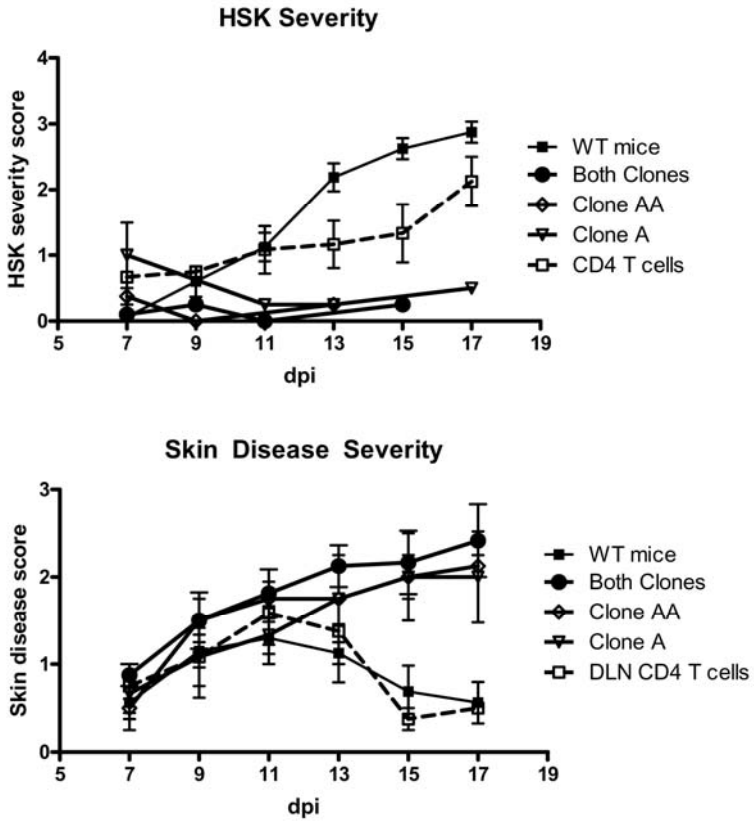

Figure 21 – SCID mice receiving HSV-1 Clones do not develop HSK or control skin disease

SCID mice hosts received $5x10^6$ clones A or AA, or $2.5x10^6$ of both clones at 2 dpi via i.v. injection. T cell clones were activated via CD3/CD28 prior to transfer. A control group of mice received $5x10^6$ MACS purified $CD4^+$ T cells from 7 dpi DLN from a WT BALB/c donor. All mice received regular 4mg/mL ACV in drinking water to control viral replication starting at 7 dpi. HSK and skin disease were evaluated every 2 days from 7 to 17 dpi (n=8 mice/group).

Further analysis of these mice via flow cytometry revealed that no $CD4^+$ T cell clones infiltrated the infected cornea (Figure 22A). Examination of the spleens of these mice revealed a small population of these clones did take up residence, implying that these clones survive within the host following adoptive transfer (Figure 22B). We also looked within the TG, and saw little, if any infiltration of our clones (data not shown), suggesting that these cells were impaired in infiltrating into the TG and cornea. This raises a major concern that these clones may not be functionally capable of acting as a model effector cell when transferred into a host mouse.

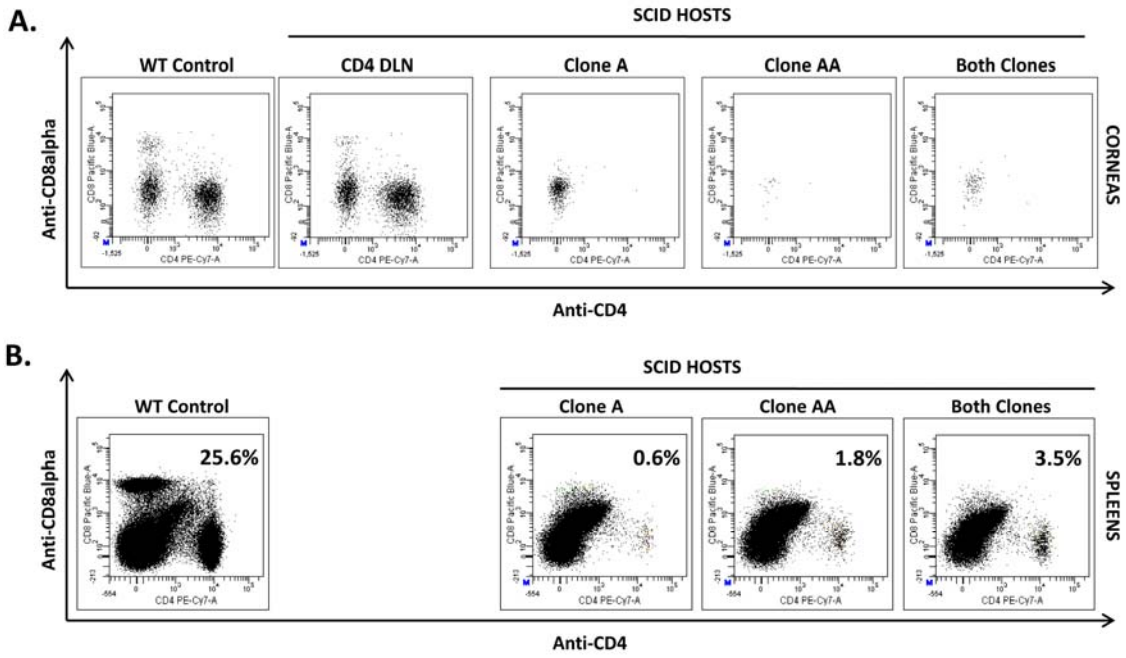

Figure 22 – HSV-1 Clones survive adoptive transfer into SCID hosts, but do not enter the infected cornea

SCID mice hosts received $5x10^6$ clones A or AA, or $2.5x10^6$ of both clones at 2 dpi via i.v. injection. T cell clones were activated via CD3/CD28 prior to transfer. A control group of mice received $5x10^6$ MACS purified $CD4^+$ T cells from 7 dpi DLN from a WT BALB/c donor. At 17 dpi, corneas and spleens were dispersed into single cell suspension and stained with antibodies for CD4, CD8α and CD45. Representative flow plots of **A)** Corneas and **B)** spleens are shown gated on $CD45^+$ cells. (total data n=4-6 mice/group)

A number of different approaches were attempted with our adoptive transfer model in hopes of observing more effective peripheral migration of clones *in vivo*: method of activation the clones, time of transfer after or before infection, and host mouse strain ($CD4^{-/-}$, RAG, and SCID models) (Data not shown). No approaches resulted in these HSV-1 specific $CD4^+$ T cell clones entering the infected cornea. With this alarming observation considered, we moved on to an adoptive transfer method where we could track infiltration of our cells with a high resolution within an immunologically intact animal.

We repeated our adoptive transfer approach of our clones into Thy 1.1 hosts, which have a small congenic change to the Thy 1 receptor. Thy 1.2 is expressed on the HSV-1 specific clones, which allows us to track these cells via antibodies to Thy 1.2 and 1.1. As seen in Figure 23A, we could track these cells effectively within the blood of these mice at various points following infection; donor clones remained stable at 4% frequency in the blood from 11-15 dpi, before doubling in frequency to 10% of all $CD4^+$ T cells within the blood at 21 dpi. When we looked within the cornea, we observed a low level of infiltration of our clones (Figure 23B). At the later stages when HSK has progressed to severe disease (15 and 21 dpi), our clones make up 1% of the infiltrating $CD4^+$ T cells. This is 4 fold and 10 fold lower than the frequency within the blood at 15 and 21 dpi, respectively. Given that all of these cells are HSV-1 specific, we anticipated enrichment in frequency as these cells infiltrate the cornea, not a sharp decline. Lepisto et al has observed that the frequency of HSV-1 reactive $CD4^+$ T cells within the cornea at 17 dpi is ~20% (193). The clones were significantly lower than the normal frequency of HSV-1 reactive cells infiltrating into the infected cornea. Given that we and others are able to see robust of WT $CD4^+$ T cells into the cornea following adoptive transfer, this deficiency appears to be restricted to our $CD4^+$ T cell clones. (Figure 22)

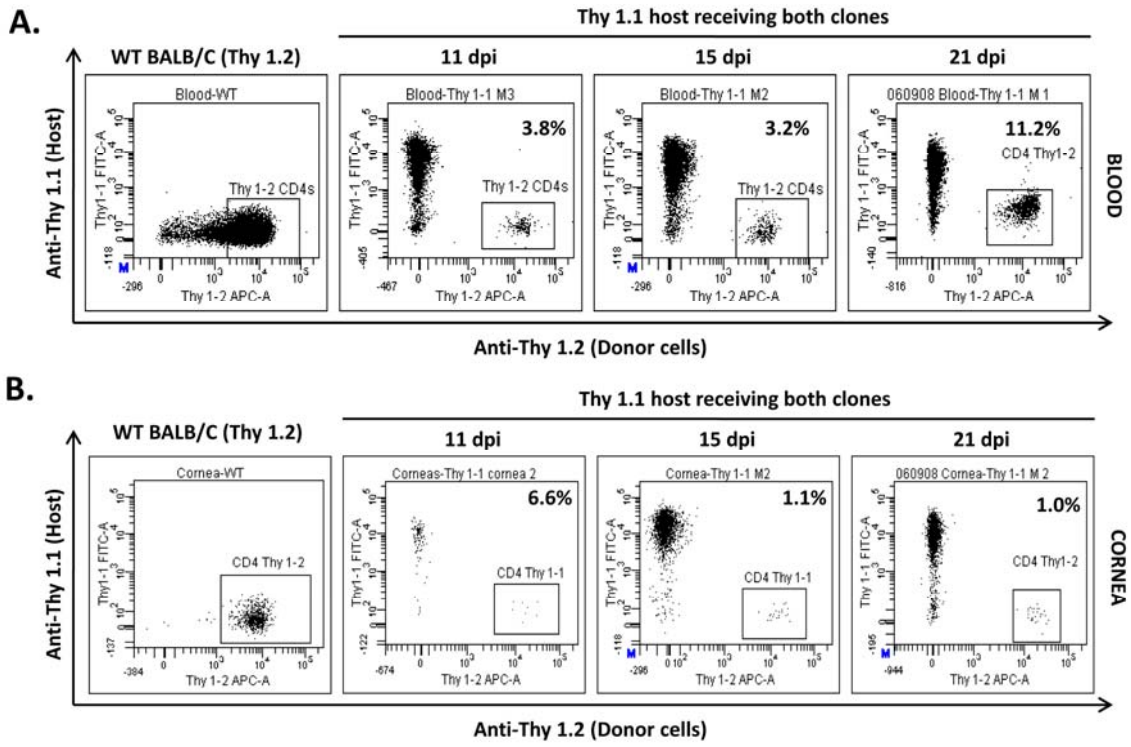

Figure 23 – HSV-1 CD4$^+$ T cell clones are impaired in entry into the cornea in immunocompetent hosts

Thy 1.1 mice hosts received 2.5x10^6 of Clone A and AA at 2 dpi via i.v. injection. T cell clones were activated via CD3/CD28 prior to transfer. At 11, 15, and 21 dpi, blood and corneas were harvested for flow cytometric analysis and stained with antibodies for CD4, CD45, Thy 1.1, and Thy 1.2. Representative flow plots of **A)** the blood and **B)** blood are shown gated on CD45$^+$ cells. (n=6-8 mice/group)

5.6 HSV-1 SPECIFIC CD4$^+$ T CELL CLONES CONSTITUTIVELY EXPRESS CD43 AND ARE IMPAIRED IN VLA-4 EXPRESSION

We further examined our clones phenotypically for potential mechanisms as to why these clones have impaired infiltration into the cornea. When resting and activated clones are phenotypically characterized, we do observe a number of stark differences in the expression of activation and

adhesion molecules to what is normally expressed on naïve and effector $CD4^+$ T cells *in vivo*. When we examine our clones under resting conditions, we found that they constitutively express the activated isoform of CD43, a T cell activation marker normally expressed on effector T cells (Figure 25A) (194). We also checked two of the primary adhesion molecules that effector T cells require to efficiently enter peripheral sites of infection, LFA-1 (CD11a), and VLA-4 (CD49D) (195-197). As depicted in Figure 25B, we establish that activated clones (as defined by CD69 expression; data not shown) do express LFA-1 (100%), but do not upregulate VLA-4 effectively (Clone A 12%, Clone AA 19%).

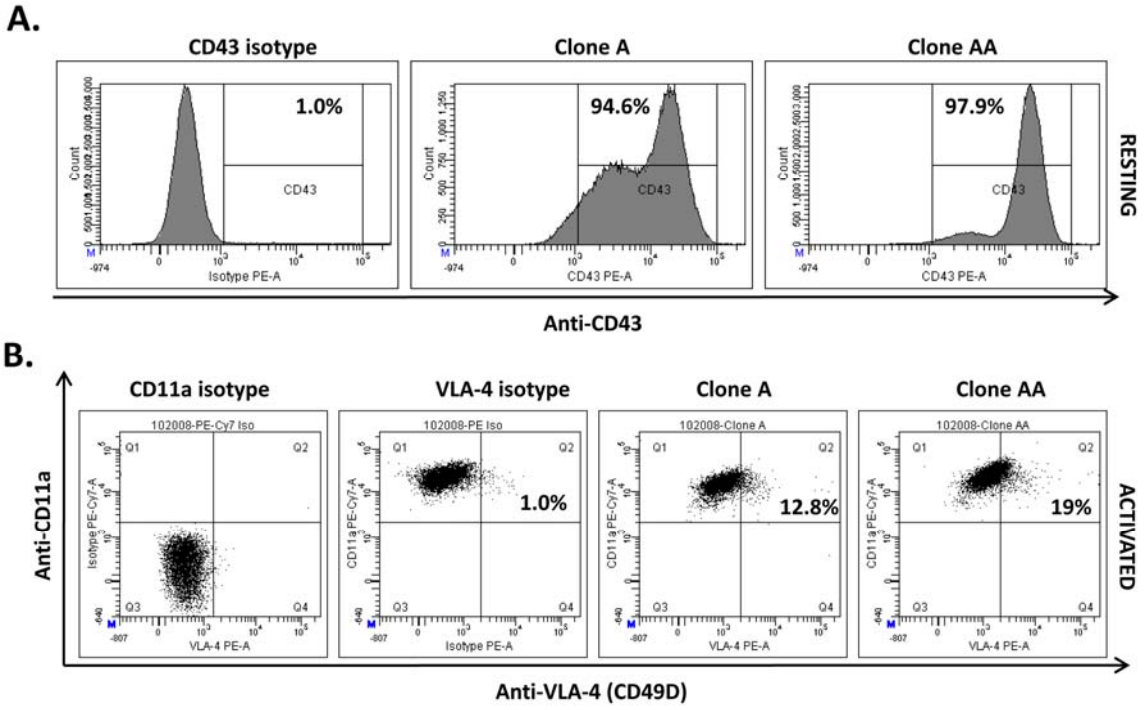

Figure 24 – Clones have dysregulated CD43 expression and fail to upregulate VLA-4 when activated.

Clones under resting conditions or stimulated with anti-CD3/CD28 for 24 hours were analyzed via flow cytometry. Cells were stained with CD4, CD43, VLA-4, and CD11a. Representative flow plots depicting **A**) CD43 expression on resting clone A and AA, and **B)** CD11a and VLA-4 co-expression on activated Clones. (total data is indicative of 3 replicate experiments)

These observations lead us to conclude that these T cell clones have too many phenotypic differences from that of an effector cell *in vivo.* This renders it difficult to accurately test the hypothesis that HSV-1 specific cells are necessary for the HSK development. Efforts were taken early in these studies towards the generation of a $CD4^+$ T cell TCR transgenic mouse. At the time of this dissertation, pups have been successfully generated for both the alpha and beta TCR chains.

A few key observations from the development of the TCR transgenic mouse need to be mentioned here in order to properly discuss the findings presented by this study. Corroborating early phenotypic analysis of the clones, we observed all cells have the identical V-beta TCR chain by sequencing. Surprisingly we also found that the cells have identical TCR V-alpha chains and the variable regions of both TCR chains of the cell line and clones were identical by sequencing. This piece of evidence demonstrates the T cell line is a homogeneous population of cells, and suggests other factors may control why certain clones exhibit a TH1 or a TH17 phenotype.

5.7 DISCUSSION – CHAPTER 5

The mechanism by which $CD4^+$ T cells initiate the complex cascade of events that leads to HSK remains contentious after years of concentrated study. Here we find that HSV-1 specific T cells can be isolated from the cornea during the initial stages of HSK progression. This corroborates with a previous study identifying HSV-specific $CD4^+$ T cells within the cornea both during HSK progression and during its chronic phase (193). A number of clinical studies have also observed

HSV-specific cells isolated from the corneal buttons from patients with necrotizing keratitis (149,155,198). Furthermore, we find that all of our clones are specific for glycoprotein B. This bares startling (though probably coincidental) similarity to the B6 model of infection, where the $CD8^+$ T cell immunodominant epitope is also directed at gB (105). The only other group of studies attempting to identify $CD4^+$ T cell viral specifities have also observed that a "late" viral protein glycoprotein D was recognized (199,200).

The observation the T cell clones were specific for gB was a surprising observation. Furthermore the T cell line these clones were derived from responds equally as well to gB as it does to HSV-1, strongly suggesting that all cells within the T cell respond to the same antigen. When sequencing of the TCR of the clones and their parent cell line was undertaken, all cells had the identical alpha chain (Vα8.2) and beta chain (Vβ8.3), including all hyper variable regions. This is indicative that the T cell line at the time of cloning was a single population of cells, based on their TCR. There a number of possibilities to account for this observation. Firstly, the selective pressures during the cell line passaging may have driven the outgrowth of a diverse repertoire of T cells within the cell line to a single specificity over time. Another alternative could be the cells specific for HSV-1 at the time of harvest for may have been all of one clone and specificity. While unlikely, it possible that an immunodominant epitope to HSV-1 is recognized early, thus driving a homogenous response of HSV-specific T cells into the cornea early; it is likely that if this is the case, the repertoire of T cells recognizing HSV-1 antigens would expand as HSK progression continues.

Previous work has observed that these clones direct a differential response (via IFN-γ) to HSV-1 antigens, and here we have continued these studies by identifying some clones produce IL-17, fitting a TH17 phenotype, while others produce IFN-γ, matching up with that of a TH1

phenotype. This observation has some profound implications, given that the cells all recognize glycoprotein B and the TCR of these cells is identical. It raises the question of how, when, and where did these cells diverged functionally. One possibility is this is an artifact of the T cell line growth and passaging; this appears unlikely, as the cells were passaged by CD3/CD28 stimulation, which has no precedence in the literature for causing divergence of a T cell helper phenotype. The second possibility remains that this change in effector subset machinery occurred *in vivo*, either in the draining lymph nodes during priming or following the entry of these cells into the cornea. There have been observations that the dogmatic mantra of "commitment to functional subset" may be more dynamic than previously understood. A handful of studies looking at natural T-regs have observed a loss of FoxP3 expression and a shift towards a classical memory T cell phenotype and functionality, notably the ability to produce IFN-γ (201-203). A study from the clinic found T-regs that had lower levels of FoxP3 could revert to a TH17 phenotype in patients suffering from a flare of systemic lupus erythematosus (204). Another study reported that RORγT, previously established as a "defining" transcription factor for TH17 cells is also found in $FoxP3^+$ T-cells, and that T-regs are capable of shifting to a TH17 phenotype when levels of TGF-β decline locally (205). One group also observed an identified T cell subset isolated from the draining lymph nodes can produce IFN-γ, but when isolated from the gut parenchyma produces IL-17 (202). Taken together, it appears that based on local microenvironmental factors, the once thought stable T helper subsets may be capable of changing based on the milieu of signals around them.

When one studies the cornea, we find that it is characterized by high levels of TGF-β under steady state conditions (43-46). It is thought the high levels of this immunomodulatory cytokine help maintain immune privilege within the cornea. As HSK development begins, large

numbers of cytokines are present within the cornea, most notably IL-6 (206,207). This provides a potential shift in the microenvironment towards concentrated local amounts of IL-6 and TGF-β in the cornea at the onset of HSK. It is within the realm of possibility that clonally expanding $CD4^+$ T cells can shift from either a T-regulatory or TH1 phenotype to that of a TH17 phenotype as they persist within the cornea. As new cells infiltrate into the cornea they would still retain their initial phenotype for a short period of time. This could explain why a mix of cells with identical TCR could have diverged to both a TH17 and TH1 phenotype. We will have to await the generation of the transgenic TCR mouse in order to properly address this hypothesis.

We identified these cells are functionally impaired in their ability to enter the cornea and ganglion after infection, a trait not shared by isolated $CD4^+$ T cells from a host animal. We found that these cells have dysregulated expression of the activated isoform of CD43, and also failed to upregulate VLA-4 when stimulated. These findings are instructive to why these cells fail to behave as an effector T cell would *in vivo*. CD43 has been implicated in negatively regulating T cell activation and also in negatively controlling T cell migration, especially into immune privileged sites such as the CNS (194,208). One potential mechanism for this regulation of migration is an observation that galectin-CD43 interactions can cause T cell death (209). Furthermore, galectin expression has been reported within the cornea (210). It possible that these clones, upon entry within the cornea, retain high levels of CD43 and may undergo preferential cell death from prolonged galectin-CD43 interactions. The more likely explanation for this low level infiltration into the cornea by the T cell clones is due to their lack of VLA-4. A recent study singled out VLA-4 as being the most important adhesion molecule for effector $CD4^+$ T cell infiltration into the infected cornea (211). As these cells lack expression of VLA-4

and also could be induced to undergo cell death if they gain entry to the cornea, it is not surprising we see poor infiltration of our cells into the infected cornea.

While we have identified many key phenotypic and functional characteristics of the HSV-specific T cell clones, we still were unable to adequately address the overarching hypothesis of this aim: to test if HSV-1 specific cells are necessary for HSK. However, we have found that these cells are a mix of both TH1 and TH17 subsets, and have identical TCRs, suggesting that the microenvironment of the cornea may be altering T helper subset machinery as HSK begins. This raises the possibility that HSV-1 specific TH17 cells may trigger the early events in HSK, being driven from either a TH1 or even T-reg phenotype by the unique microenvironment of the cornea. As TH1 cytokines have been identified to be important in HSK, it is likely that TH1 T cells as well as bystander activated cells continue mediating the ongoing inflammation initiated by TH17 cells (Figure 25). Unfortunately, the TCR transgenic mouse under development will be needed to properly address these newly generated hypotheses.

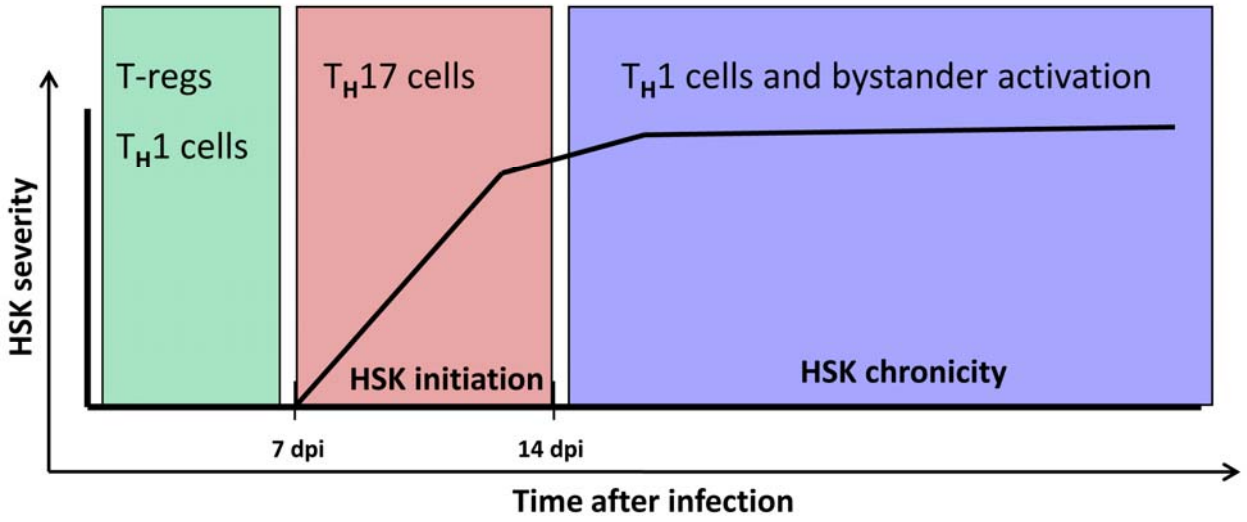

Figure 25 – Model for T helper subsets and their contribution to herpes stromal keratitis

We propose that either resident T-regs or TH1 $CD4^+$ T cells may be shifting towards an IL-17 phenotype early in HSK development, providing the needed inflammatory signals to ramp up t pathogenesis of keratitis. Once high levels of inflammatory mediators are established, TH1 HSV-1 specific $CD4^+$ T cells and as time goes on, bystander activated cells, contribute to the chronicity of disease.

6.0 THE ROLE IL-12 SUBUNITS IN HERPES STROMAL K ERATITIS

Interleukin (IL)-12p40 can couple with IL-12p35 or p19 chains to form the molecules IL-12p70 and IL-23, respectively that promote TH1 cytokine responses. IL-12p35 can bind to EBI3 to form an anti-inflammatory molecule IL-p35, but a proinflammatory function of IL-12p35 independent of IL-12p40 has not been described. IL-12 has been previous implicated in the progression of herpes stromal keratitis. Here we observed the roles of IL-12p35 and IL-12p40 in a mouse model of HSK.

6.1 MICE LACKING THE IL-12P35 SUBUNIT DEVELOP TRANSIENT HSK

The corneas of IL-12p35$^{-/-}$, IL-12p40$^{-/-}$, IL-12p35$^{-/-}$p40$^{-/-}$ (double knockout), and WT mice were infected with HSV-1. All four strains of mice developed moderate to severe HSK marked by increasing corneal opacity and peripheral neovascularization by 15 dpi (Fig. 1). HSK severity progressed steadily through 21 dpi in both WT and IL-12p40$^{-/-}$ mice with complete opacity, expanded neovascularization encroaching from the periphery into the central cornea, and corneal edema. In contrast, HSK severity began to regress by 15 dpi and 11 dpi in IL-12p35$^{-/-}$ mice and IL-12p35$^{-/-}$p40$^{-/-}$ mice, respectively. Disease regression in both groups of IL-12p35 deficient mice was marked by rapidly decreased peripheral opacity with thinning of peripheral vasculature and a more gradual decrease in central opacity.

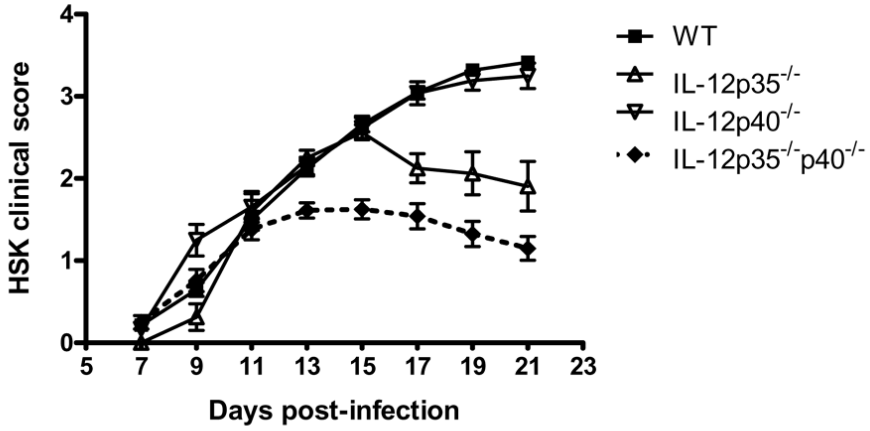

Figure 26 – Mice lacking IL-12 develop HSK

IL-12p35$^{-/-}$, IL-12p40$^{-/-}$, IL-12p35$^{-/-}$p40$^{-/-}$ (double knockout), and WT mice infected with HSV-1 RE were scored for HSK by slit-lamp examination from 7 – 21 dpi. Data shown reflect n values of at least 5 mice per group and are representative of 2 or more independent experiments.

6.2 CORNEAL INFLAMMATORY INFILTRATE OF MICE LACKING IL-12P35

Early in HSK development (13 dpi) the infected corneas of WT, IL-12p35$^{-/-}$, IL-12p40$^{-/-}$, and IL-12p35$^{-/-}$p40$^{-/-}$ mice showed comparable infiltrates of CD4^{+} T cells and Gr1^{bright} neutrophils (Fig. 2A), which comprised the majority of the bone marrow-derived CD45^{+} cells in the cornea (data not shown). At 17 dpi, IL-12p35$^{-/-}$p40$^{-/-}$ mice exhibited a significant reduction in neutrophilic infiltrate and a reduction in the mean number of CD4^{+} T cells in the cornea that did not achieve statistical significance (Fig. 2B). The composition of the corneal infiltrate in the p35$^{-/-}$ and p40$^{-/-}$ mice at 17 dpi was not significantly different than that of WT mice. At the peak of HSK severity (21 dpi), both IL-12p35$^{-/-}$ and IL-12p35$^{-/-}$p40$^{-/-}$ mice showed significantly reduced numbers of

$CD4^+$ T cells and neutrophils within their corneal infiltrates relative to WT mice (Fig. 2C). In both IL-12p35$^{-/-}$ and IL-12p35$^{-/-}$p40$^{-/-}$ mice reduction in clinical HSK severity preceded changes in the composition of the inflammatory infiltrate in the cornea by approximately 2 days. The p40$^{-/-}$ mice had a significantly higher $CD4^+$ T cell and neutrophilic corneal infiltrate than WT mice at 21 dpi, though this did not translate into a higher clinical HSK score (Fig. 1).

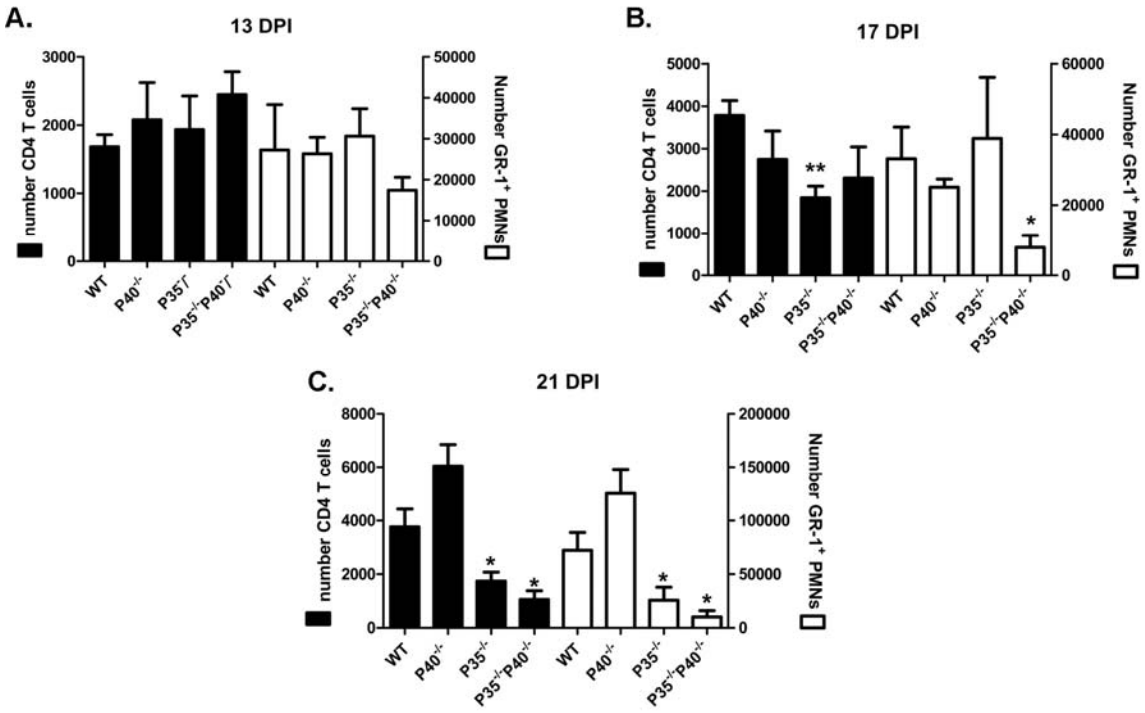

Figure 27 - Mice lacking IL-12p35 have a reduced corneal leukocytic infiltrate

At 13, 17, and 21 dpi, corneas were dispersed into single cell suspensions and stained with anti-CD45, CD4, and Gr-1 mAb. Cell suspensions were analyzed by flow cytometry. Data are represented as mean ± SEM number of $CD4^+$ T cells (Left axis), and GR-1^{bright} neutrophils (Right axis). Data reflect the average of 2 independent experiments with n values of at least 4 corneas per group. (* $p < .05$; ** $p < .01$.)

We hypothesized that the HSK regression would be associated with an increased frequency of $CD4^+$ $CD25^+$ $FoxP3^+$ Tregs in the corneas of p35 deficient mice. In fact, the $CD4^+$ T cell

population in the corneas of IL-12p35$^{-/-}$ mice did show an increased frequency of CD25^{+} FoxP3^{+} cells during HSK regression at17 dpi (Fig. 3). However, an increased frequency of Tregs was not observed in the IL-12p35$^{-/-}$p40$^{-/-}$ mice despite more rapid HSK regression (Fig. 3).

6.3 NATURAL TREGS DO NOT ACCOUNT FOR HSK REGRESSION IN IL-12P35$^{-/-}$ MICE

To determine if the increased frequency of CD4^{+} CD25^{+} FoxP3^{+} cells in infected corneas of 12p35$^{-/-}$ mice was responsible for HSK regression, we determined if in vivo depletion of CD25^{+} cells prior to HSV-1 corneal infection would alter the course of HSK in these mice. A single treatment with 100 µg of anti-CD25 mAb or control mAb 3 days before HSV-1 corneal infection, effectively depleted CD25^{+} Foxp3^{+} cells from corneas through 21 dpi (Fig. 4A).

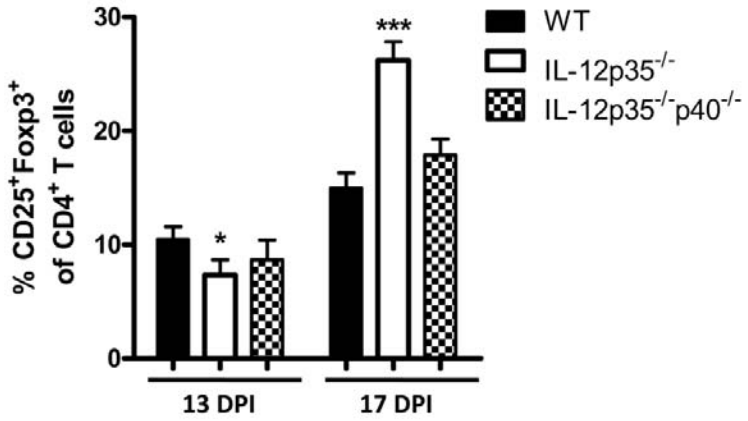

Figure 28 - IL-12p35$^{-/-}$ corneas contain an increased Treg population during disease regression.

Corneas were dispersed into single cell suspensions at 13 and 17 dpi and were stained with anti-CD4, CD25, and Foxp3 mAb. Corneal suspensions were analyzed by flow cytometry. Data are represented as mean % ± SEM CD25^{+}FoxP3^{+} cells in the CD4^{+} T cell population. Groups consisted of 5 or more individual corneas and results reflect the average of 2 independent experiments. (* $p < .05$, *** $p < .001$.)

However, Treg depletion did not significantly impact the course of HSK in IL-12p35$^{-/-}$ mice, with both depleted and non-depleted mice exhibiting HSK regression (Fig. 4B). As established in previous studies(212,213), Treg depletion did significantly increase the leukocytic infiltrate in infected corneas of WT mice (Fig. 4C), but did not significantly influence the size of the infiltrate in corneas of IL-12p35$^{-/-}$ mice (Fig. 4D). Thus, while CD25^{+} Tregs do modulate HSK severity in WT mice, they do not account for HSK regression in mice lacking IL-12p35. However, it is noteworthy that there remained in the corneas of the anti-CD25 mAb-treated IL-12p35$^{-/-}$ mice a substantial population of CD4^{+} FoxP3^{+} cells that did not express CD25 (Fig. 4A). These cells did not stain with anti-rat Ig, suggesting that CD25 was not simply masked by the rat anti-mouse CD25 mAb used for depletion. A contribution of these FoxP3^{+} cells to HSK regression cannot be ruled out.

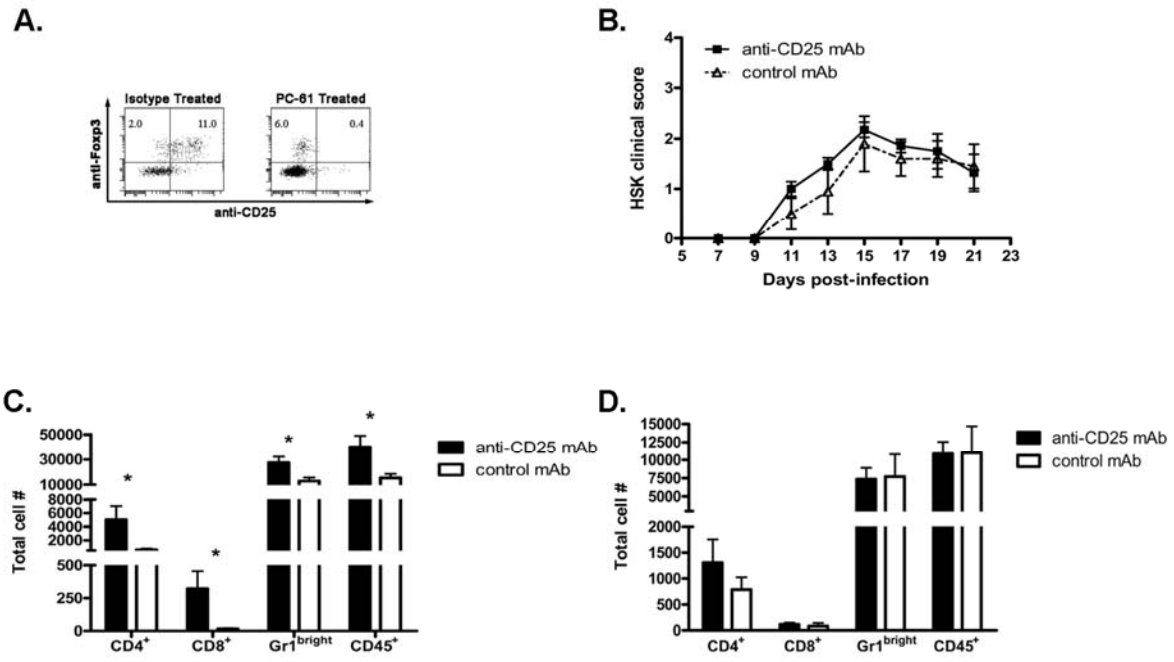

Figure 29 - Regulatory T cells do not cause disease attenuation in IL-12p35$^{-/-}$ mice.

IL-12p35$^{-/-}$ and WT mice were ~80% depleted of Treg cells by treatment with anti-CD25 mAb (PC61) 3 days prior to infection with HSV-1 RE (A, comparing depletion in WT mice). WT and IL-12p35$^{-/-}$ mice were followed for HSK (data not shown and B, respectively), and at 21 dpi, dispersed corneas were stained with anti-CD4, CD8, CD45, and GR-1 and analyzed by flow cytometry (WT, C and IL-12p35$^{-/-}$ D). Data are represented as mean ± SEM number of cells per cornea. Results represent the average of 2 independent experiments with an n value of at least 6 mice per group. * $p < .05$.

6.4 IL-12P35 INFLUENCES THE CYTOKINE AND CHEMOKINE PROFILE IN INFECTED CORNEAS

To determine if HSK progression and regression was associated with different chemokine and cytokine profiles, corneas of WT, IL-12p40$^{-/-}$, IL-12p35$^{-/-}$, and IL-12p35$^{-/-}$p40$^{-/-}$ mice were

excised at 17 dpi, and cytokine and chemokine proteins were quantified using a multiplex bead array assay (Fig. 5). During HSK regression (17 dpi) the corneas of both IL-12p35$^{-/-}$ and IL-12p35$^{-/-}$p40$^{-/-}$ mice exhibited significantly reduced expression of the neutrophil chemoattractants KC/CXCL3 (Fig. 5A) and MIP-2/CXCL2 (Fig. 5B), relative to those of WT mice. This correlated with a reduction in the neutrophilic infiltrate in IL-12p35$^{-/-}$p40$^{-/-}$ mice and slightly preceded their reduction in IL-12p35$^{-/-}$ mice (Fig. 2B). In conjunction with a reduced CD4^{+} T cell infiltrate, the corneas of IL-12p35$^{-/-}$ and IL-12p35$^{-/-}$p40$^{-/-}$ mice also exhibited significantly reduced levels of the chemotactic factor MCP-1/CCL2 (Fig. 5C), a chemokine that one study suggested regulates CD4^{+} T cell infiltration into infected corneas(214). The attenuation of blood vessels in infected corneas of IL-12p35$^{-/-}$ and IL-12p35$^{-/-}$p40$^{-/-}$ mice was also associated with significantly reduced levels of the angiogenic factor VEGF (Fig. 5D). Infected corneas of IL-12p40$^{-/-}$ mice compared to infected WT corneas exhibited elevated levels of MIP-2/CXCL2 and VEGF, but similar levels of KC/CXCL3 and MCP-1/CCL2. The increased levels of MIP-2/CXCL2 and VEGF preceded the increased leukocytic infiltrate at 21 dpi (Fig. 2C), but were not associated with increased clinical HSK scores (Fig. 1). Of interest was the lack of detectable levels of IL-6 within the corneas of the IL-12p35$^{-/-}$ mice while levels of this cytokine were similar in WT, IL-12p40$^{-/-}$, and IL-12p35$^{-/-}$p40$^{-/-}$ mice (Fig. 5E). As mice lacking IL-12 p35 still underwent a regression of disease (Fig. 1), it appears IL-6 while important for HSK development, is not alone sufficient to promote HSK progression.

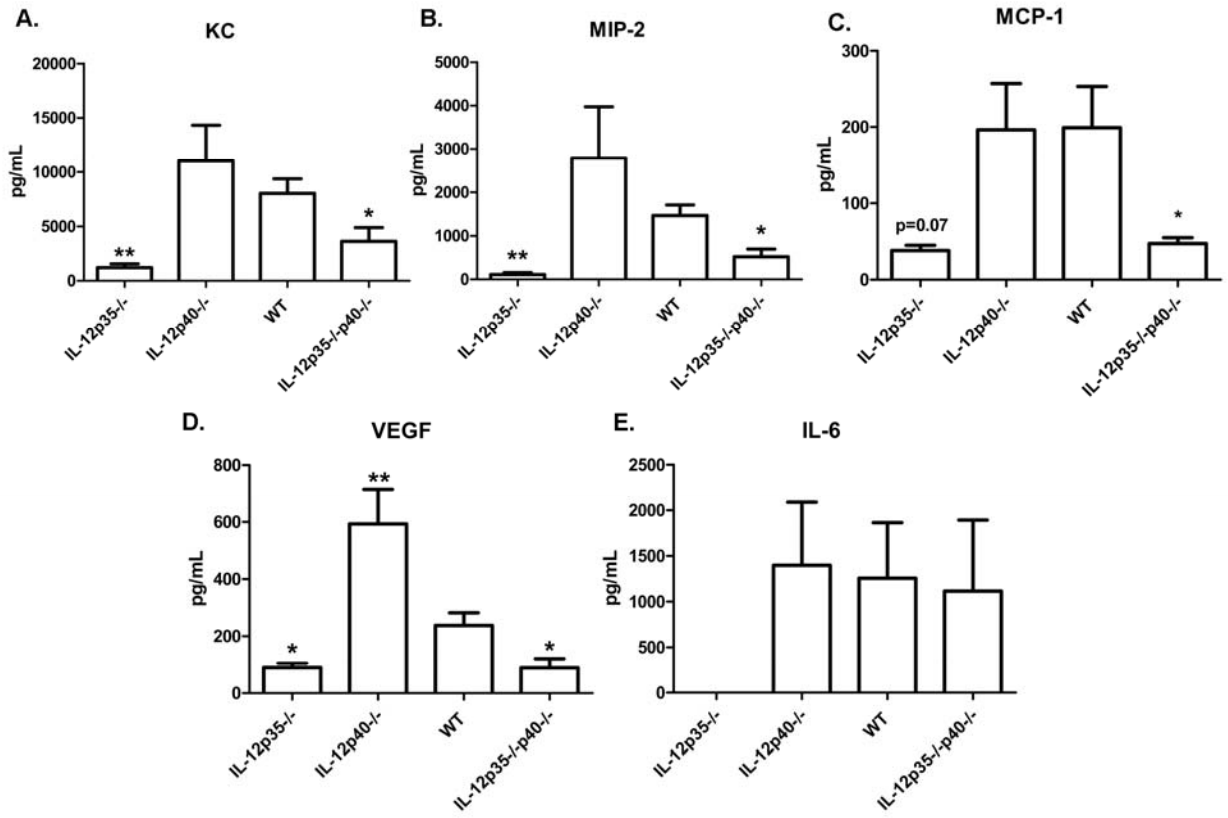

Figure 30 - Absence of IL-12 alters expression of cytokines and chemoattractants in corneas.

WT, IL-12p35$^{-/-}$, IL-12p40$^{-/-}$, and IL-12p35$^{-/-}$p40$^{-/-}$ corneas were harvested at 17 dpi. Corneas were homogenized by sonic dismembranation in PBS $^{+}$ protease inhibitor, and analyzed by multiplex bead array for cytokine and chemokine expression. Data are represented as mean ± SEM pg/ml of analyte. Groups consisted of 5 or more corneas and results were averaged between two independent experiments. (* $p < .05$, ** $p < .01$.)

6.5 DISCUSSION CHAPTER 6

The established regulatory role of TH1 cytokines in HSK immunopathology strongly implicates the involvement of the IL-12 cytokine family. Indeed, a previous study using the same BALB/c WT, IL-12p40$^{-/-}$, and IL-12p35$^{-/-}$ mice employed in our study supported a role for IL-12 in HSK by showing reduced HSK in IL-12p35$^{-/-}$ mice and no HSK in IL-12p40$^{-/-}$ mice (175). The authors

concluded that IL-12 was required for HSK. Those findings stand in stark contrast to the findings in this report. In our hands IL-12p40$^{-/-}$ mice developed HSK with similar kinetics and severity to that seen in WT control mice. Indeed, infected corneas of IL-12p40$^{-/-}$ mice exhibited a more robust inflammatory infiltrate at the peak of HSK (21 dpi) compared to their WT counterparts. These findings demonstrate that in our HSK model neither IL-12 nor IL-23 has a requisite role in HSK development since both molecules incorporate an IL-12p40 chain. We further establish that the IL-12p35 chain has a requisite role in the progression of HSK beyond 11 dpi, which is independent of the IL-12p40 chain as indicated by the transient nature of HSK in corneas of IL-12p35$^{-/-}$ mice and IL-12p35/p40 double knockout mice. The genotype of all the mice used in these experiments was confirmed by PCR, and the pattern of HSK was observed in multiple experiments.

We surmise that a likely explanation for the differences in findings of the two studies lies in the virus used to infect the mice. Ghiasi and colleagues used the McKrae strain of HSV-1 at an infectious dose of 2 x 10^5 PFU to infect corneas. The McKrae strain is highly neurovirulent and at the dose employed only 20% of WT and IL-12p40$^{-/-}$ mice and 50% of IL-12p35$^{-/-}$ mice survived to the time of HSK evaluation. Thus, in that study HSK was evaluated only in those few mice that survived the infection, and the general health of those surviving mice was not described. Our study employed a much less neurovirulent RE strain of HSV-1 at a much lower infectious dose that induced HSK in 80-100% of WT mice while permitting 100% survival with no clinically apparent disease other than HSK. We previously established that HSK is highly dependent on the function of CD4$^+$ T cells at the RE HSV-1 infectious dose used in these studies (193), and our model better reflects human disease where infections are rarely fatal and HSK usually occurs in otherwise healthy individuals. One interesting parallel between the two studies

is the fact that the IL-12p35 chain appears to function independent of IL-12p40; in our study prolonging HSK and in the previous study enhancing the lethality of HSV-1 infection. These findings are consistent with an important role for IL-12p35 in regulating the immunopathology in the cornea and in the CNS independent of IL-12p40.

The IL-12p40 chain can form an IL-12p40 homodimer, which has been shown to inhibit T cell responses by binding to the IL-12Rβ1 chain and inhibiting binding of IL-12 and IL-23 (165,166). We considered the possibility that IL-12p35$^{-/-}$ mice might have a propensity to produce more IL-12p40 homodimer, which might account for the transient nature of HSK in these mice. This possibility was addressed by monitoring HSK in mice that lack both the p35 and p40 subunits. We observed a transient pattern of HSK in the double knockout mice that was similar to that seen in IL-12p35$^{-/-}$ mice. These findings demonstrated that HSK regression was due to the lack of the IL-12p35 subunit rather than to an altered function of the IL-12p40 subunit. The increased level of infiltrate within the IL-12P40$^{-/-}$ corneas is in agreement with the recent study in IL-23 deficient mice, where more severe HSK lesions develop over WT mice(176). However, the observation that mice deficient in both IL-12p35 and p40 regress in HSK earlier than IL-12p35$^{-/-}$ mice suggests more complex relationships exist for p40 in the development of HSK.

We were intrigued by the dramatic increase in the frequency of Foxp3^{+} Tregs in the infected corneas of IL-12p35$^{-/-}$ mice during HSK regression. The reduced overall CD4^{+} T cell population in the infected corneas of IL-12p35$^{-/-}$ mice during HSK regression, combined with the elevated frequency of Tregs among the CD4^{+} T cells would suggest a very high Treg: effector T cell ratio in the infected corneas of these mice. The cytokine TGF-β regulates the differentiation of CD4^{+} T cells into Tregs and into TH17 cells, with co-stimulation by IL-6 favoring the latter

(215,216). We noted dramatically reduced levels of IL-6 in the corneas of IL-12p35$^{-/-}$ mice during HSK regression when compared with those of WT mice with progressive HSK. The known presence of TGF-β in the cornea (44,217) and the low levels of IL-6 in the corneas of IL-12p35$^{-/-}$ mice might provide a cytokine milieu that favors the differentiation and/or expansion of Tregs.

However, depletion of CD25^{+} cells failed to influence HSK regression in IL-12p35$^{-/-}$ mice. The possible explanation that our anti-CD25 treatment effected HSK regression by inadvertently depleting CD4^{+} effector T cells along with Tregs appears highly unlikely. In our hands the majority of CD4^{+} CD25^{+} cells in infected corneas co-express Foxp3 (not shown) suggesting that predominantly Tregs would be depleted by anti-CD25 treatment. Moreover, similar anti-CD25 mAb treatment increased CD4^{+} T cell numbers and augmented the overall leukocytic infiltrate in HSV-1 infected corneas of WT mice, suggesting that the CD4^{+} T cells that mediate HSK do not express CD25. To further corroborate this evidence, IL-12p35$^{-/-}$p40$^{-/-}$ did not exhibit any increase in Treg frequency in their corneas, despite HSK regression. Thus, although the frequency of CD4^{+} CD25^{+} Foxp3^{+} Tregs is dramatically increased in infected corneas of IL-12p35$^{-/-}$ mice during HSK regression, these cells are either inactive or their effector molecules inhibit an IL-12p35-dependent activation pathway. However as noted above, depletion of CD25^{+} cells leaves a substantial population of CD4^{+} FoxP3^{+} CD25^{-} cells in the cornea that might contribute to HSK regression.

Our findings demonstrate that IL-12p35 and p40 regulate the production of several chemokines and cytokines in corneas with HSK. Levels of the macrophage chemoattractant MCP-1/CCL2 were significantly and equivalently reduced in infected corneas of IL-12p35$^{-/-}$ and IL-12p35$^{-/-}$p40$^{-/-}$ mice at 17 dpi. This observation is consistent with a role for IL-12 in regulating

production of this chemokine. A recent study does suggest a role of MCP-1 in regulating the infiltration of $CD4^+$ T cells into the HSK inflamed cornea (214), although such studies are complicated by the fact that $MCP1^{-/-}$ mice exhibit enhanced IL-12 production and increased HSK (218,219). Together these findings suggest a regulatory circuit in which IL-12 induces MCP-1/CCL2 production, while MCP-1/CCL2 provides feedback inhibition of IL-12 production.

We also observed that IL-12p35 regulates neutrophil infiltration and production of the neutrophil chemoattractants KC/CXCL3 and MIP-2/CXCL2 as these chemokines were significantly reduced in infected corneas of IL-$12p35^{-/-}$ and IL-$12p35/40^{-/-}$ mice relative to WT mice. This function of IL-12p35 is independent of IL-12p40 since neutrophilic infiltration and levels of these chemokines were somewhat elevated in infected corneas of IL-$12p40^{-/-}$ mice. These findings are consistent with previous studies identifying KC/CXCL3, and to a greater extent MIP-2/CXCL2 as important factors for neutrophil recruitment and HSK development (220-222).

Several studies have established a critical role for neovascularization in HSK progression (206,206,207,223-225). Here we demonstrate that IL-12p35 independent of IL-12p40 regulates VEGF production in corneas with HSK. In fact, IL-12p40 appears to inhibit the induction of VEGF production by IL-12p35 as corneas of IL-$12p40^{-/-}$ mice exhibit dramatically increased VEGF production whereas the IL-12p35/p40 double knockouts show reduced VEGF levels comparable to those seen in IL-12p35 single knockouts.

The current understanding of IL-12p35 synthesis indicates that this subunit is not released by cells unbound (226). The recent description of IL-35, a IL-12p35 EBI3 heterodimeric sets the precedence for more p35 binding partners (170,226). The exact contribution of IL-12p35 subunit

to the maintenance of HSK remains unclear, but reflects an exciting development in the study of the IL-12 cytokine family in the pathogenesis of HSK immunopathology.

7.0 THE ROLE OF DENDRITIC CELLS IN CONTROL OF HSV-1 OCULAR INFECTION

A number of studies have recently identified that the local APCs that reside or infiltrate a site of infection may diverge from the classic notion of antigen uptake for presentation in the lymph node, as discussed in the introduction. Here we examined the role of local resident and early recruited DCs within the cornea after HSV-1 infection and how they contribute to the immune response. We took advantage of CD11c-DTR transgenic mice, which contain the high affinity human *diphtheria* toxin (DT) receptor only on $CD11c^+$ DCs. We used local depletion *only* within the cornea as well as systemic depletions to effectively dissect the roles of both resident and responding DCs within the cornea in ocular HSV-1 infection.

7.1 CD11C-EGFP$^+$ DC CAN BE DETECTED WITHIN THE NORMAL CORNEA

Within the normal cornea we have recently identified, using CD11c-DTR mice, the presence of a distinct population of CD11c$^+$ DCs that reside at the epithelial stromal interface (Knickelbein et al., publication accepted). Given this novel observation, studies were undertaken to identify their function in the context of HSV-1 ocular infection. In the studies here, we used chimeras reconstituted with the bone marrow from CD11c-DTR hosts. This ensures that only bone marrow derived CD11c$^+$ cells are ablated following diphtheria toxin (DT) treatment, as reported in previous studies (227). For the purpose of this chapter, unless specified, we shall call these bone marrow chimeras CD11c-DTR mice. As seen in figure 31 we can detect pCD11c-EGFP$^+$CD11c surface$^+$ cells within the cornea. The peripheral region of the cornea contains a more dense concentration of DCs that begins to the thin as one moves toward the central regions of the cornea. These DCs within the cornea are of the classic dendritic morphology. These DCs are bright for pCD11c-EFGP, but also have dim surface CD11c expression.

A recent study observed that the cornea requires at least 5-6 weeks for full reconstitution following irradiation (228). As indicated in Figure 32, we can see that at 1 month post reconstitution – a time frame most studies rely on for "complete reconstitution," the cornea is not completely reconstituted with dendritic cells. However, by 6 weeks post reconstitution we see similar levels of DCs within the central cornea as an intact regular CD11c-DTR mouse. This time frame for corneal recovery is similar to what was previously reported.

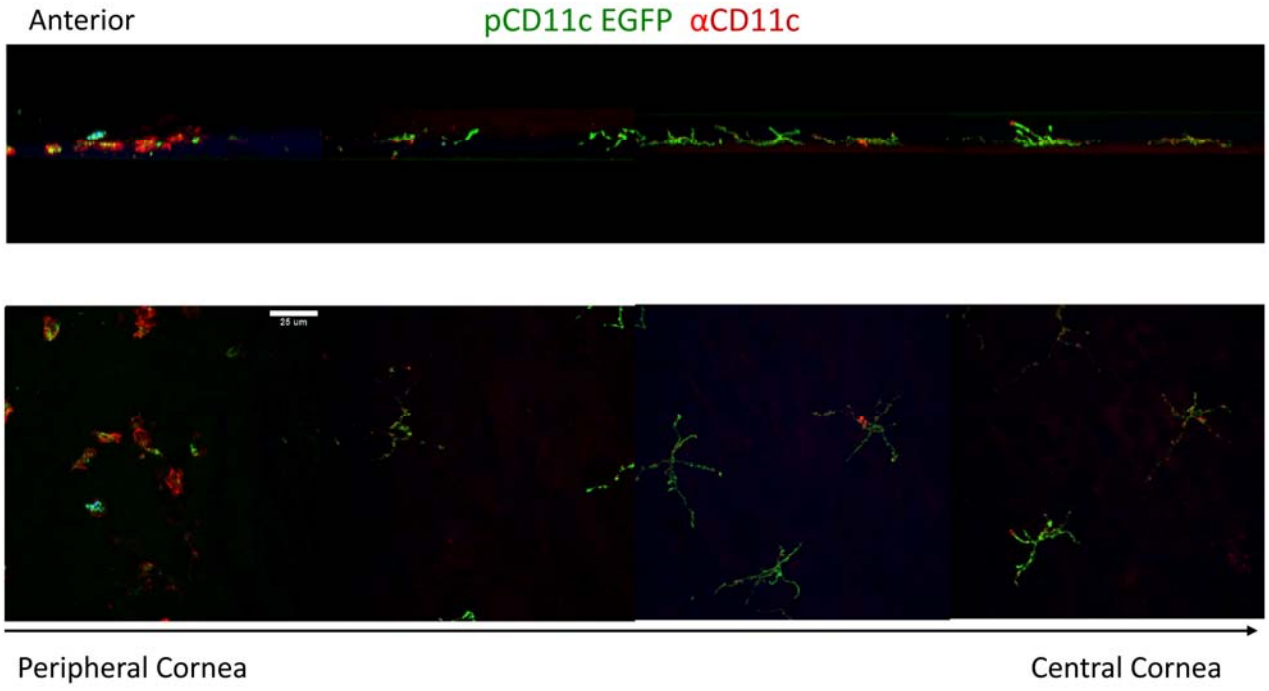

Figure 31 – CD11c^{+} DCs are present within the normal cornea.

Naïve corneas from CD11c-DTR mice were stained with anti-CD11c antibody, fixed and whole mounted onto slides for confocal analysis. Images are representative serial Z-stack confocal microscopy images. The top set of images portrays a cross sectional view of the image, with the anterior cornea top, moving down into the corneal stroma. The lower sets of images depict a set of images looking downwards into the corneal stroma, moving from the peripheral cornea right towards the central cornea. Representative images (n=4 mice, 2 independent experiments)

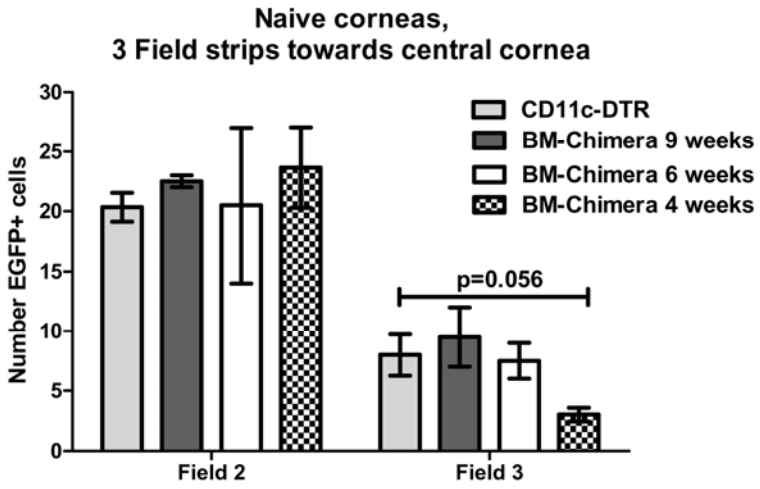

Figure 32 – CD11c-DTR Bone Marrow Chimeras require 6 weeks for full reconstitution of the cornea.

WT BALB/C mice were dosed with 1000 rads, and reconstituted with $2x10^5$ bone marrow cells from CD11c-DTR donors. At indicated times post reconstitution, naïve corneas were excised, fixed and whole mounted onto slides for confocal analysis. Data represents the mean± SEM number of pCD11c-$EGFP^+$ cells per 40x field, in the serial strips moving towards the central cornea. Field 2 and 3 are indicative of the two most central fields in the strip. Data is indicative of 2 independent experiments, n=6.

7.2 LOCAL AND SYSTEMIC DT TX EFFECTIVELY ABLATES DCS FROM THE CORNEA

With a corneal population identified by pCD11c-EGFP expression, our first steps were to establish that we can effectively ablate this population from the cornea with both a local and systemic treatment of DT. Naïve CD11c-DTR mice were locally depleted via subconjunctival

injection or systemically with an i.p. DT treatment. Prior studies have observed that a single systemic injection of DT effectively ablates $CD11c^+$ cells for 2 days, after which recovery begins (227,229,230). With this in mind, 2 days following injections, both DT treatments appeared to effectively remove $pCD11c^+$ cells from the cornea (Figure 32). A concern of treatments was the enhanced infiltration of PMN neutronphils or monocytes into the tissue in response to the inflammation by the DC ablation. Based on $CD11b^+$ cell infiltration into the cornea following treatment there was little, if any increased infiltration of $CD11b^+$ cells into the cornea. Within the naïve cornea, MHC-II^+ expression is also seen on $CD11b^+$ cells that lack pCD11c. This is similar to a prior observation by our group (49). A second concern of the local injection was the increase in MHC-II expression on these cells following ablation, which could alter the progression of the immune response to HSV-1. As also seen in Figure 32, frequency of MCH-II^+CD11b^+ cells remains similar within the cornea following local or systemic DT treatment.

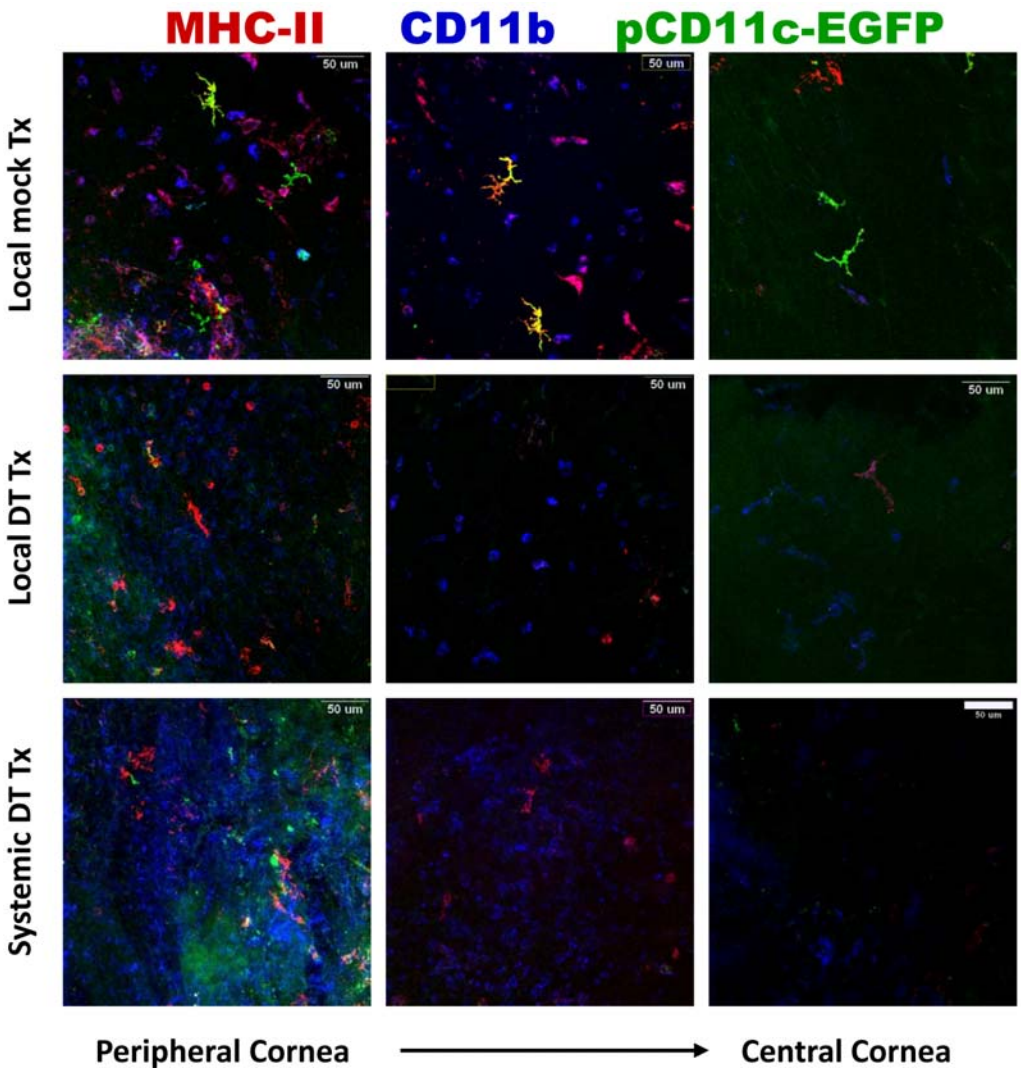

Figure 33 – Local or systemic *Diphtheria* toxin treatment effectively ablates CD11c^{+} cells from the cornea

Naïve CD11c-DTR mice received subconjunctival injections of 50ng DT or PBS, or they received 150ng DT systemically via i.p. injection. 2 days following injections whole corneas were harvested, stained for antibodies to CD11b and MHC-II, fixed, and whole mounted for confocal microscopy. Figure depicts representative Z-stack images from areas within the peripheral cornea moving out to the central corneal regions. N=3 mice per group, representative images from 2 independent experiments.

7.3 LOCAL DT TX DOES NOT ABLATE CELLS IN THE DRAINING LYMPH NODES

An important concern of local DT treatment was that of leakage of toxin into the blood stream or down the lymphatics to the lymphoid tissues. Leakage and subsequent depletion of DCs in lymphoid organs as a byproduct of a local depletion would greatly complicate interpretation of these findings. Within the draining lymph nodes and spleens of CD11-DTR mice treated locally with DT, we saw no appreciable loss of $CD11c^+$ cells compared to that of mock PBS treated controls (Figure 34A). Of note was the observation that pCD11c-EGFP and surface $CD11c^+$ cells had great concordance in expression (Figure 34B). Systemic DT treatment completely ablated these cells from the lymphoid organs. As summarized in Figure 34C, local treatment caused no significant change in the frequency of $CD11c^+$ in lymphoid organs, while systemic injections removed these cells effectively.

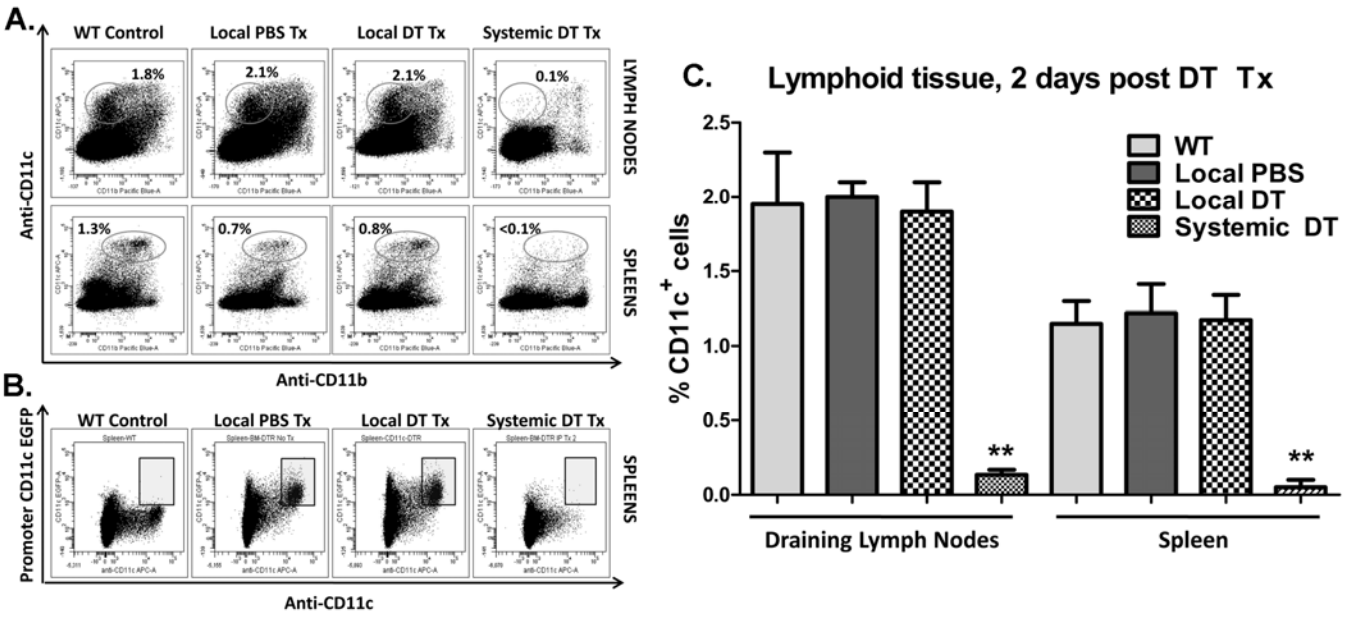

Figure 34 – Local *Diphtheria* toxin treatment does not ablate systemically

Naïve CD11c-DTR mice received subconjunctival injections of 50ng DT or PBS, or they received 150ng DT systemically via i.p. injection. 2 days following injections draining lymph nodes and spleens were harvested and dispersed into single cell suspensions, and stained for antibodies to CD11c and CD11b, and analyzed via flow cytometry. **A)** Representative flow plots depicting $CD11c^+$ cells within the draining lymph nodes and spleens. **B)** Representative flow plots from the spleen depicting concordance of expression between surface CD11c and promoter drive EGFP. **C)** Graphical representation of $CD11c^+$ frequency in the DLN and spleen. Data is presented as mean ± SEM frequency of $CD11c^+$ cells (* $p < .05$, ** $p < .01$). n=7-9/group, 2 independent experiments.

7.4 NK CELLS AND PLASMACYTOID DCS ARE NOT LOST FOLLOWING DT TREATMENT

A number of studies have observed NK cells can express CD11c and that either NK cell depletion or DC depletion approaches may inadvertently remove the other population (231). While pDCs have not been reported to be ablated in CD11c-DTR mice, we nevertheless

established that this cell population remained unaffected following DT treatment in our model. We assayed for the secondary depletion of these two important innate arm populations in naïve CD11c-DTR mice systemically treated with DT. Both populations appeared to remain intact following systemic DT treatment (Figure 35). NK cells residing within the spleen did not appear to express significant levels of CD11c (Figure 35A, B), and no detectable loss of these cells was observed following treatment. pDCs also remained stable following DT treatment; these cells also appeared to be completely negative for pCD11c-EGFP (Figure 35C), correlating with previous studies that reported these cell populations were not altered by DT treatment (227).

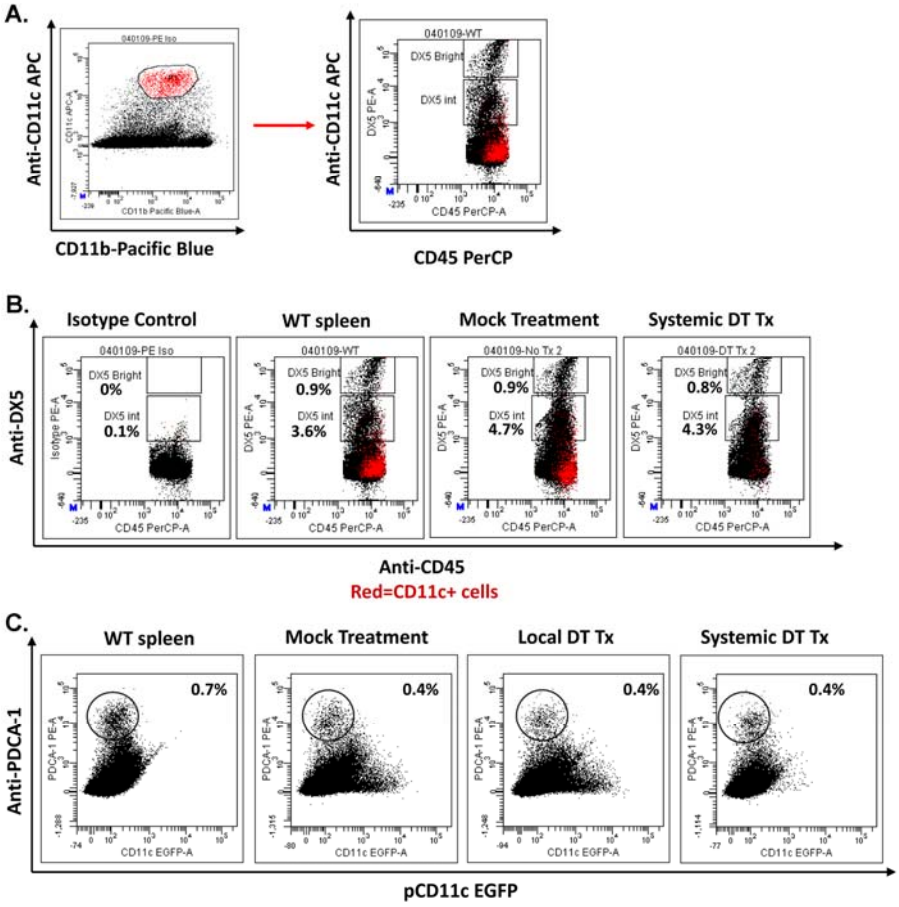

Figure 35 – Neither NK cells nor pDCs are affected by DT depletion of CD11c$^+$ cells

Naïve CD11c-DTR mice received subconjunctival injections of 50ng DT or PBS, or they received 150ng DT systemically via i.p. injection. 2 days following injections spleens were harvested and dispersed into single cell

suspensions, and stained for antibodies to CD11c and DX5, or PDCA-1, and analyzed via flow cytometry. **A)** Gating strategy used to observe NK cell depletion; CD11c cells in red are shown in a plot showing NK cells, to demonstrate how few $CD11c^+$ cells are $DX5^+$. **B)** Representative flow plots from the spleen showing no loss of NK cell frequency following DT treatment **C)** Representative flow plots depicting $PDCA^+$ cells are not lost when $CD11c^+$ cells are ablated.

7.5 DCS WITHIN THE CORNEA ARE NOT LANGERHANS CELLS

As discussed in this chapter's introduction, Langerhans cells (LCs) in particular have been identified to have functional properties that depart from the classical understanding of how DCs contribute to the immune response. Historically, all DCs within the cornea have been considered LCs, though few studies have used specific markers for this cell subset (133,232). We felt it necessary to establish if in fact these cells were LCs, given that their potential immunomodulatory properties could play an important role in both the immune privileged cornea as well as immune control of HSV-1. Surprisingly we did see very few $Langerin^+$ cells within the cornea, in stark contrast to the skin, where these cells were readily seen (Figure 36).

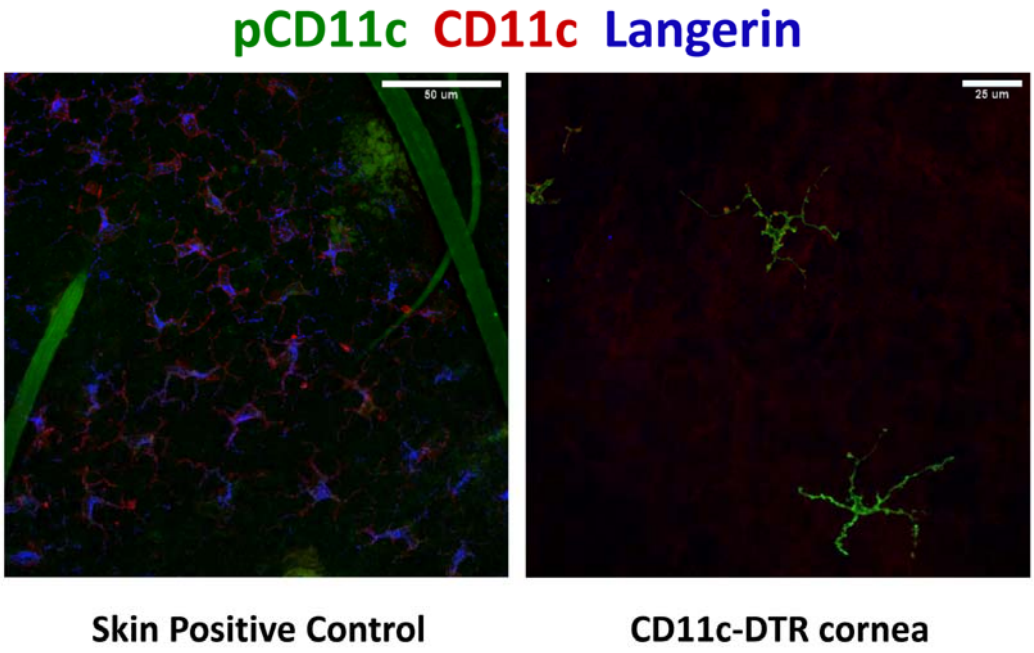

Figure 36 – CD11c$^+$ cells within the cornea are not Langerhans cells

Skin biopsies and whole corneas were harvested from CD11c-DTR mice, stained with antibodies to CD11c, fixed and permeabilized, stained with anti-langerin antibody, then whole mounted for confocal microscopy. Figure depicts representative Z-stack reconstructions from the cornea and skin. n=2,3 mice, 2 independent experiments.

More importantly LCs observed within the skin expressed no detectable EGFP, and furthermore they were not depleted with systemic DT treatment (data not shown). This is similar to other observed studies using CD11c-DTR mice that reported poor, if any loss of LCs after DT treatment, despite the fact that these cells do express low levels of surface CD11c (227). This data demonstrates that the classical notion LCs exist throughout the cornea were incorrect, being based on less accurate phenotypic markers for LCs than used here.

7.6 MICE LACKING DCS SYSTEMICALLY THROUGHOUT INFECTION ARE IMPAIRED IN VIRAL CONTROL AND HSV $CD4^+$ T CELL RESPONSE

After establishing our depletion model, we initiated experimentation that observe DC depletion in the context of ocular HSV-1 infection. A recent study presented results that systemic DT treatment can impair the ability of mice to respond to HSV-1 infection (233). This study used the HSV-1 resistant B6 strain of mice and also used a different route of infection (the footpad). We first wanted to establish how ocular HSV-1 infection is controlled in the more HSV-1 susceptible BALB/c mice when DCs are absence throughout infection.

When we observe mice continuously ablated of DCs throughout infection, we find there are serious deficiencies in both viral control and the generation of the adaptive immune response. In mice regularly treated with DT, we find a significant increase in viral burden within the cornea (Figure 37). At 2 dpi it appears there is similar viral control (or lack thereof) regardless of whether the DC compartment is intact. At 4 and 6 dpi, DC-intact mice rapidly reduce their viral load, which is almost non-existent by 6 dpi. In contrast viral load is significantly higher at both 4 dpi and 6 dpi in DC ablated corneas. Viral load does decline over time, suggesting that control is not completely lost, only impaired. These findings demonstrate there is a significant impairment in the innate immune responses' ability to control virus within the cornea while the adaptive immune response is being generated.

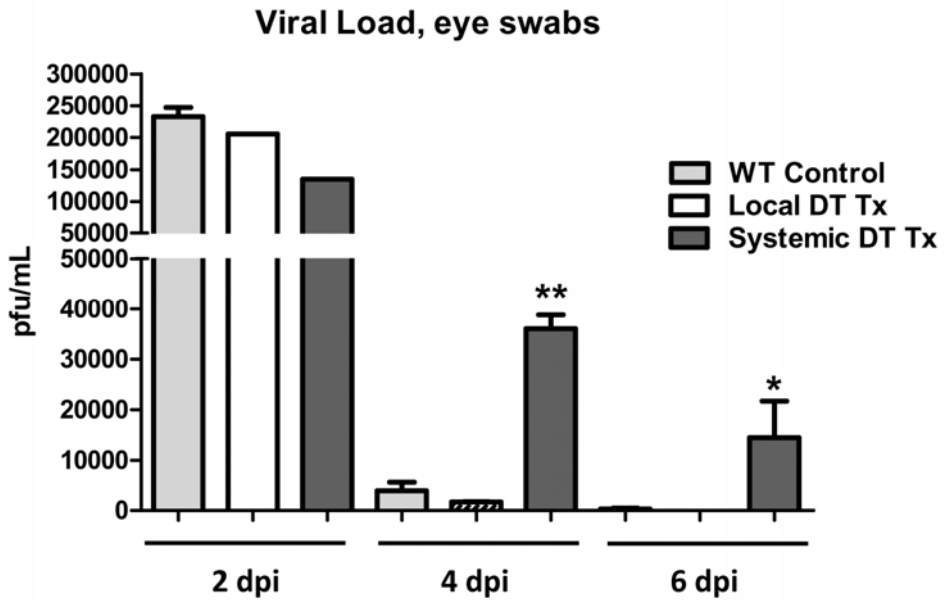

Figure 37 – Mice continuously depleted of DCs have an impaired ability to control corneal HSV-1 infection.

Naïve CD11c-DTR mice received subconjunctival injections of PBS or they received 150ng DT systemically via i.p. injection. 2 days following injections mice were ocular infected with HSV-1. Repeat injections of PBS or DT were given at 3 and 6 dpi to maintain depletion. At indicated days post infection (dpi), eyes were swabbed with a sterile surgical spear and assayed for live virus by standard plaque assay. The data are presented as the mean ± SEM viral plaque forming units (pfu) per cornea of WT controls, locally PBS DT Tx CD11c-DTR mice, and systemically DT Tx mice. (** $p<0.01$, * $p<0.05$)

We also observed how the adaptive immune response is generated in these mice. When whole DLNs from mice systemically DT treated were stimulated with APCs loaded with HSV-1 infected target lysate, we saw a significant impairment in the $CD4^+$ T cell IFN-γ responses (Figure 38). In response to HSV-1, $CD4^+$ T cells from WT control mice and CD11c-DTR PBS mock treated mice responded with IFN-γ to HSV-1 at a frequency of ~1.5%. Only 0.2% of $CD4^+$ T cells responded with IFN-γ in DC ablated mice, close to a 10 fold reduction. This

strongly suggests that the adaptive response is not effectively generated in the absence of DCs, which is similar to the findings of the early study that ablated DCs during HSV-1 infection (227).

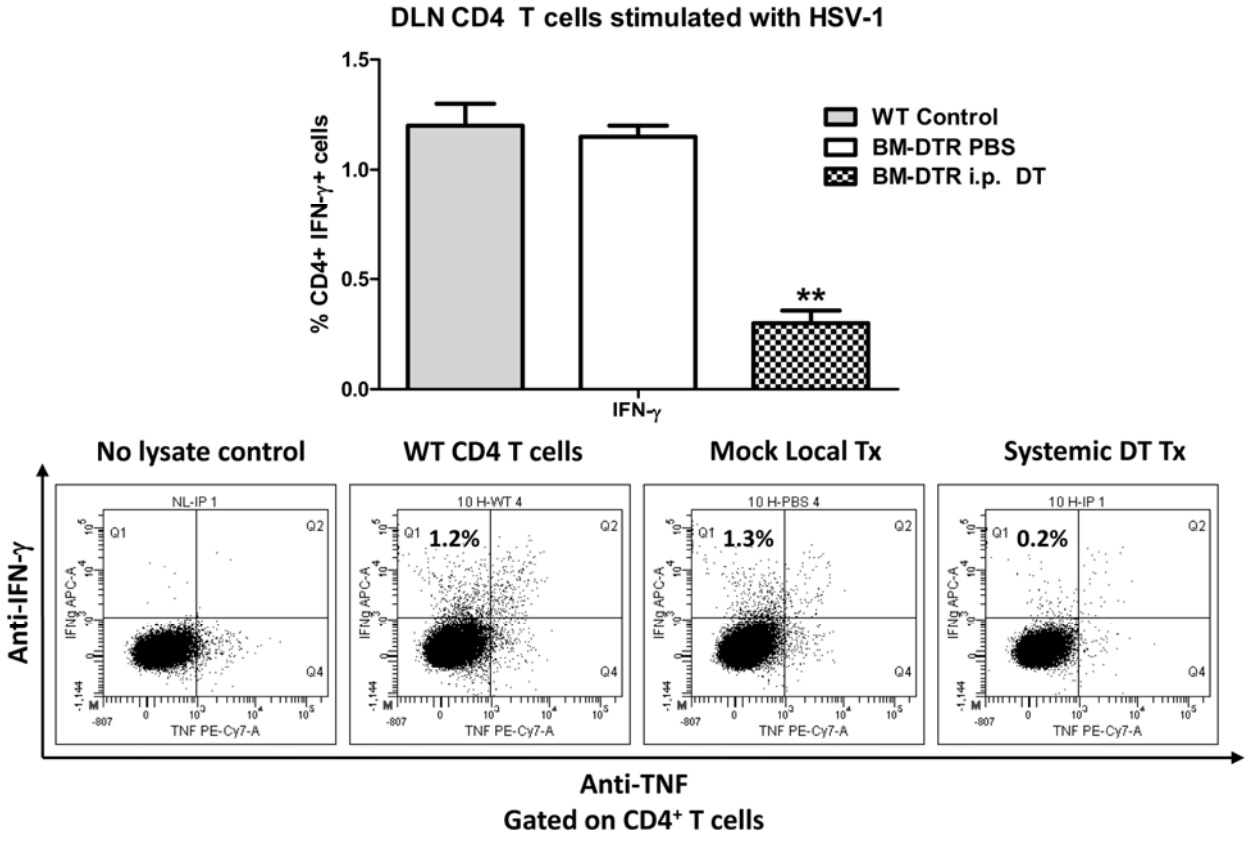

Figure 38 – Mice deficient in DCs generated a diminished HSV-1 CD4$^+$ T cell response

Naïve CD11c-DTR mice received subconjunctival injections of PBS or they received 150ng DT systemically via i.p. injection. 2 days following injections mice were ocular infected with HSV-1. Repeat injections of PBS or DT were given at 3 and 6 dpi to maintain depletion. At 7 dpi, whole DLN were harvested, and dispersed into a single cell suspension, and incubated for 72 hours at a 1:5 effector to target ratio with APCs pulsed with HSV-1 antigens. During the last 12 hours of stimulation, golgi plug was added, and cultures were subsequently stained for antibodies to CD4, IFN-γ, and TNF. Graph depicts mean ± SEM frequency of CD4$^+$ cells responding with IFN-γ only to HSV-1 (** $p < .01$). n=3 mice per group, one independent experiment.

7.7 EARLY INFILTRATING DCS ARE NECCESARY TO FOR HSV-1 VIRAL CONTROL AND MOBILIATION OF THE ADAPTIVE IMMUNE RESPONSE

We have established that removal of DCs during the entire course of infection is extremely detrimental to early viral control as well as the mobilization of the adaptive immune response. We endeavored to ask the more complex question of whether local DCs or early responding DCs were important to this process. To this end, we used an approach where only a single injection of DT was given prior to infection. Based on previous observations that depletion lasts 2-3 days, we would have recovery of DCs in treated mice by 2 dpi (4 days post injection). We find that mice depleted once before infection either locally or systemically have intact DC populations within their lymphoid organs at 7 dpi, or 9 days after injection (Figure 39). The two distinct DC populations within the spleen, $CD8\alpha^+$ and CD8α- DCs, are both intact after DT treatment, and in the case of systemic depletion, are actually almost 3 times larger in frequency then mock treated controls. This data does establish that DC repopulation has already occurred prior to 7 dpi, and that there is an intact lymphoid APC population to present antigens to T cells.

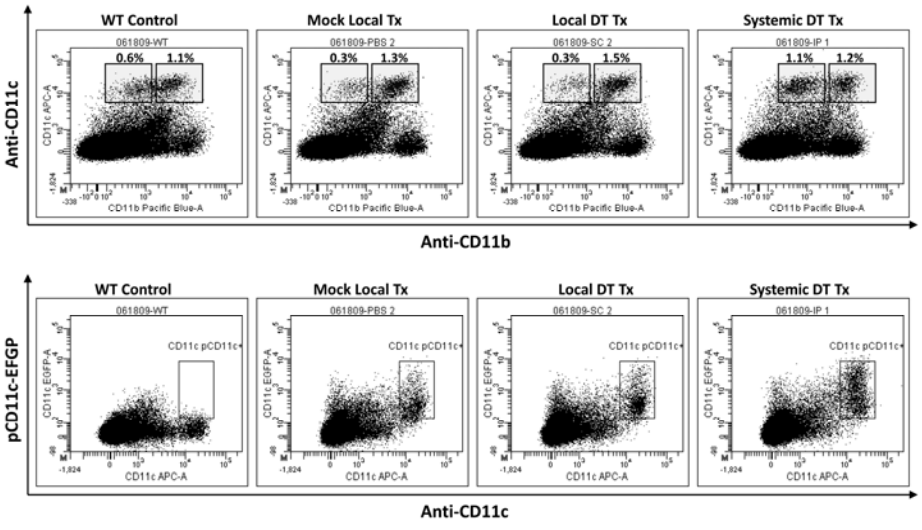

Figure 39 – Mice treated with DT locally or systemically prior to infection have intact lymphoid DCs populations at 7 dpi.

Naïve CD11c-DTR mice received subconjunctival injections of PBS or they received 150ng DT systemically via i.p. injection. 2 days following injections mice were ocular infected with HSV-1. At 7 dpi dispersed spleens were stained with anti-CD11b and CD11c. Data represents representative flow plots depicting $Cd11c^+$ cells recovered in the lymphoid organs. The boxes identify $CD8\alpha^+$ DCs (left box) and $CD8\alpha^-$ DCs (right box). Lower panel represents $EGFP^+$ cells and their concordant expression with surface CD11c. n=5-8 mice/group, 2 independent experiments.

When we look at the ability of these mice to control HSV-1 infection, we find that local depletion of DCs appeared to only have a minor impairment in viral control, while mice that received a systemic dose of DCs prior to infection had significant increases in viral burden (Figure 40). Viral load in locally depleted mice had a moderate, but not significant elevation in viral burden at 4 dpi (10000 pfu/mL) when compared to mock treated controls (5000 pfu/mL), but went on to clear virus in similar fashion by 6 dpi. Systemically DT treated mice had significantly higher levels of viral load at both 4 and 6 dpi. Surprisingly, these mice had viral burden very similar to those mice whose DCs were continuously depleted throughout infection

(36000 pfu/mL continuous, 44000 pfu/mL single at 4 dpi and 14400 pfu/mL continuous, 10880 pfu/mL single at 6 dpi). This similar impairment of viral control suggests an early role for DCs in mobilizing the innate immune response against the corneal infection. As locally depleted DCs only have a minor impairment in viral burden early, this suggests that DCs that infiltrate the cornea, not those present at the time of infection, contribute more towards innate control of HSV-1.

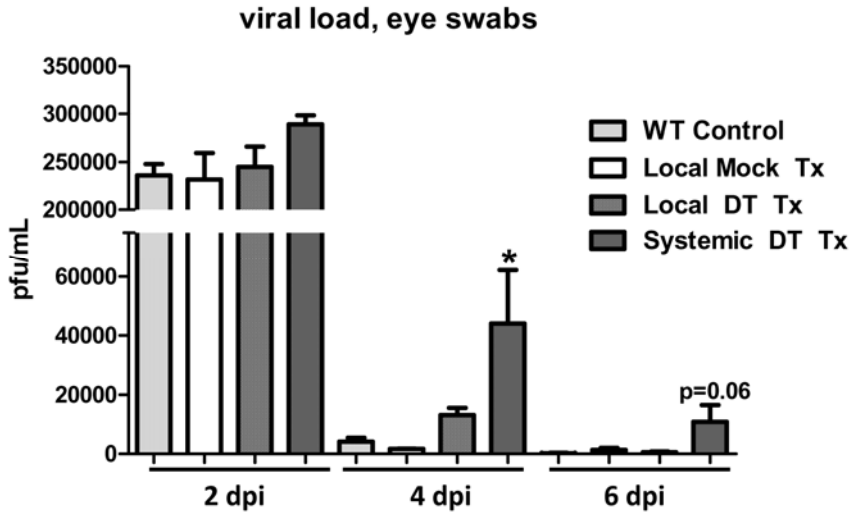

Figure 40 – Mice lacking DCs systemically at the time of HSV-1 infection have impaired ability to control HSV-1.

Naïve CD11c-DTR mice received subconjunctival injections of PBS or 50 ng DT, or they received 150ng DT systemically via i.p. injection. 2 days following injections mice were ocular infected with HSV-1. At indicated days post infection (dpi), eyes were swabbed with a sterile surgical spear and assayed for live virus by standard plaque assay. The data are presented as the mean ± SEM viral plaque forming units (pfu) per mL of WT controls, locally PBS DT Tx CD11c-DTR mice, locally DT, and systemically DT Tx mice. (* $p<0.05$), n=3-5 mice/group, 2 independent experiments.

Also surprising was the impairment of the $CD4^+$ T cell response to HSV-1 in systemically DT treated mice prior to infection. When equivalent numbers of $CD4^+$ T cells from the DLN of systemically DT treated mice were stimulated with HSV-1 at 7 dpi, they produced 50% less IFN-γ when compared to mock treated counterparts (Figure 41). Mice locally DT treated before infection had a similar response, suggesting that local resident DCs are dispensable for generating the adaptive immune response.

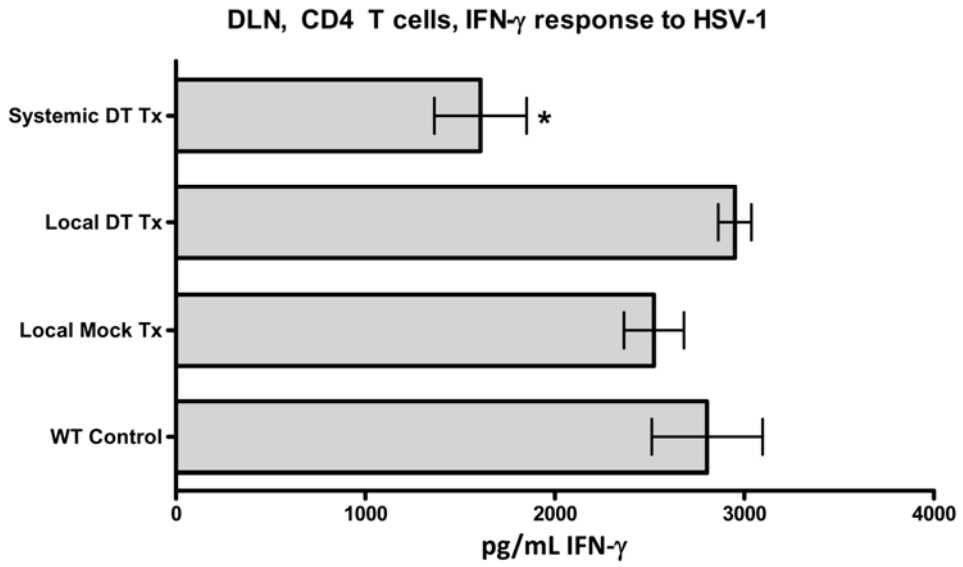

Figure 41 – Mice lacking DCs systemically at the time of infection develop an impaired HSV-$CD4^+$ T cell response.

Naïve CD11c-DTR mice received subconjunctival injections of PBS or they received 150ng DT systemically via i.p. injection. 2 days following injections mice were ocular infected with HSV-1. Repeat injections of PBS or DT were given at 3 and 6 dpi to maintain depletion. At 7 dpi, whole DLN were harvested, and dispersed into a single cell suspension, $CD4^+$ T cells were isolated via MACS columns, and then were incubated for 72 hours at a 1:5 effector to target ratio with APCs pulsed with HSV-1 antigens. At the end of the stimulation, supernatants were tested by standard ELISA for the IFN-γ. Graph depicts mean ± SEM pg/mL IFN-γ (* $p < .05$).

Based on these observations it appears that the DCs that infiltrate into the cornea shortly after infection are integral for both early viral control as well as ultimately contributing to the mobilization of the adaptive immune response.

7.8 EARLY INFILTRATING DCS DIRECT MIGRATION OF NK CELLS AND PDCS INTO THE CENTRAL CORNEA

Our observations that early responding DCs had such a drastic effect on viral control in the cornea pointed to a deficiency in the innate immune response within the cornea. The literature observed that NK cells, γδ T cells, and PMNs all play a role in the initial control of HSV-l ocular infection(52-55), (234-236).

Due to our approach to HSV-1 infection, viral replication will be confined to the central areas of the cornea. Armed with this knowledge, we hypothesized that in mice lacking DCs one or more of these populations are not effectively entering the central cornea, or they are reaching the central cornea but are functionally deficient. We used a 2mm trephine to remove the central cornea, and assayed by flow cytometry the migration of NK cells, PMNs, and inflammatory monocytes into the central corneas of mice treated once before infection with systemic dose of DT. One can see that of the three populations assayed, inflammatory monocytes and PMNs make up the largest infiltrating cell populations, followed by NK cells within the cornea (Figure 42A).

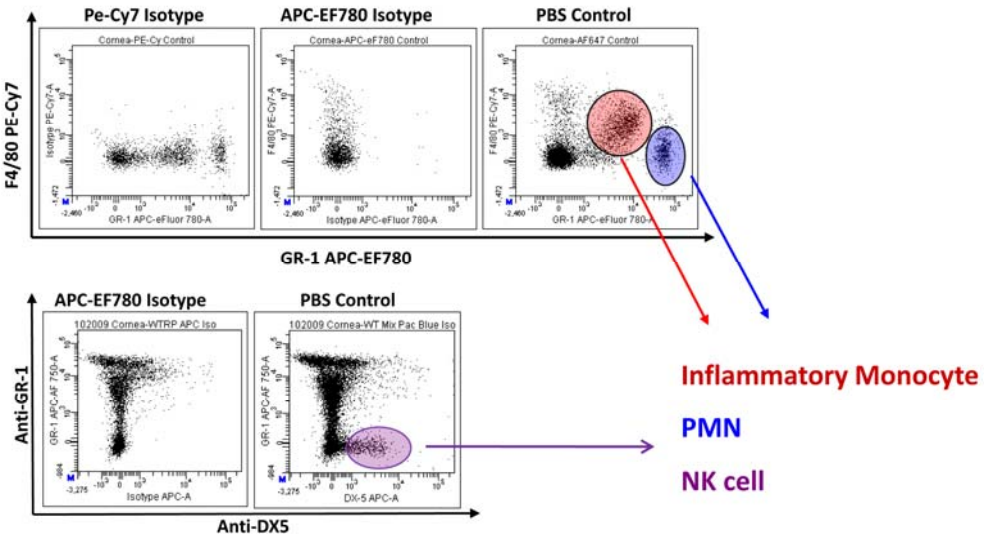

Figure 42- Gating Strategy for identification of innate immune responders, cornea 3 dpi

Naïve CD11c-DTR mice received subconjunctival injections of PBS or they received 150ng DT systemically via i.p. injection. 2 days following injections mice were ocular infected with HSV-1. At 3 dpi, corneas were harvested for flow cytometric analysis. The central cornea was removed via a 2mm trephine, and pooled central corneas were dispersed, stained with mAb to CD49b (DX5), F4/80, and GR-1. Data are representative flow plots depicting the gating strategy to identify PMN neutrophils, NK cells, and inflammatory monocytes.

At 3 dpi, we observed that similar numbers of innate immune cells extravasate into the corneal periphery whether the DC compartment is ablated or intact (Figure 43). Similar numbers of PMNs, inflammatory monocytes, and NK cells were observed within the peripheral cornea of DC ablated mice. We see significantly fewer cells in the periphery of naïve corneas, even after DT treatment. Notably, NK cells and to a greater extent inflammatory monocytes are a much smaller presence in the periphery of naïve corneas (Figure 43). This agrees with the notion that these cells are infiltrating into the cornea in response to viral infection. We do note an increase in the number PMNs in the corneas of DT Tx mice, a reflection of the lingering inflammation from DC ablation.

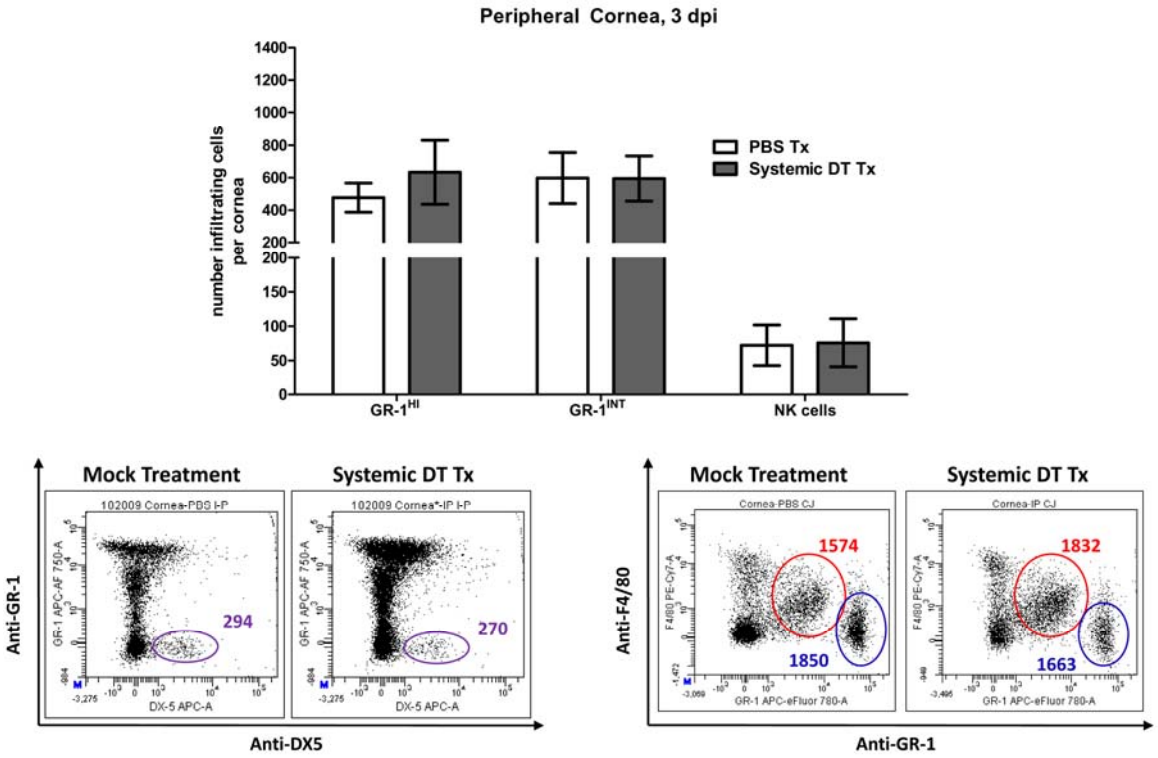

Figure 43 – Equivalent, or greater numbers of innate immune cells are present within the peripheral corneas of DT treated mice.

Naïve CD11c-DTR mice received subconjunctival injections of PBS or they received 150ng DT systemically via i.p. injection. 2 days following injections mice were ocular infected with HSV-1. At 3 dpi, corneas were harvested for flow cytometric analysis. The central cornea was removed via a 2mm trephine, and peripheral corneas were dispersed, stained with mAb to CD49b (DX5), F4/80, and GR-1. Graph depicts mean ± SEM absolute number of cells per cornea in PBS or Systemically DT Tx mice. Dot plots below graph indicate raw flow data from representative samples (each 5 pooled corneas). (n=7 samples (each 3-5 pooled corneas), 5 independent experiments).

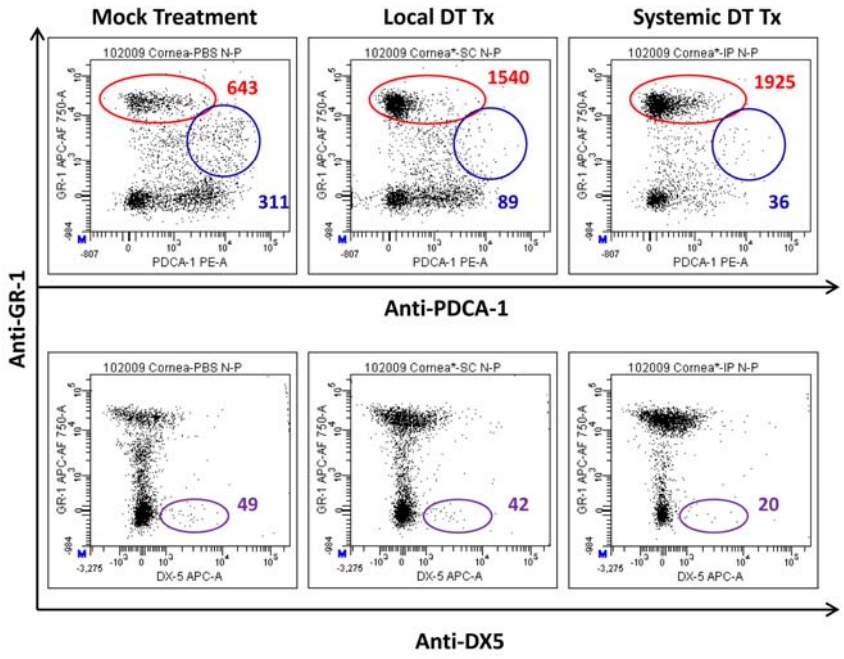

Figure 44 Innate immune cells are not present in large numbers in the naïve peripheral cornea.

Naïve CD11c-DTR mice received subconjunctival injections of PBS or they received 150ng DT systemically via i.p. injection. At 3 days post injection (which is 5 dpi for infected corneas), corneas were harvested for flow cytometric analysis. The central cornea was removed via a 2mm trephine, and peripheral corneas were dispersed, stained with mAb to CD49b (DX5), PDCA-1, and GR-1. Data are representative flow plots depicting the number of infiltrating innate immune cells into the peripheral corneas of WT controls, Mock Tx, Local DT, or systemically DT mice. Data is representative of 2 independent experiments, each with consisting of 5 pooled corneas.

When we observe the central corneas at 3 dpi, we see significant impairment in the infiltration of inflammatory monocytes (2 fold reduction), and NK cells (close to a 90% reduction) in DT treated mice (Figure 45). We do observe similar numbers of neutrophils within the central cornea following DT treatment, suggesting that only certain innate subsets were reliant on DCs to home to sites of viral infection. When taken together, we conclude DCs that infiltrate early after infection are required to direct recently extravasated NK cells and

inflammatory monocytes into the central cornea. PMNs do not appear to need local or early infiltrating DCs to migrate into the central cornea.

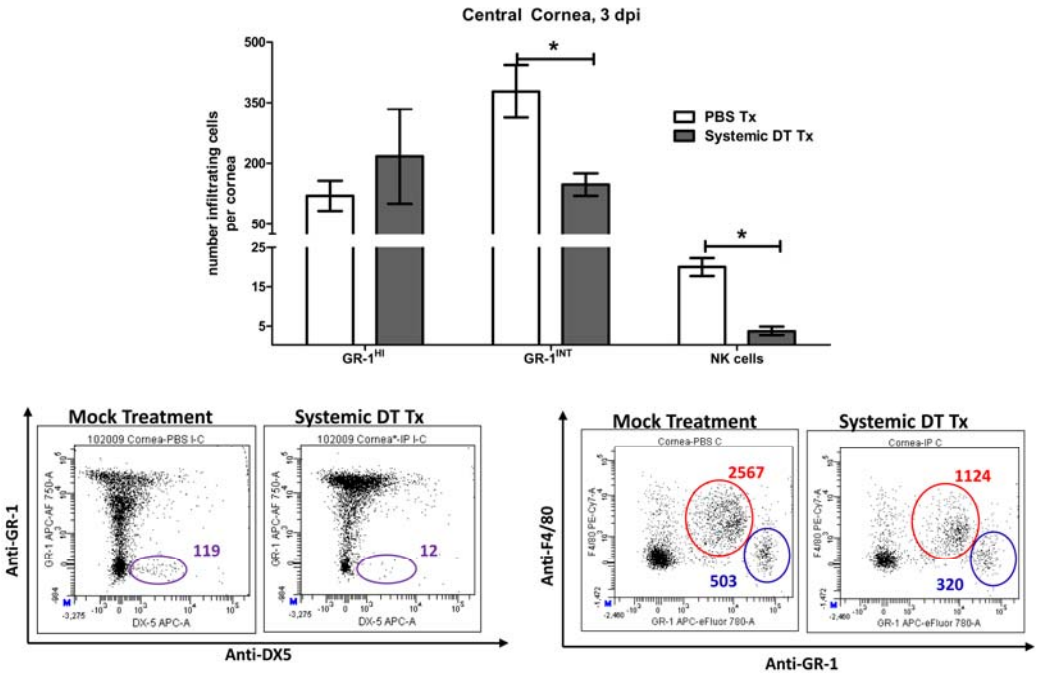

Figure 45 – Fewer NK cells and inflammatory monocytes enter the central cornea following DT Treatment at 3 dpi

Naïve CD11c-DTR mice received subconjunctival injections of PBS or they received 150ng DT systemically via i.p. injection. 2 days following injections mice were ocular infected with HSV-1. At 3 dpi, corneas were harvested for flow cytometric analysis. The central cornea was removed via a 2mm trephine, and peripheral corneas were dispersed, stained with mAb to CD49b (DX5), F4/80, and GR-1. Graph depicts mean ± SEM absolute number of cells per cornea in PBS or Systemically DT Tx mice. Dot plots below graph indicate raw flow data from representative samples (5 pooled corneas). (n=7 samples (each 3-5 pooled corneas), 5 independent experiments). * $p < .05$.

7.9 IFN-γ AND INOS ARE REDUCED THE CORNEAS OF DT TX MICE

Given that we see significantly fewer NK cells and inflammatory monocytes within the central cornea, we would expect that we would see a corresponding loss of effector mechanisms used by these subsets. NK cells, in addition to their lytic granules, have been reported to produce IFN-γ in response to viral infection (237). Inflammatory monocytes are potent producers of nitric oxide (NO) in models of viral infection (238). In 3 dpi corneas, we see a large upregulation of IFN-γ message over mock infected corneas in PBS treated mice (Figure 46). In contrast we see close to 100 fold less IFN-γ message within the corneas of DT treated mice after infection. We also observe a 2.5 fold less iNOS upregulation in the corneas of DT treated mice following infection. Both of these observations demonstrate a reduction in critical innate effector mechanisms needed to combat viral infection. Of interest was the observation that DT mice had impaired upregulation of IFN-γ even following mock infection of the eye (scarification, without the addition of virus). This likely indicates that either resident or early responding DCs play a role in the innate immune response to tissue damage, in addition to viral infection.

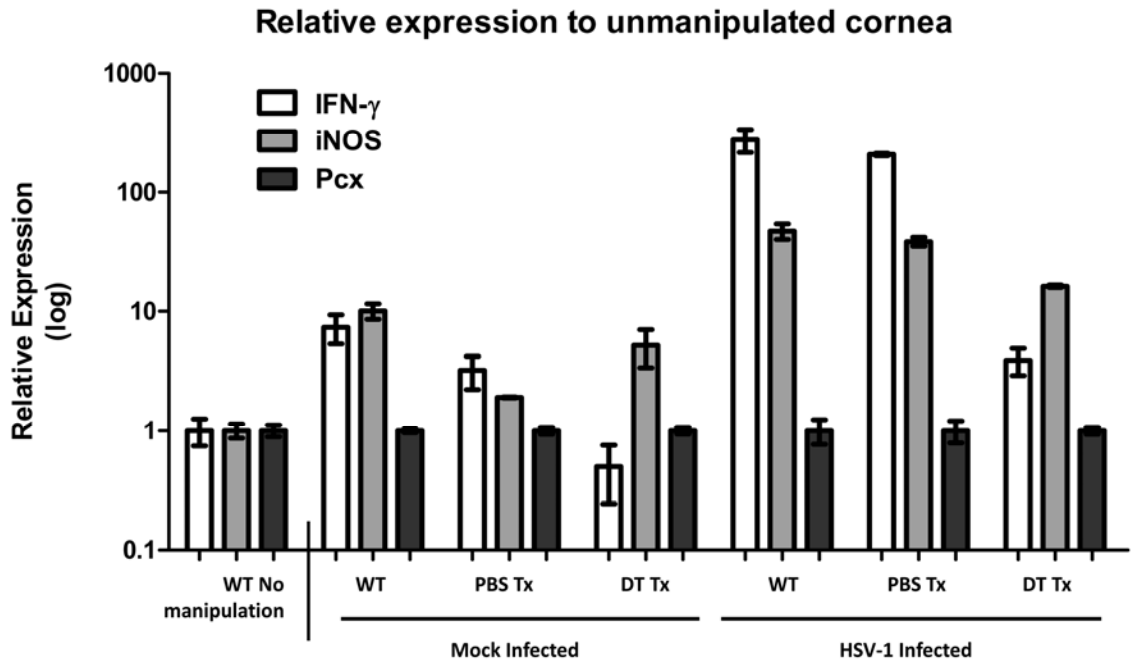

Figure 46 – IFN-γ and iNOS are reduced within the corneas of DT Tx mice at 3 dpi

Naïve CD11c-DTR mice received subconjunctival injections of PBS or they received 150ng DT systemically via i.p. injection. 2 days following injections mice were ocular infected with HSV-1. At 3 dpi, corneas were harvested for RNA isolation. cDNA was generated from isolated RNA, and quantitative real-time PCR was performed using primers to PCX (a house keeping gene), IFN-γ, and iNOS. Data is represented as mean ± SEM fold differences from an unmanipulated WT cornea. n=2 (3-4 pooled corneas) per group, 1 experiment.

7.10 DISCUSSION – CHAPTER SEVEN

A number of recent studies have found that peripheral DCs have divergent functions from that of transporting antigen to prime the adaptive immune response to invading pathogens. Notably epidermal resident LCs tend to play an immunomodulatory role against the immune response, while dermal resident LCs play classic role of mobilizing the immune system (65,66). Here we

find that local resident DCs do not appear to play a major role in the mobilization of either the innate or adaptive immune response to HSV-1 ocular infection. In fact, it appears that responding DCs that infiltrate into the cornea play a larger role in both control of virus within the cornea as well as initiating the adaptive immune response to HSV-1.

The finding there was no apparent role for local resident DCs in the control of HSV-1 infection was surprising. Also surprising was the observation that these cells are not phenotypically identified as LCs, as is the established dogma in corneal immune research (156). A number of researchers have hypothesized that LCs within the cornea may help to play an immunomodulatory role in order to protect corneal immune privilege. We saw no such change when we removed these cells prior to infection. Other than a minor delay in viral clearance, mice deficient in resident DCs ultimately clear virus and generate an adaptive immune response effectively. Studies using UV irradiation of the eye in A/J mice found that that removal of DCs from the corneal epithelium resulted in a reduced DTH response, suggesting a diminished adaptive immune response was being mobilized in response to HSV-1 (239). As the authors state, UV-B irradiation can ablate more than the observed DCs from the corneal epithelium. Depletion of other subsets along with the different strain of mouse used in these studies can arguably account for the differences seen in the role of local DCs seen here with our more specific CD11c-DTR depletion system. A number of recent studies have found that subsets other then the epidermal (in our case, epithelial) LC/DCs are more important in generating the adaptive immune response to HSV-1 and HSV-2, which appears similar to our observations in the ocular model of infection (64,67,240,241).

More profound were the effects when DCs were systemically depleted throughout or prior to HSV-1 infection. We observed that mice deficient of DCs only early after infection

were equally impaired in viral control as mice lacking DCs throughout, suggesting an early role of recruited DCs to site of infection. Recent studies have observed differential roles of DC subpopulations early after response to HSV-1 infection. In the model of flank infection, epidermal LCs emigrated from the tissue rapidly following viral encounter, after which a dermal resident DC population accumulated around the areas of viral infection (68). A second study, using a model of vaginal HSV-2 infection, observed a similar sub-epithelial accumulation of recruited DCs to the site of infection (241). While neither of these studies focused on the innate immune response, this accumulation of recruited DCs suggest these cells could be playing a local role in the innate immune response to viral infection. In our model, -2 dpi depleted DCs should recover by 2-3 days following infection; therefore DCs would be available to respond within 48 hours following HSV-1 infection (229). This demonstrates a critical window for DC function within the cornea.

In HSV-1 ocular infection, γδ T cells, NK cells, and PMNs have all been assigned important roles in control of HSV-1 ocular infection (52 – 55). We observe fewer NK cells and inflammatory monocytes within the central cornea following DC depletion. Also, we observe significant reductions in IFN-γ and iNOS, both the primary effector mechanisms of these cells, respectively. What are the potential roles DCs play in directing these cells to control virus in the cornea? DC interplay with the innate immune response has been well documented. Particularly, DCs have been assigned a critical role in the survival and function of NK cells by a large body of work (70,230,233,242). IL-15 in particular has been identified as the primary mechanism of DC mediated activation of NK cell function (71). DCs are necessary to prime NK cells in the lymphoid organs, after which they migrate to the periphery and exert their effector functions at the site of infection. However this study observed a rapid recovery of NK cell functionality as

soon as DCs recovered. In contrast, we observe impaired viral control up to a week following infection in mice only depleted of DCs prior to infection. Less has been established concerning a direct role of DCs in macrophage activation. A number of studies have also implicated NK cells and their cytokines in the activation of monocytes, however (59,243). Given our observations, it possible that the lack of NK cells at the site of infection results in less macrophage activation, and thus fewer inflammatory monocytes at the site of infection. Further experimentations that remove NK cells from the cornea are required to address these hypotheses adequately. Taken together, our observations suggest two possibilities: either NK cell activation by DCs is critical for viral control early after infection, or that a local role of DCs is needed at the site of viral infection.

We believe the latter hypothesis may be correct. We do see drastic diminishment of innate immune infiltration to the sites of viral replication within the cornea following DC ablation. Both NK cells and inflammatory monocytes did not effectively enter the central cornea following systemic DT treatment. Similar numbers of these were cells are present within the peripheral tissues of the cornea. This suggests the innate immune cells are capable entering the cornea from the blood vessels, but are unable to migrate to the site of viral replication. In contrast it appears that PMN neutrophil infiltration into the central cornea was unaffected by DC ablation. This observation points to a different mechanism of PMN infiltration into the central cornea when compared to that of NK cells and monocytes. Given the PMN neutrophil role of "first responding" innate immune cells, it is reasonable that these cells have large amount of redundancy in their chemotactic machinery (244). Regardless, it appears these PMN neutrophils present within the cornea of DC ablated mice are either unable to control viral replication alone, or are functionally impaired, given the high viral load within the cornea. Both possibilities point

to the necessity of a combined innate immune response for control HSV-1. We have also not observed whether the infiltration of γδ T cells is impeded following DC ablation. Given their important role in viral control in the cornea we plan to include this subset in future experimentation.

What are the potential DC directed chemokines and cytokines that direct the homing of these cells to the site of infection? In the context of HSK, IL-2 has been implicated in infiltration of PMN neutrophils into the central cornea as well as their survival (245). Another study observed IL-6 drove MIP-1α and MIP-2 production by DCs in the cornea to promote infiltration of PMN neutrophils into the cornea (225). In mice lacking CCR5, PMN neutrophil infiltration into the infected cornea was diminished (246). These studies may be instructive to what is needed for the infiltration of inflammatory monocytes and NK cells. Few studies observed the chemokines needed for NK cells and inflammatory monocyte homing within the cornea. However a studies in the context of other infections have implicated a large number of chemokines in the migration of these cells (247,248). Given the complex redundancies that exist in chemokine function, it is likely a large number of chemokines are produced either directly or indirectly by early responding DCs. While neutrophils may be capable of infiltrating to danger signals and other viral replication induced factors, noted DC produced chemokines such as these may be integral for the proper homing of other innate immune cells to the site of infection. Further experimentation will be needed to dissect the role of chemokines in innate immune migration into the central cornea, and how local responding DCs contribute to these processes.

We found that removal of DCs also has a dramatic effect on the adaptive immune response. In continuously DC depleted mice, we saw over a tenfold decline in the frequency of HSV-1 reactive cells within the DLN at 7 dpi. Viral antigen can travel directly down the

lymphatics directly to the DLNs, where other APCs, such as macrophages or B cells can present these antigens, albeit with a reduced efficiency to prime the adaptive immune response (249). We believe these factors could account for the remaining reactivity in continuously DC ablated mice.

In mice depleted only of DCs systemically prior to infection, we saw an approximate 50% reduction in IFN-γ response to HSV-1 from DLN $CD4^+$ T cells. Given this intermediate impairment of the adaptive immune response, it could be that the delay in DCs in reaching the cornea, and presenting the antigen within the DLNs could be explain this reduction in the adaptive immune response. Further study will be needed to clarify if there is an ancillary role of early responding DCs in the priming of the adaptive immune response, or if this is a delay in the kinetics of the immune response. In either case, the adaptive immune response only contributes to viral control within the cornea late in the infection (6-8 dpi), suggesting against the possibility that deficiencies in the adaptive immune response is accounting for the viral control in the cornea early (37,250). Nevertheless, this hypothesis will need to be clarified with further experimentation.

To conclude this chapter, our model of DT treatment can ablate DCs to observe their role both temporally and spatially within the context of HSV-1 corneal infection. We observed resident DCs within the cornea at the time of infection are not absolutely necessary to generate the adaptive immune response, although they may play a minor role in the innate directed control of virus early after infection. In contrast, early recruited DCs appear to play a more important role in directing the innate immune response to HSV-1. We suspect this to be a local role, which may be in the production of a chemotactic gradient which directs innate immune responders to the site of infection from the peripheral cornea. While more experimental approaches will be

needed to clarify these questions, we believe that this study represents an unappreciated role of recruited DCs in mobilizing localized innate responses to viral infection.

8.0 SUMMARY AND CONCLUDING REMARKS

The mechanisms that drive the normally protective immune response to that of a damaging pathology consist of a variety of complex factors. The pathology of herpes stromal keratitis is no exception. The immune response can direct a protective mechanism that minimizes viral replication and reactivation. It can also drive a more damaging dysregulated immune response that ultimately leads to corneal blindness.

Our group and others have observed the importance of a strong HSV-CD8 response in the control of HSV-1 reactivation from latently infected neurons. Here we demonstrate $CD4^+$ T cells provide important aid to these $CD8^+$ T cells during their priming and expansion which we suspect regulates the threshold of TCR stimulation that causes PD-1 upregulation. This help allows HSV-CD8 to remain functionally competent within the TG, where these cells experience high levels of antigen and PD-1 ligands over a long period of time. Thus CD4 T cells provide important signals that help the immune system combat HSV-1 viral infection.

In contrast to the supporting role in the context of $CD8^+$ T cell immunosurveillance of latency, $CD4^+$ T cells are the main orchestrators of HSK. This immune mediated disease overwhelms the anti-inflammatory protections in place within the cornea, resulting in progressive damage to corneal architecture and blindness. Understanding why $CD4^+$ T cells drive HSK is paramount to developing therapeutic treatments. Here we identified HSV-1 specific $CD4^+$ T cells from the HSK-inflamed cornea. We found that these cells responded to

glycoprotein B. More importantly, we identified that while these cells retained an identical TCR, some cells appeared to be TH1 cells while other cells were TH17. Unfortunately we were unable to demonstrate these cells were able to initiate HSK, due to differences in expression of adhesion molecules compared to that of effector cells *in vivo*. Nevertheless our findings do raise a number of interesting concepts to how HSK is initiated. The cornea microenvironment usually has large amounts of TGF-β, an immunomodulating cytokine. As TH1 $CD4^+$ T cells respond to the HSV-1 infected cornea, they encounter large amounts of TGF-β, along with inflammatory cytokines such as IL-6. It is possible this combination of cytokines (known to drive differentiation of inflammatory TH-17 cells) might promote peripheral differentiation of non-pathogenic TH1 cells to pathogenic TH17 cells. Given that TH-17 cells have been implicated in a large number of immunopathologies, it is reasonable that these newly minted TH-17 cells initiate the cascade of events that leads to HSK. If these hypotheses hold true, we would have a situation where the barriers put into place by the cornea to combat excessive inflammation may, in fact, drive just that. Regardless of the mechanism, here we can see two clear examples in the murine model of HSV-1 ocular infection where $CD4^+$ T cells can provide both helpful and pathological signals to the immune response to HSV-1.

Dendritic cells are the sentinels of the immune system as well as an important line of communications between the innate and adaptive immune response. Here we observed what DCs do to contribute to the local innate immune response early after HSV-1 ocular infection. We found when DCs were removed from the cornea prior to infection viral control was impaired during the first week of infection. In the absence of DCs, certain innate immune responders, notably inflammatory monocytes and NK cells were unable to traffic from the peripheral cornea to the sites of viral infection in the central cornea. We hypothesize that DCs must respond early

to infection in order to drive the production of the chemokine gradient the innate immune response requires to home to sites of infection *in situ.* This data forwards a concept where in addition to their role in activating the adaptive immune response, DCs can play a local role in directing the innate immune response at the site of infection.

A number of studies have also implicated APCs in helping to drive HSK. Here we found that IL-12p70, a cytokine classically produced by APCs, is important for HSK. We find that mice lacking the subunit IL-12p35 develop transient HSK. These observations hold true even when mice lack both IL-12p35 and p40. In mice lacking IL-12p35 we see significant reductions in soluble factors important for HSK (VEGF, MCP-1, and KC). Based on these findings we conclude IL-12p35 is operating in an IL-12p40 independent fashion that contributes to HSK progression. While we did not establish DCs were the source of this cytokine, a large body of work would indicate APCs, whether DCs or macrophages, are the probable source of these cytokines. Here, as with CD4+ T cells, we see that DCs can also aid in controlling viral replication or assist in immunopathology in response to HSV-1.

A large number of immune-mediated diseases exist within the clinic; only through enhanced understanding of *both* the protective and pathogenic roles of infiltrating can we better understand these diseases and devise effective therapy. When it comes to ocular HSV-1 infection, we must be cautious that attempts to enhance immune surveillance of latently infected neurons do not lead to exacerbation of immunopathology in the infected cornea. A better understanding of the mechanisms of HSK and immune protection from HSV-1 reactivation from latency will enhance prospects for developing therapeutic vaccines capable of enhancing protection while minimizing immunopathology. . In the context of this body of work, understanding $CD4^+$ T cell and DC functions help further us along our path of understanding

both the beneficial and detrimental effects of the immune response to HSV-1. This data and the studies it will lead to not only allow us to better design therapeutic vaccines to HSV-1 and potentially HSK, but contribute to the understanding of the immune response in a general fashion. This will help provide the building blocks other models of infection can use to understand their respective mechanisms of immune control and pathogenesis.

APPENDIX A

[LIST OF WORKS PUBLISHED]

1) **Frank GM** and Hendricks RL (2010) "First responding" dendritic cells, but not resident dendritic cells are critical for mobilizing the innate immune response to herpes simplex virus ocular infection. Manuscript in preparation.
2) **Frank GM,** Lepisto AJ, Freeman ML, Hendricks RL (2010) $CD8^+$ T cell memory generated without $CD4^+$ help is transiently compromised in latent infection. Journal of Immunology. 1;184(1):277-86.
3) **Frank GM**, Divito, SJ, Xu M, Maker DM, Hendricks RL (2010) A novel p40-independent function of IL-12p35 is required for progression and maintenance of herpes stromal keratitis. In Press. Investigative Ophthalmology and Visual Science.
4) Buela KA, **Frank GM**, Knickelbein, JE, Hendricks RL (2009) Eye Chapter 12: Immunopathogenesis of HSV Keratitis. Encyclopedia of the Eye.
5) **Frank GM** and Hendricks RL (2007) Recent Developments in Herpes Stromal Keratitis. Essentials of Ophthalmology.
6) Lepisto AJ, **Frank GM**, Hendricks RL (2007) How herpes simplex virus type 1 (HSV-1) rescinds corneal privilege. Chemical Immunology. 92:203-12.
7) Sheridan BS, Khanna KM, **Frank GM**, Hendricks RL (2006) Latent virus influences the generation and maintenance of $CD8^+$ T cell Memory. Journal of Immunology. 177(12):8356-64.

8) Lepisto AJ, **Frank GM,** Xu M, Stuart PM, Hendricks RL (2006) $CD8^+$ T cells mediate transient herpes stromal keratitis (HSK) in CD4 deficient mice. Investigative Ophthalmology and Visual Science. 47(8):3400-9.

BIBLIOGRAPHY

Bibliography

1. Xu, F., M. R. Sternberg, B. J. Kottiri, G. M. McQuillan, F. K. Lee, A. J. Nahmias, S. M. Berman, and L. E. Markowitz. 2006. Trends in herpes simplex virus type 1 and type 2 seroprevalence in the United States. *JAMA* 296:964-973.

2. Smith, J. S., M. Rosinska, A. Trzcinska, J. M. Pimenta, B. Litwinska, and J. Siennicka. 2006. Type specific seroprevalence of HSV-1 and HSV-2 in four geographical regions of Poland. *Sex Transm.Infect.* 82:159-163.

3. Smith, J. S. and N. J. Robinson. 2002. Age-specific prevalence of infection with herpes simplex virus types 2 and 1: a global review. *J.Infect.Dis.* 186 Suppl 1:S3-28.

4. Whitley RJ. 1996. Herpes simplex viruses. In *Fields virology, 3rd ed.* Fields BN et al, ed. Lippincott-Raven, Philadelphia, pp. 2297-2342.

5. Roberts, C. M., J. R. Pfister, and S. J. Spear. 2003. Increasing proportion of herpes simplex virus type 1 as a cause of genital herpes infection in college students. *Sex Transm.Dis.* 30:797-800.

6. Decman, V., M. L. Freeman, P. R. Kinchington, and R. L. Hendricks. 2005. Immune Control of HSV-1 Latency. *Viral Immunol* 18:466-473.

7. Liesegang, T. J., L. J. Melton, P. J. Daly, and D. M. Ilstrup. 1989. Epidemiology of ocular herpes simplex. Incidence in Rochester, MN, 1950 through 1982. *Arch.Ophthalmol.* 107:1155-1159.

8. Liesegang, T. J. 2001. Herpes simplex virus epidemiology and ocular importance. *Cornea* 20:1-13.

9. Cosar, C. B., M. S. Sridhar, E. J. Cohen, E. L. Held, T. Alvim Pde, C. J. Rapuano, I. M. Raber, and P. R. Laibson. 2002. Indications for penetrating keratoplasty and associated procedures, 1996-2000. *Cornea* 21:148-151.

10. Whitley, R. J. 1985. Therapy for human herpesvirus infections. A perspective. *Ala.J.Med.Sci.* 22:193-207.

11. Roizman, B. and D. M. Knipe. 2001. Herpes simplex viruses and their replication. In *Fields Virology*. Fields BN, ed. Lippincott-Raven, Philadelphia, pp. 2399-2459.

12. Koelle, D. M. and L. Corey. 2003. Recent progress in herpes simplex virus immunobiology and vaccine research. *Clin.Microbiol.Rev.* 16:96-113.

13. Divito, S., T. L. Cherpes, and R. L. Hendricks. 2006. A triple entente: virus, neurons, and CD8+ T cells maintain HSV-1 latency. *Immunol.Res.* 36:119-126.

14. Pinnoji, R. C., G. R. Bedadala, B. George, T. C. Holland, J. M. Hill, and S. C. Hsia. 2007. Repressor element-1 silencing transcription factor/neuronal restrictive silencer factor (REST/NRSF) can regulate HSV-1 immediate-early transcription via histone modification. *Virol.J.* 4:56.

15. Steiner, I., J. G. Spivack, D. R. O'Boyle, E. Lavi, and N. W. Fraser. 1988. Latent herpes simplex virus type 1 transcription in human trigeminal ganglia. *J.Virol.* 62:3493-3496.

16. Stevens, J. G., E. K. Wagner, G. B. Devi-Rao, M. L. Cook, and L. T. Feldman. 1987. RNA complementary to a herpesvirus alpha gene mRNA is prominent in latently infected neurons. *Science* 235:1056-1059.

17. Stevens, J. G., L. Haarr, D. D. Porter, M. L. Cook, and E. K. Wagner. 1988. Prominence of the herpes simplex virus latency-associated transcript in trigeminal ganglia from seropositive humans. *J.Infect.Dis.* 158:117-123.

18. Javier, R. T., J. G. Stevens, V. B. Dissette, and E. K. Wagner. 1988. A herpes simplex virus transcript abundant in latently infected neurons is dispensable for establishment of the latent state. *Virology* 166:254-257.

19. Sedarati, F., K. M. Izumi, E. K. Wagner, and J. G. Stevens. 1989. Herpes simplex virus type 1 latency-associated transcription plays no role in establishment or maintenance of a latent infection in murine sensory neurons. *J.Virol.* 63:4455-4458.

20. Ho, D. Y. and E. S. Mocarski. 1989. Herpes simplex virus latent RNA (LAT) is not required for latent infection in the mouse. *Proc.Natl.Acad.Sci.U.S.A* 86:7596-7600.

21. Thompson, R. L. and N. M. Sawtell. 2001. Herpes simplex virus type 1 latency-associated transcript gene promotes neuronal survival. *J.Virol.* 75:6660-6675.

22. Perng, G. C., C. Jones, J. Ciacci-Zanella, M. Stone, G. Henderson, A. Yukht, S. M. Slanina, F. M. Hofman, H. Ghiasi, A. B. Nesburn, and S. L. Wechsler. 2000. Virus-induced neuronal apoptosis blocked by the herpes simplex virus latency-associated transcript. *Science* 287:1500-1503.

23. Margolis, T. P., Y. Imai, L. Yang, V. Vallas, and P. R. Krause. 2007. Herpes simplex virus type 2 (HSV-2) establishes latent infection in a different population of ganglionic neurons than HSV-1: role of latency-associated transcripts. *J.Virol.* 81:1872-1878.

24. Umbach, J. L., M. F. Kramer, I. Jurak, H. W. Karnowski, D. M. Coen, and B. R. Cullen. 2008. MicroRNAs expressed by herpes simplex virus 1 during latent infection regulate viral mRNAs. *Nature*.

25. Sawtell, N. M. and R. L. Thompson. 1992. Rapid in vivo reactivation of herpes simplex virus in latently infected murine ganglionic neurons after transient hyperthermia. *J.Virol.* 66:2150-2156.

26. Padgett, D. A., J. F. Sheridan, J. Dorne, G. G. Berntson, J. Candelora, and R. Glaser. 1998. Social stress and the reactivation of latent herpes simplex virus type 1. *Proc.Natl.Acad.Sci.U.S.A.* 95:7231-7235.

27. Pereira, D. B., M. H. Antoni, A. Danielson, T. Simon, J. Efantis-Potter, C. S. Carver, R. E. Duran, G. Ironson, N. Klimas, M. A. Fletcher, and M. J. O'Sullivan. 2003. Stress as a predictor of symptomatic genital herpes virus recurrence in women with human immunodeficiency virus. *J Psychosom.Res.* 54:237-244.

28. Sainz, B., J. M. Loutsch, M. E. Marquart, and J. M. Hill. 2001. Stress-associated immunomodulation and herpes simplex virus infections. *Med.Hypotheses* 56:348-356.

29. Freeman, M. L., B. S. Sheridan, R. H. Bonneau, and R. L. Hendricks. 2007. Psychological stress compromises CD8(+) T cell control of latent herpes simplex virus type 1 infections. *J.Immunol.* 179:322-328.

30. Posavad, C. M., D. M. Koelle, M. F. Shaughnessy, and L. Corey. 1997. Severe genital herpes infections in HIV-infected individuals with impaired herpes simplex virus-specific CD8+ cytotoxic T lymphocyte responses. *Proc.Natl.Acad.Sci.U.S.A.* 94:10289-10294.

31. Porteous, C., J. A. Bradley, D. N. Hamilton, I. M. Ledingham, G. B. Clements, and C. G. Robinson. 1984. Herpes simplex virus reactivation in surgical patients. *Crit.Care Med.* 12:626-628.

32. Dohlman, C. H. 1971. The function of the corneal epithelium in health and disease. The Jonas S. Friedenwald Memorial Lecture. *Invest Ophthalmol.* 10:383-407.

33. Marchant, J. K., G. Zhang, and D. E. Birk. 2002. Association of type XII collagen with regions of increased stability and keratocyte density in the cornea. *Exp.Eye Res.* 75:683-694.

34. Patel, S., D. Z. Reinstein, R. H. Silverman, and D. J. Coleman. 1998. The shape of Bowman's layer in the human cornea. *J.Refract.Surg.* 14:636-640.

35. Bron, A. J. 2001. The architecture of the corneal stroma. *Br.J.Ophthalmol.* 85:379-381.

36. Meek, K. M. and C. Boote. 2009. The use of X-ray scattering techniques to quantify the orientation and distribution of collagen in the corneal stroma. *Prog.Retin.Eye Res.* 28:369-392.

37. Biswas, P. S. and B. T. Rouse. 2005. Early events in HSV keratitis--setting the stage for a blinding disease. *Microbes.Infect.* 7:799-810.

38. O'Brien, W. J., M. L. Palmer, J. Guy, and J. L. Taylor. 1996. Endothelial barrier function and Na+/K(+)-ATPase pump density in herpetic stromal disease. *Invest Ophthalmol.Vis.Sci.* 37:29-36.

39. Bonanno, J. A. 2003. Identity and regulation of ion transport mechanisms in the corneal endothelium. *Prog.Retin.Eye Res.* 22:69-94.

40. Ambati, B. K., M. Nozaki, N. Singh, A. Takeda, P. D. Jani, T. Suthar, R. J. Albuquerque, E. Richter, E. Sakurai, M. T. Newcomb, M. E. Kleinman, R. B. Caldwell, Q. Lin, Y. Ogura, A. Orecchia, D. A. Samuelson, D. W. Agnew, J. St Leger, W. R. Green, P. J. Mahasreshti, D. T. Curiel, D. Kwan, H. Marsh, S. Ikeda, L. J. Leiper, J. M. Collinson, S. Bogdanovich, T. S. Khurana, M. Shibuya, M. E. Baldwin, N. Ferrara, H. P. Gerber, S. De Falco, J. Witta, J. Z. Baffi, B. J. Raisler, and J. Ambati. 2006. Corneal avascularity is due to soluble VEGF receptor-1. *Nature* 443:993-997.

41. Niederkorn, J. Y. 2007. Immune mechanisms of corneal allograft rejection. *Curr.Eye Res.* 32:1005-1016.

42. Hori, J. and J. Y. Niederkorn. 2007. Immunogenicity and immune privilege of corneal allografts. *Chem.Immunol.Allergy* 92:290-299.

43. Mochizuki, M., S. Sugita, N. Ishikawa, and T. Watanabe. 2000. Immunoregulation by aqueous humor. *Cornea* 19:S24-S25.

44. Jampel, H. D., N. Roche, W. J. Stark, and A. B. Roberts. 1990. Transforming growth factor-beta in human aqueous humor. *Curr.Eye Res.* 9:963-969.

45. Granstein, R. D., R. Staszewski, T. L. Knisely, E. Zeira, R. Nazareno, M. Latina, and D. M. Albert. 1990. Aqueous humor contains transforming growth factor-beta and a small (<3500 daltons) inhibitor of thymocyte proliferation. *J.Immunol.* 144:3021-3027.

46. Streilein, J. W., S. Okamoto, Y. Sano, and A. W. Taylor. 2000. Neural control of ocular immune privilege. *Ann.N.Y.Acad.Sci.* 917:297-306.

47. Hamrah, P., Q. Zhang, Y. Liu, and M. R. Dana. 2002. Novel characterization of MHC class II-negative population of resident corneal Langerhans cell-type dendritic cells. *Investigative Ophthalmology & Visual Science* 43:639-646.

48. Hamrah, P., Y. Liu, Q. Zhang, and M. R. Dana. 2003. The corneal stroma is endowed with a significant number of resident dendritic cells. *Investigative Ophthalmology & Visual Science* 44:581-589.

49. Brissette-Storkus, C. S., S. M. Reynolds, A. J. Lepisto, and R. L. Hendricks. 2002. Identification of a novel macrophage population in the normal mouse corneal stroma. *Invest Ophthalmol Vis Sci* 43:2264-2271.

50. Chinnery, H. R., E. Pearlman, and P. G. McMenamin. 2008. Cutting edge: Membrane nanotubes in vivo: a feature of MHC class II+ cells in the mouse cornea. *J.Immunol.* 180:5779-5783.

51. Hendricks, R. L., P. C. Weber, J. L. Taylor, A. Koumbis, T. M. Tumpey, and J. C. Glorioso. 1991. Endogenously produced interferon alpha protects mice from herpes simplex virus type 1 corneal disease. *J Gen Virol* 72 (Pt 7):1601-1610.

52. Liu, T., Q. Tang, and R. L. Hendricks. 1996. Inflammatory infiltration of the trigeminal ganglion after herpes simplex virus type 1 corneal infection. *J.Virol.* 70:264-271.

53. Heiligenhaus, A., D. Bauer, M. Zheng, S. Mrzyk, and K. P. Steuhl. 1999. CD4+ T-cell type 1 and type 2 cytokines in the HSV-1 infected cornea. *Graefes Arch.Clin.Exp.Ophthalmol.* 237:399-406.

54. Ghiasi, H., S. Cai, G. C. Perng, A. B. Nesburn, and S. L. Wechsler. 2000. The role of natural killer cells in protection of mice against death and corneal scarring following ocular HSV-1 infection. *Antiviral Res.* 45:33-45.

55. Carr, D. J., P. Harle, and B. M. Gebhardt. 2001. The immune response to ocular herpes simplex virus type 1 infection. *Exp.Biol.Med.(Maywood.)* 226:353-366.

56. Shimeld, C., S. Efstathiou, and T. Hill. 2001. Tracking the spread of a lacZ-tagged herpes simplex virus type 1 between the eye and the nervous system of the mouse: comparison of primary and recurrent infection. *J.Virol.* 75:5252-5262.

57. Kodukula, P., T. Liu, N. V. Rooijen, M. J. Jager, and R. L. Hendricks. 1999. Macrophage control of herpes simplex virus type 1 replication in the peripheral nervous system. *J Immunol* 162:2895-2905.

58. Sciammas, R., P. Kodukula, Q. Tang, R. L. Hendricks, and J. A. Bluestone. 1997. T cell receptor-gamma/delta cells protect mice from herpes simplex virus type 1-induced lethal encephalitis. *J Exp Med* 185:1969-1975.

59. Heise, M. T. and H. W. Virgin. 1995. The T-cell-independent role of gamma interferon and tumor necrosis factor alpha in macrophage activation during murine cytomegalovirus and herpes simplex virus infections. *J.Virol.* 69:904-909.

60. Shortman, K. and Y. J. Liu. 2002. Mouse and human dendritic cell subtypes. *Nat.Rev.Immunol.* 2:151-161.

61. Wolff, K. and R. K. Winkelmann. 1967. Quantitative studies on the Langerhans cell population of guninea pig epidermis. *J.Invest.Dermatol.* 48:504-513.

62. Kaisho, T. and S. Akira. 2001. Dendritic-cell function in Toll-like receptor- and MyD88-knockout mice. *Trends Immunol.* 22:78-83.

63. Kaisho, T. and S. Akira. 2001. Toll-like receptors and their signaling mechanism in innate immunity. *Acta Odontol.Scand.* 59:124-130.

64. Allan, R. S., C. M. Smith, G. T. Belz, A. L. van Lint, L. M. Wakim, W. R. Heath, and F. R. Carbone. 2003. Epidermal viral immunity induced by CD8 alpha(+) dendritic cells but not by Langerhans cells. *Science* 301:1925-1928.

65. Bursch, L. S., L. Wang, B. Igyarto, A. Kissenpfennig, B. Malissen, D. H. Kaplan, and K. A. Hogquist. 2007. Identification of a novel population of Langerin+ dendritic cells. *J.Exp.Med.* 204:3147-3156.

66. Kaplan, D. H., M. C. Jenison, S. Saeland, W. D. Shlomchik, and M. J. Shlomchik. 2005. Epidermal Langerhans cell-deficient mice develop enhanced contact hypersensitivity. *Immunity* 23:611-620.

67. Bedoui, S., P. G. Whitney, J. Waithman, L. Eidsmo, L. Wakim, I. Caminschi, R. S. Allan, M. Wojtasiak, K. Shortman, F. R. Carbone, A. G. Brooks, and W. R. Heath. 2009. Cross-presentation of viral and self antigens by skin-derived CD103+ dendritic cells. *Nat.Immunol.* 10:488-495.

68. Eidsmo, L., R. Allan, I. Caminschi, N. van Rooijen, W. R. Heath, and F. R. Carbone. 2009. Differential migration of epidermal and dermal dendritic cells during skin infection. *J.Immunol.* 182:3165-3172.

69. Ferlazzo, G., D. Thomas, S. L. Lin, K. Goodman, B. Morandi, W. A. Muller, A. Moretta, and C. Munz. 2004. The abundant NK cells in human secondary lymphoid tissues require activation to express killer cell Ig-like receptors and become cytolytic. *J.Immunol.* 172:1455-1462.

70. Ferlazzo, G., M. Pack, D. Thomas, C. Paludan, D. Schmid, T. Strowig, G. Bougras, W. A. Muller, L. Moretta, and C. Munz. 2004. Distinct roles of IL-12 and IL-15 in human natural killer cell activation by dendritic cells from secondary lymphoid organs. *Proc.Natl.Acad.Sci.U.S.A* 101:16606-16611.

71. Lucas, M., W. Schachterle, K. Oberle, P. Aichele, and A. Diefenbach. 2007. Dendritic cells prime natural killer cells by trans-presenting interleukin 15. *Immunity.* 26:503-517.

72. Mosmann, T. R., H. Cherwinski, M. W. Bond, M. A. Giedlin, and R. L. Coffman. 1986. Two types of murine helper T cell clones. I. Definition according to profiles of lymphokine activities and secreted proteins. *J.Immunol.* 136:2348-2357.

73. Ahmed, R., L. D. Butler, and L. Bhatti. 1988. $T4^+$ T helper cell function in vivo: Differential requirement for induction of antiviral cytotoxic T-cell and antibody responses. *J.Virol.* 62:2102-2106.

74. Kopf, M., G. Le Gros, M. Bachmann, M. C. Lamers, H. Bluethmann, and G. Kohler. 1993. Disruption of the murine IL-4 gene blocks Th2 cytokine responses. *Nature* 362:245-248.

75. Weaver, C. T., L. E. Harrington, P. R. Mangan, M. Gavrieli, and K. M. Murphy. 2006. Th17: an effector CD4 T cell lineage with regulatory T cell ties. *Immunity* 24:677-688.

76. Marie, J. C., J. J. Letterio, M. Gavin, and A. Y. Rudensky. 2005. TGF-beta 1 maintains suppressor function and Foxp3 expression in CD4(+)CD25(+) regulatory T cells. *J.Exp.Med.* 201:1061-1067.

77. Dai, Z., Q. Li, Y. Wang, G. Gao, L. S. Diggs, G. Tellides, and F. G. Lakkis. 2004. CD4+CD25+ regulatory T cells suppress allograft rejection mediated by memory CD8+ T cells via a CD30-dependent mechanism. *J.Clin.Invest* 113:310-317.

78. Sundstedt, A., E. J. O'Neill, K. S. Nicolson, and D. C. Wraith. 2003. Role for IL-10 in suppression mediated by peptide-induced regulatory T cells in vivo. *J.Immunol.* 170:1240-1248.

79. Gesser, R. M., T. Valyi-Nagy, and N. W. Fraser. 1994. Restricted herpes simplex virus type 1 gene expression within sensory neurons in the absence of functional B and T lymphocytes. *Virology* 200:791-795.

80. Simmons, A. and D. C. Tscharke. 1992. Anti-CD8 impairs clearance of herpes simplex virus from the nervous system: implications for the fate of virally infected neurons. *J.Exp.Med.* 175:1337-1344.

81. Griffiths, G. M. 1995. The cell biology of CTL killing. *Curr.Opin.Immunol.* 7:343-348.

82. Lenschow, D. J., T. L. Walunas, and J. A. Bluestone. 1996. CD28/B7 system of T cell costimulation. *Annu.Rev.Immunol.* 14:233.

83. Sperling, A. I. and J. A. Bluestone. 1996. The complexities of T-cell co-stimulation: CD28 and beyond. *Immunol.Rev.* 153:155-182.

84. Orange, J. S. and C. A. Biron. 1997. An absolute and restricted requirement for IL-12 in natural killer cell IFN-γ production and antiviral defense. *J.Immunol.* 156:1138-1142.

85. Yap, G., M. Pesin, and A. Sher. 2000. Cutting edge: IL-12 is required for the maintenance of IFN-gamma production in T cells mediating chronic resistance to the intracellular pathogen, Toxoplasma gondii. *J.Immunol.* 165:628-631.

86. Butz, E. A. and M. J. Bevan. 1998. Massive expansion of antigen-specific CD8+ T cells during an acute virus infection. *Immunity* 8:167-175.

87. Schluns, K. S. and L. Lefrancois. 2003. Cytokine control of memory T-cell development and survival. *Nat.Rev.Immunol.* 3:269-279.

88. Chang, J. T., V. R. Palanivel, I. Kinjyo, F. Schambach, A. M. Intlekofer, A. Banerjee, S. A. Longworth, K. E. Vinup, P. Mrass, J. Oliaro, N. Killeen, J. S. Orange, S. M. Russell, W. Weninger, and S. L. Reiner. 2007. Asymmetric T lymphocyte division in the initiation of adaptive immune responses. *Science* 315:1687-1691.

89. Kaech, S. M., J. T. Tan, E. J. Wherry, B. T. Konieczny, C. D. Surh, and R. Ahmed. 2003. Selective expression of the interleukin 7 receptor identifies effector CD8 T cells that give rise to long-lived memory cells. *Nat.Immunol.* 4:1191-1198.

90. Hand, T. W., M. Morre, and S. M. Kaech. 2007. Expression of IL-7 receptor alpha is necessary but not sufficient for the formation of memory CD8 T cells during viral infection. *Proc.Natl.Acad.Sci.U.S.A* 104:11730-11735.

91. Joshi, N. S., W. Cui, A. Chandele, H. K. Lee, D. R. Urso, J. Hagman, L. Gapin, and S. M. Kaech. 2007. Inflammation directs memory precursor and short-lived effector CD8(+) T cell fates via the graded expression of T-bet transcription factor. *Immunity.* 27:281-295.

92. Sallusto, F., J. Geginat, and A. Lanzavecchia. 2004. Central memory and effector memory T cell subsets: function, generation, and maintenance. *Annu.Rev.Immunol* 22:745-763.

93. Masopust, D., V. Vezys, A. L. Marzo, and L. Lefrancois. 2001. Preferential localization of effector memory cells in nonlymphoid tissue. *Science* 291:2413-2417.

94. Kaech, S. M. and R. Ahmed. 2001. Memory CD8+ T cell differentiation: initial antigen encounter triggers a developmental program in naive cells. *Nat.Immunol.* 2:415-422.

95. Kaech, S. M., E. J. Wherry, and R. Ahmed. 2002. Effector and memory T-cell differentiation: implications for vaccine development. *Nat.Rev.Immunol.* 2:251-262.

96. Bullock, T. N. J. and H. Yagita. 2005. Induction of CD70 on Dendritic Cells through CD40 or TLR Stimulation Contributes to the Development of CD8+ T Cell Responses in the Absence of CD4+ T Cells. *J Immunol* 174:710-717.

97. Bennett, S. R., F. R. Carbone, F. Karamalis, R. A. Flavell, Miller, JF, and W. R. Heath. 1998. Help for cytotoxic-T-cell responses is mediated by CD40 signalling [see comments]. *Nature* 393:478-480.

98. Shedlock, D. J. and H. Shen. 2003. Requirement for CD4 T cell help in generating functional CD8 T cell memory. *Science* 300:337-339.

99. Sun, J. C. and M. J. Bevan. 2003. Defective CD8 T cell memory following acute infection without CD4 T cell help. *Science* 300:339-342.

100. Williams, M. A., A. J. Tyznik, and M. J. Bevan. 2006. Interleukin-2 signals during priming are required for secondary expansion of CD8(+) memory T cells. *Nature* 441:890-893.

101. Wilson, E. B. and A. M. Livingstone. 2008. Cutting edge: CD4+ T cell-derived IL-2 is essential for help-dependent primary CD8+ T cell responses. *J.Immunol.* 181:7445-7448.

102. Oh, S., L. P. Perera, M. Terabe, L. Ni, T. A. Waldmann, and J. A. Berzofsky. 2008. IL-15 as a mediator of CD4(+) help for CD8(+) T cell longevity and avoidance of TRAIL-mediated apoptosis. *Proceedings of the National Academy of Sciences of the United States of America* 105:5201-5206.

103. Sun, J. C., M. A. Williams, and M. J. Bevan. 2004. CD4(+) T cells are required for the maintenance, not programming, of memory CD8(+) T cells after acute infection. *Nature Immunology* 5:927-933.

104. Schluns, K. S., W. C. Kieper, S. C. Jameson, and L. Lefrancois. 2000. Interleukin-7 mediates the homeostasis of naive and memory CD8 T cells in vivo. *Nat.Immunol.* 1:426-432.

105. Wallace, M. E., R. Keating, W. R. Heath, and F. R. Carbone. 1999. The cytotoxic T-cell response to herpes simplex virus type 1 infection of C57BL/6 mice is almost entirely directed against a single immunodominant determinant. *J.Virol.* 73:7619-7626.

106. Khanna, K. M., R. H. Bonneau, P. R. Kinchington, and R. L. Hendricks. 2003. Herpes simplex virus-specific memory CD8+ T cells are selectively activated and retained in latently infected sensory ganglia. *Immunity* 18:593-603.

107. Suvas, S., A. K. Azkur, and B. T. Rouse. 2006. Qa-1b and CD94-NKG2a interaction regulate cytolytic activity of herpes simplex virus-specific memory CD8+ T cells in the latently infected trigeminal ganglia. *J.Immunol.* 176:1703-1711.

108. Shimeld, C., J. L. Whiteland, S. M. Nicholls, E. Grinfeld, D. L. Easty, H. Gao, and T. J. Hill. 1995. Immune cell infiltration and persistence in the mouse trigeminal ganglion after infection of the cornea with herpes simplex virus type 1. *J.Neuroimmunol.* 61:7-16.

109. Halford, W. P., B. M. Gebhardt, and D. J. Carr. 1996. Persistent cytokine expression in trigeminal ganglion latently infected with herpes simplex virus type 1. *J.Immunol.* 157:3542-3549.

110. Cantin, E. M., D. R. Hinton, J. Chen, and H. Openshaw. 1995. Gamma interferon expression during acute and latent nervous system infection by herpes simplex virus type 1. *J.Virol.* 69:4898-4905.

111. Liu, T., K. M. Khanna, X. Chen, D. J. Fink, and R. L. Hendricks. 2000. CD8(+) T cells can block herpes simplex virus type 1 (HSV-1) reactivation from latency in sensory neurons. *J.Exp.Med.* 191:1459-1466.

112. Liu, T., K. M. Khanna, B. N. Carriere, and R. L. Hendricks. 2001. Gamma interferon can prevent herpes simplex virus type 1 reactivation from latency in sensory neurons. *J.Virol.* 75:11178-11184.

113. Decman, V., P. R. Kinchington, S. A. Harvey, and R. L. Hendricks. 2005. Gamma interferon can block herpes simplex virus type 1 reactivation from latency, even in the presence of late gene expression. *J.Virol.* 79:10339-10347.

114. Knickelbein, J. E., K. M. Khanna, M. B. Yee, C. J. Baty, P. R. Kinchington, and R. L. Hendricks. 2008. Noncytotoxic lytic granule-mediated CD8(+) T cell inhibition of HSV-1 reactivation from neuronal latency. *Science* 322:268-271.

115. Barber, D. L., E. J. Wherry, D. Masopust, B. Zhu, J. P. Allison, A. H. Sharpe, G. J. Freeman, and R. Ahmed. 2006. Restoring function in exhausted CD8 T cells during chronic viral infection. *Nature* 439:682-687.

116. Urbani, S., B. Amadei, D. Tola, M. Massari, S. Schivazappa, G. Missale, and C. Ferrari. 2006. PD-1 expression in acute hepatitis C virus (HCV) infection is associated with HCV-specific CD8 exhaustion. *J.Virol.* 80:11398-11403.

117. Velu, V., S. Kannanganat, C. Ibegbu, L. Chennareddi, F. Villinger, G. J. Freeman, R. Ahmed, and R. R. Amara. 2007. Elevated expression levels of inhibitory receptor programmed death 1 on simian immunodeficiency virus-specific CD8 T cells during chronic infection but not after vaccination. *J.Virol.* 81:5819-5828.

118. Wherry, E. J., S. J. Ha, S. M. Kaech, W. N. Haining, S. Sarkar, V. Kalia, S. Subramaniam, J. N. Blattman, D. L. Barber, and R. Ahmed. 2007. Molecular signature of CD8+ T cell exhaustion during chronic viral infection. *Immunity.* 27:670-684.

119. Ejrnaes, M., C. M. Filippi, M. M. Martinic, E. M. Ling, L. M. Togher, S. Crotty, and M. G. von Herrath. 2006. Resolution of a chronic viral infection after interleukin-10 receptor blockade. *J.Exp.Med.* 203:2461-2472.

120. Blackburn, S. D., H. Shin, W. N. Haining, T. Zou, C. J. Workman, A. Polley, M. R. Betts, G. J. Freeman, D. A. Vignali, and E. J. Wherry. 2009. Coregulation of CD8+ T cell exhaustion by multiple inhibitory receptors during chronic viral infection. *Nat.Immunol.* 10:29-37.

121. Greenwald, R. J., G. J. Freeman, and A. H. Sharpe. 2005. The B7 family revisited. *Annu.Rev.Immunol* 23:515-548.

122. Okazaki, T. and T. Honjo. 2006. The PD-1-PD-L pathway in immunological tolerance. *Trends Immunol.* 27:195-201.

123. Chen, L. 2004. Co-inhibitory molecules of the B7-CD28 family in the control of T-cell immunity. *Nat.Rev.Immunol.* 4:336-347.

124. Latchman, Y., C. R. Wood, T. Chernova, D. Chaudhary, M. Borde, I. Chernova, Y. Iwai, A. J. Long, J. A. Brown, R. Nunes, E. A. Greenfield, K. Bourque, V. A. Boussiotis, L. L. Carter, B. M. Carreno, N. Malenkovich, H. Nishimura, T. Okazaki, T. Honjo, A. H. Sharpe, and G. J. Freeman. 2001. PD-L2 is a second ligand for PD-I and inhibits T cell activation. *Nat.Immunol.* 2:261-268.

125. Augello, A., R. Tasso, S. M. Negrini, A. Amateis, F. Indiveri, R. Cancedda, and G. Pennesi. 2005. Bone marrow mesenchymal progenitor cells inhibit lymphocyte proliferation by activation of the programmed death 1 pathway. *Eur.J.Immunol.* 35:1482-1490.

126. Eppihimer, M. J., J. Gunn, G. J. Freeman, E. A. Greenfield, T. Chernova, J. Erickson, and J. P. Leonard. 2002. Expression and regulation of the PD-L1 immunoinhibitory molecule on microvascular endothelial cells. *Microcirculation.* 9:133-145.

127. Schreiner, B., M. Mitsdoerffer, B. C. Kieseier, L. Chen, H. P. Hartung, M. Weller, and H. Wiendl. 2004. Interferon-beta enhances monocyte and dendritic cell expression of B7-H1 (PD-L1), a strong inhibitor of autologous T-cell activation: relevance for the immune modulatory effect in multiple sclerosis. *J.Neuroimmunol.* 155:172-182.

128. Zajac, A. J., J. N. Blattman, K. Murali-Krishna, D. J. Sourdive, M. Suresh, J. D. Altman, and R. Ahmed. 1998. Viral immune evasion due to persistence of activated T cells without effector function [see comments]. *J.Exp.Med.* 188:2205-2213.

129. Matloubian, M., R. J. Concepcion, and R. Ahmed. 1994. CD4+ T cells are required to sustain CD8+ cytotoxic T-cell responses during chronic viral infection. *J.Virol.* 68:8056-8063.

130. Sheridan, B. S., K. M. Khanna, G. M. Frank, and R. L. Hendricks. 2006. Latent virus influences the generation and maintenance of CD8+ T cell memory. *J.Immunol.* 177:8356-8364.

131. Cardin, R. D., J. W. Brooks, S. R. Sarawar, and P. C. Doherty. 1996. Progressive loss of CD8+ T cell-mediated control of a gamma-herpesvirus in the absence of CD4+ T cells. *J.Exp.Med.* 184:863-871.

132. Dias, P., A. L. Shea, C. Inglis, F. Giannoni, L. N. Lee, and S. R. Sarawar. 2008. Primary clearance of murine gammaherpesvirus 68 by PKCtheta-/- CD8 T cells is compromised in the absence of help from CD4 T cells. *J.Virol.* 82:11970-11975.

133. Miller, J. K., K. A. Laycock, M. M. Nash, and J. S. Pepose. 1993. Corneal Langerhans cell dynamics after herpes simplex virus reactivation. *Invest Ophthalmol.Vis.Sci.* 34:2282-2290.

134. Keadle, T. L., J. L. Morris, J. S. Pepose, and P. M. Stuart. 2002. CD4(+) and CD8(+) cells are key participants in the development of recurrent herpetic stromal keratitis in mice. *Microb.Pathog.* 32:255-262.

135. Tang, Q. and R. L. Hendricks. 1996. Interferon gamma regulates platelet endothelial cell adhesion molecule 1 expression and neutrophil infiltration into herpes simplex virus-infected mouse corneas. *J.Exp.Med.* 184:1435-1447.

136. Lee, S., M. Zheng, B. Kim, and B. T. Rouse. 2002. Role of matrix metalloproteinase-9 in angiogenesis caused by ocular infection with herpes simplex virus. *J.Clin.Invest* 110:1105-1111.

137. Metcalf, J. F., D. S. Hamilton, and R. W. Reichert. 1979. Herpetic keratitis in athymic (nude) mice. *Infect.Immun.* 26:1164-1171.

138. Russell, R. G., M. P. Nasisse, H. S. Larsen, and B. T. Rouse. 1984. Role of T-lymphocytes in the pathogenesis of herpetic stromal keratitis. *Invest.Ophthalmol.Vis.Sci.* 25:938-944.

139. Newell, C. K., S. Martin, D. Sendele, C. M. Mercadal, and B. T. Rouse. 1989. Herpes simplex virus-induced stromal keratitis: role of T-lymphocyte subsets in immunopathology. *J.Virol.* 63:769-775.

140. Hendricks, R. L. and T. M. Tumpey. 1990. Contribution of virus and immune factors to herpes simplex virus type 1 induced corneal pathology. *Invest.Ophthalmol.Vis.Sci.* 31:1929-1939.

141. Mercadal, C. M., D. M. Bousley, D. Destephano, and B. Rouse. 1993. Herpetic stromal keratitis in the reconstituted SCID mouse model. *J.Virol.* 67:3404-3408.

142. Tang, Q., W. Chen, and R. L. Hendricks. 1997. Proinflammatory functions of IL-2 in herpes simplex virus corneal infection. *J.Immunol.* 158:1275-1283.

143. Tang, Q. and R. L. Hendricks. 1996. IFN-gamma regulates PECAM-1 expression and neutrophil infiltration into herpes simplex virus-infected mouse corneas. *J.Exp.Med.* 184:1435-1447.

144. Avery, A. C., Z.-S. Zhao, A. Rodriguez, E. K. Bikoff, M. Soheilian, C. S. Foster, and H. Cantor. 1995. Resistance to herpes stromal keratitis conferred by an IgG2a-derived peptide. *Nature* 376:431-433.

145. Huster, K. M., V. Panoutsakopoulou, K. Prince, M. E. Sanchirico, and H. Cantor. 2002. T cell-dependent and -independent pathways to tissue destruction following herpes simplex virus-1 infection. *Eur.J.Immunol.* 32:1414-1419.

146. Panoutsakopoulou, V., M. E. Sanchirico, K. M. Huster, M. Jansson, F. Granucci, D. J. Shim, K. W. Wucherpfennig, and H. Cantor. 2001. Analysis of the Relationship between Viral Infection and Autoimmune Disease. *Immunity.* 15:137-147.

147. Zhao, Z.-S., F. Granucci, L. Yeh, P. A. Schaffer, and H. Cantor. 1998. Molecular mimicry by herpes simplex virus-type 1: Autoimmune disease after viral infection. *Science* 279:1344-1347.

148. Deshpande, S. P., S. Lee, M. Zheng, B. Song, D. Knipe, J. A. Kapp, and B. T. Rouse. 2001. Herpes simplex virus-induced keratitis: evaluation of the role of molecular mimicry in lesion pathogenesis. *J.Virol.* 75:3077-3088.

149. Verjans, G. M., L. Remeijer, C. M. Mooy, and A. D. Osterhaus. 2000. Herpes simplex virus-specific T cells infiltrate the cornea of patients with herpetic stromal keratitis: no evidence for autoreactive T cells. *Invest Ophthalmol.Vis.Sci.* 41:2607-2612.

150. Gangappa, S., J. S. Babu, J. Thomas, M. Daheshia, and B. T. Rouse. 1998. Virus-induced immunoinflammatory lesions in the absence of viral antigen recognition. *J.Immunol.* 161:4289-4300.

151. Deshpande, S., M. Zheng, S. Lee, K. Banerjee, S. Gangappa, U. Kumaraguru, and B. T. Rouse. 2001. Bystander activation involving T lymphocytes in herpetic stromal keratitis. *J Immunol.* 167:2902-2910.

152. Whittum, J. A., J. Y. Niederkorn, J. P. McCulley, and J. W. Streilein. 1983. Intracameral inoculation of herpes simplex virus type I induces anterior chamber associated immune deviation. *Curr.Eye Res.* 2:691-697.

153. Streilein, J. W. 1987. Immune regulation and the eye: a dangerous compromise. *FASEB J.* 1:199-208.

154. Ksander, B. R. and R. L. Hendricks. 1987. Cell-mediated immune tolerance to HSV-1 antigens associated with reduced susceptibility to HSV-1 corneal lesions. *Invest Ophthalmol.Vis.Sci.* 28:1986-1993.

155. Verjans, G. M., L. Remeijer, R. S. van Binnendijk, J. G. Cornelissen, H. J. Volker-Dieben, S. G. Baarsma, and A. D. Osterhaus. 1998. Identification and characterization of herpes simplex virus-specific CD4+ T cells in corneas of herpetic stromal keratitis patients. *J.Infect.Dis.* 177:484-488.

156. Jager, M. J. 1992. Corneal Langerhans cells and ocular immunology. *Regional Immunol.* 4:186-195.

157. Hendricks, R. L., M. Janowicz, and T. M. Tumpey. 1992. Critical role of corneal Langerhans cells in the CD4- but not CD8-mediated immunopathology in herpes simplex virus-1-infected mouse corneas. *J.Immunol.* 148:2522-2529.

158. Chen, H. and R. L. Hendricks. 1998. B7 costimulatory requirements of T cells at an inflammatory site. *J.Immunol.* 160:5045-5052.

159. Xu, M., A. J. Lepisto, and R. L. Hendricks. 2004. CD154 signaling regulates the Th1 response to herpes simplex virus-1 and inflammation in infected corneas. *J Immunol* 173:1232-1239.

160. Lepisto, A. J., M. Xu, H. Yagita, A. D. Weinberg, and R. L. Hendricks. 2007. Expression and function of the OX40/OX40L costimulatory pair during herpes stromal keratitis. *J Leukoc.Biol.* 81:766-774.

161. Wolf, S. F., P. A. Temple, M. Kobayashi, D. Young, M. Dicig, L. Lowe, R. Dzialo, L. Fitz, C. Ferenz, R. M. Hewick, and . 1991. Cloning of cDNA for natural killer cell

stimulatory factor, a heterodimeric cytokine with multiple biologic effects on T and natural killer cells. *J.Immunol.* 146:3074-3081.

162. Heinzel, F. P., R. M. Rerko, F. Ahmed, and E. Pearlman. 1995. Endogenous IL-12 is required for control of Th2 cytokine responses capable of exacerbating leishmaniasis in normally resistant mice. *J.Immunol.* 155:730-739.

163. Oppmann, B., R. Lesley, B. Blom, J. C. Timans, Y. Xu, B. Hunte, F. Vega, N. Yu, J. Wang, K. Singh, F. Zonin, E. Vaisberg, T. Churakova, M. Liu, D. Gorman, J. Wagner, S. Zurawski, Y. Liu, J. S. Abrams, K. W. Moore, D. Rennick, R. Waal-Malefyt, C. Hannum, J. F. Bazan, and R. A. Kastelein. 2000. Novel p19 protein engages IL-12p40 to form a cytokine, IL-23, with biological activities similar as well as distinct from IL-12 [In Process Citation]. *Immunity.* 13:715-725.

164. Aggarwal, S., N. Ghilardi, M. H. Xie, F. J. de Sauvage, and A. L. Gurney. 2003. Interleukin-23 promotes a distinct CD4 T cell activation state characterized by the production of interleukin-17. *J.Biol.Chem.* 278:1910-1914.

165. Ling, P., M. K. Gately, U. Gubler, A. S. Stern, P. Lin, K. Hollfelder, C. Su, Y. C. E. Pan, and J. Hakimi. 1995. Human Il-12 P40 Homodimer Binds to the Il-12 Receptor But Does Not Mediate Biologic Activity. *J.Immunol.* 154:116-127.

166. Piccotti, J. R., S. Y. Chan, K. W. Li, E. J. Eichwald, and D. K. Bishop. 1997. Differential effects of IL-12 receptor blockade with IL-12 p40 homodimer on the induction of CD4(+) and CD8(+) IFN-gamma-producing cells. *J.Immunol.* 158:643-648.

167. Khader, S. A., S. Partida-Sanchez, G. Bell, D. M. Jelley-Gibbs, S. SWAIN, J. E. Pearl, N. Ghilardi, F. J. deSauvage, F. E. Lund, and A. M. Cooper. 2006. Interleukin 12p40 is required for dendritic cell migration and T cell priming after Mycobacterium tuberculosis infection. *J.Exp.Med.* 203:1805-1815.

168. Russell, T. D., Q. Yan, G. Fan, A. P. Khalifah, D. K. Bishop, S. L. Brody, and M. J. Walter. 2003. IL-12 p40 homodimer-dependent macrophage chemotaxis and respiratory viral inflammation are mediated through IL-12 receptor beta 1. *J Immunol* 171:6866-6874.

169. Nieuwenhuis, E. E., M. F. Neurath, N. Corazza, H. Iijima, J. Trgovcich, S. Wirtz, J. Glickman, D. Bailey, M. Yoshida, P. R. Galle, M. Kronenberg, M. Birkenbach, and R. S. Blumberg. 2002. Disruption of T helper 2-immune responses in Epstein-Barr virus-induced gene 3-deficient mice. *Proc.Natl.Acad.Sci.U.S.A* 99:16951-16956.

170. Collison, L. W., C. J. Workman, T. T. Kuo, K. Boyd, Y. Wang, K. M. Vignali, R. Cross, D. Sehy, R. S. Blumberg, and D. A. Vignali. 2007. The inhibitory cytokine IL-35 contributes to regulatory T-cell function. *Nature* 450:566-569.

171. Pflanz, S., J. C. Timans, J. Cheung, R. Rosales, H. Kanzler, J. Gilbert, L. Hibbert, T. Churakova, M. Travis, E. Vaisberg, W. M. Blumenschein, J. D. Mattson, J. L. Wagner, W. To, S. Zurawski, T. K. McClanahan, D. M. Gorman, J. F. Bazan, M. R. de Waal, D.

Rennick, and R. A. Kastelein. 2002. IL-27, a heterodimeric cytokine composed of EBI3 and p28 protein, induces proliferation of naive CD4(+) T cells. *Immunity.* 16:779-790.

172. Kanangat, S., J. Thomas, S. Gangappa, J. S. Babu, and B. T. Rouse. 1996. Herpes simplex virus type 1-mediated up-regulation of IL-12 (p40) mRNA expression. Implications in immunopathogenesis and protection. *J.Immunol.* 156:1110-1116.

173. Kumaraguru, U. and B. T. Rouse. 2002. The IL-12 response to herpes simplex virus is mainly a paracrine response of reactive inflammatory cells. *J.Leukoc.Biol.* 72:564-570.

174. Al khatib, K., I. L. Campbell, and D. J. Carr. 2002. Resistance to ocular herpes simplex virus type 1 infection in IL-12 transgenic mice. *J.Neuroimmunol.* 132:41-48.

175. Osorio, Y., S. L. Wechsler, A. B. Nesburn, and H. Ghiasi. 2002. Reduced severity of HSV-1-induced corneal scarring in IL-12-deficient mice. *Virus Res.* 90:317-326.

176. Kim, B., P. P. Sarangi, A. K. Azkur, S. D. Kaistha, and B. T. Rouse. 2008. Enhanced viral immunoinflammatory lesions in mice lacking IL-23 responses. *Microbes.Infect.* 10:302-312.

177. Wolint, P., M. R. Betts, R. A. Koup, and A. Oxenius. 2004. Immediate cytotoxicity but not degranulation distinguishes effector and memory subsets of CD8+ T cells. *J.Exp.Med.* 199:925-936.

178. Betts, M. R., D. A. Price, J. M. Brenchley, K. Lore, F. J. Guenaga, A. Smed-Sorensen, D. R. Ambrozak, S. A. Migueles, M. Connors, M. Roederer, D. C. Douek, and R. A. Koup. 2004. The functional profile of primary human antiviral CD8+ T cell effector activity is dictated by cognate peptide concentration. *J.Immunol.* 172:6407-6417.

179. La Gruta, N. L., P. C. Doherty, and S. J. Turner. 2006. A correlation between function and selected measures of T cell avidity in influenza virus-specific CD8+ T cell responses. *Eur.J.Immunol.* 36:2951-2959.

180. Cherpes, T. L., J. L. Busch, B. S. Sheridan, S. A. Harvey, and R. L. Hendricks. 2008. Medroxyprogesterone acetate inhibits CD8+ T cell viral-specific effector function and induces herpes simplex virus type 1 reactivation. *J.Immunol.* 181:969-975.

181. al Ramadi, B. K., M. T. Jelonek, L. F. Boyd, D. H. Margulies, and A. L. Bothwell. 1995. Lack of strict correlation of functional sensitization with the apparent affinity of MHC/peptide complexes for the TCR. *J.Immunol.* 155:662-673.

182. Slifka, M. K. and J. L. Whitton. 2001. Functional avidity maturation of CD8(+) T cells without selection of higher affinity TCR. *Nat.Immunol.* 2:711-717.

183. Sawtell, N. M. and R. L. Thompson. 2004. Comparison of herpes simplex virus reactivation in ganglia in vivo and in explants demonstrates quantitative and qualitative differences. *J.Virol.* 78:7784-7794.

184. Rajasagi, N. K., S. H. Kassim, C. M. Kollias, X. Zhao, R. Chervenak, and S. R. Jennings. 2009. CD4+ T cells are required for the priming of CD8+ T cells following infection with herpes simplex virus type 1. *J.Virol.* 83:5256-5268.

185. Wakim, L. M., J. Waithman, N. van Rooijen, W. R. Heath, and F. R. Carbone. 2008. Dendritic cell-induced memory T cell activation in nonlymphoid tissues. *Science* 319:198-202.

186. Freeman, G. J., E. J. Wherry, R. Ahmed, and A. H. Sharpe. 2006. Reinvigorating exhausted HIV-specific T cells via PD-1-PD-1 ligand blockade. *J.Exp.Med.* 203:2223-2227.

187. Blackburn, S. D., H. Shin, G. J. Freeman, and E. J. Wherry. 2008. Selective expansion of a subset of exhausted CD8 T cells by alphaPD-L1 blockade. *Proc.Natl.Acad.Sci.U.S.A* 105:15016-15021.

188. Bennett, F., D. Luxenberg, V. Ling, I. M. Wang, K. Marquette, D. Lowe, N. Khan, G. Veldman, K. A. Jacobs, V. E. Valge-Archer, M. Collins, and B. M. Carreno. 2003. Program death-1 engagement upon TCR activation has distinct effects on costimulation and cytokine-driven proliferation: Attenuation of ICOS, IL-4, and IL-21, but not CD28, IL-7, and IL-15 responses. *J.Immunol.* 170:711-718.

189. Maertzdorf, J., G. M. Verjans, L. Remeijer, K. A. van der, and A. D. Osterhaus. 2003. Restricted T cell receptor beta-chain variable region protein use by cornea-derived CD4+ and CD8+ herpes simplex virus-specific T cells in patients with herpetic stromal keratitis. *J.Infect.Dis.* 187:550-558.

190. Furuzawa-Carballeda, J., M. I. Vargas-Rojas, and A. R. Cabral. 2007. Autoimmune inflammation from the Th17 perspective. *Autoimmun.Rev.* 6:169-175.

191. Kolls, J. K. and A. Linden. 2004. Interleukin-17 family members and inflammation. *Immunity* 21:467-476.

192. Duan, R., L. Remeijer, J. M. van Dun, A. D. Osterhaus, and G. M. Verjans. 2007. Granulocyte macrophage colony-stimulating factor expression in human herpetic stromal keratitis: implications for the role of neutrophils in HSK. *Invest Ophthalmol.Vis.Sci.* 48:277-284.

193. Lepisto, A. J., G. M. Frank, M. Xu, P. M. Stuart, and R. L. Hendricks. 2006. CD8 T cells mediate transient herpes stromal keratitis in CD4-deficient mice. *Invest Ophthalmol.Vis.Sci.* 47:3400-3409.

194. Onami, T. M., L. E. Harrington, M. A. Williams, M. Galvan, C. P. Larsen, T. C. Pearson, N. Manjunath, L. G. Baum, B. D. Pearce, and R. Ahmed. 2002. Dynamic regulation of T cell immunity by CD43. *J.Immunol.* 168:6022-6031.

195. Whitcup, S. M., L. R. DeBarge, R. R. Caspi, R. Harning, R. B. Nussenblatt, and C.-C. Chan. 1993. Monoclonal antibodies against ICAM-1 (CD54) and LFA-1 (CD11a/CD18) inhibit experimental autoimmune uveitis. *Clin.Immunol.Immunopathol.* 67:143-150.

196. Vennegoor, C. J. G. M., E. Van de Wiel-van Kemenade, R. J. F. Huijbens, F. Sanchez-Madrid, C. J. M. Melief, and C. G. Figdor. 1992. Role of LFA-1 and VLA-4 in the adhesion of cloned normal and LFA- 1 (CD11/CD18)-deficient T cells to cultured endothelial cells: Indication for a new adhesion pathway. *J.Immunol.* 148:1093-1101.

197. Baron, J. L., J. A. Madri, N. H. Ruddle, G. Hashim, and C. A. Janeway, Jr. 1993. Surface expression of α4 integrin by CD4 T cells is required for their entry into brain parenchyma. *J.Exp.Med.* 177:57-68.

198. Maertzdorf, J., G. M. Verjans, L. Remeijer, K. A. van der, and A. D. Osterhaus. 2003. Restricted T cell receptor beta-chain variable region protein use by cornea-derived CD4+ and CD8+ herpes simplex virus-specific T cells in patients with herpetic stromal keratitis. *J.Infect.Dis.* 187:550-558.

199. Johnson, R. M., D. W. Lancki, F. W. Fitch, and P. G. Spear. 1990. Herpes simplex virus glycoprotein D is recognized as antigen by CD4+ and CD8+ T lymphocytes from infected mice. Characterization of T cell clones. *J.Immunol.* 145:702-710.

200. Heiligenhaus, A., S. Jayaraman, S. Soukiasian, M. Dorf, and C. S. Foster. 1995. [Glycoprotein D (5-23) specific Th2-T-cell line induces HSV-1 keratitis]. *Ophthalmologe* 92:484-491.

201. Zhou, X., S. L. Bailey-Bucktrout, L. T. Jeker, C. Penaranda, M. Martinez-Llordella, M. Ashby, M. Nakayama, W. Rosenthal, and J. A. Bluestone. 2009. Instability of the transcription factor Foxp3 leads to the generation of pathogenic memory T cells in vivo. *Nat.Immunol.* 10:1000-1007.

202. Zhou, X., S. Bailey-Bucktrout, L. T. Jeker, and J. A. Bluestone. 2009. Plasticity of CD4(+) FoxP3(+) T cells. *Curr.Opin.Immunol.* 21:281-285.

203. Komatsu, N., M. E. Mariotti-Ferrandiz, Y. Wang, B. Malissen, H. Waldmann, and S. Hori. 2009. Heterogeneity of natural Foxp3+ T cells: a committed regulatory T-cell lineage and an uncommitted minor population retaining plasticity. *Proc.Natl.Acad.Sci.U.S.A* 106:1903-1908.

204. Miyara, M., Y. Yoshioka, A. Kitoh, T. Shima, K. Wing, A. Niwa, C. Parizot, C. Taflin, T. Heike, D. Valeyre, A. Mathian, T. Nakahata, T. Yamaguchi, T. Nomura, M. Ono, Z. Amoura, G. Gorochov, and S. Sakaguchi. 2009. Functional delineation and differentiation dynamics of human CD4+ T cells expressing the FoxP3 transcription factor. *Immunity.* 30:899-911.

205. Belperio, J. A., M. P. Keane, M. D. Burdick, J. P. Lynch, Y. Y. Xue, K. W. Li, D. J. Ross, and R. M. Strieter. 2002. Critical role for CXCR3 chemokine biology in the pathogenesis of bronchiolitis obliterans syndrome. *J.Immunol.* 169:1037-1049.

206. Biswas, P. S., K. Banerjee, P. R. Kinchington, and B. T. Rouse. 2006. Involvement of IL-6 in the paracrine production of VEGF in ocular HSV-1 infection. *Exp.Eye Res.* 82:46-54.

207. Banerjee, K., P. S. Biswas, B. Kim, S. Lee, and B. T. Rouse. 2004. CXCR2-/- mice show enhanced susceptibility to herpetic stromal keratitis: a role for IL-6-induced neovascularization. *J Immunol* 172:1237-1245.

208. He, J. and L. G. Baum. 2006. Endothelial cell expression of galectin-1 induced by prostate cancer cells inhibits T-cell transendothelial migration. *Lab Invest* 86:578-590.

209. Hernandez, J. D., J. T. Nguyen, J. He, W. Wang, B. Ardman, J. M. Green, M. Fukuda, and L. G. Baum. 2006. Galectin-1 binds different CD43 glycoforms to cluster CD43 and regulate T cell death. *J.Immunol.* 177:5328-5336.

210. Ishida, K., N. Panjwani, Z. Cao, and J. W. Streilein. 2003. Participation of pigment epithelium in ocular immune privilege. 3. Epithelia cultured from iris, ciliary body, and retina suppress T-cell activation by partially non-overlapping mechanisms. *Ocul.Immunol Inflamm.* 11:91-105.

211. Suvas, S., B. Kim, and B. T. Rouse. 2008. Homeostatic expansion of CD4(+) T cells upregulates VLA-4 and exacerbates HSV-induced corneal immunopathology. *Microbes.Infect.* 10:1192-1200.

212. Suvas, S., A. K. Azkur, B. S. Kim, U. Kumaraguru, and B. T. Rouse. 2004. CD4+CD25+ regulatory T cells control the severity of viral immunoinflammatory lesions. *J.Immunol.* 172:4123-4132.

213. Divito, S. J. and R. L. Hendricks. 2008. Activated inflammatory infiltrate in HSV-1-infected corneas without herpes stromal keratitis. *Invest Ophthalmol.Vis.Sci.* 49:1488-1495.

214. Lee, S. K., B. K. Choi, W. J. Kang, Y. H. Kim, H. Y. Park, K. H. Kim, and B. S. Kwon. 2008. MCP-1 derived from stromal keratocyte induces corneal infiltration of CD4+ T cells in herpetic stromal keratitis. *Mol.Cells* 26:67-73.

215. Bettelli, E., Y. Carrier, W. Gao, T. Korn, T. B. Strom, M. Oukka, H. L. Weiner, and V. K. Kuchroo. 2006. Reciprocal developmental pathways for the generation of pathogenic effector TH17 and regulatory T cells. *Nature* 441:235-238.

216. Veldhoen, M., R. J. Hocking, C. J. Atkins, R. M. Locksley, and B. Stockinger. 2006. TGFbeta in the context of an inflammatory cytokine milieu supports de novo differentiation of IL-17-producing T cells. *Immunity.* 24:179-189.

217. Wilson, S. E., G. S. Schultz, N. Chegini, J. Weng, and Y. G. He. 1994. Epidermal growth factor, transforming growth factor alpha, transforming growth factor beta, acidic fibroblast growth factor, basic fibroblast growth factor, and interleukin-1 proteins in the cornea. *Exp.Eye Res.* 59:63-71.

218. Thomas, J., S. Kanangat, and B. T. Rouse. 1998. Herpes simplex virus replication-induced expression of chemokines and proinflammatory cytokines in the eye: implications in herpetic stromal keratitis. *J.Interferon Cytokine Res.* 18:681-690.

219. Kim, B., P. P. Sarangi, Y. Lee, K. S. Deshpande, S. Lee, and B. T. Rouse. 2006. Depletion of MCP-1 increases development of herpetic stromal keratitis by innate immune modulation. *J.Leukoc.Biol.* 80:1405-1415.

220. Tumpey, T. M., H. Cheng, D. N. Cook, O. Smithies, J. E. Oakes, and R. N. Lausch. 1998. Absence of macrophage inflammatory protein-1alpha prevents the development of blinding herpes stromal keratitis. *J.Virol.* 72:3705-3710.

221. Tumpey, T. M., H. Cheng, X. T. Yan, J. E. Oakes, and R. N. Lausch. 1998. Chemokine synthesis in the HSV-1-infected cornea and its suppression by interleukin-10. *J Leukoc.Biol.* 63:486-492.

222. Yan, X.-T., T. M. Tumpey, S. L. Kunkel, J. E. Oakes, and R. N. Lausch. 1998. Role of MIP-2 in neutrophil migration and tissue injury in the herpes simplex virus-1-infected cornea. *Investigative Ophthalmology & Visual Science* 39:1854-1862.

223. Zheng, M., S. Deshpande, S. Lee, N. Ferrara, and B. T. Rouse. 2001. Contribution of vascular endothelial growth factor in the neovascularization process during the pathogenesis of herpetic stromal keratitis. *J Virol* 75:9828-9835.

224. Cohen, T., D. Nahari, L. W. Cerem, G. Neufeld, and B. Z. Levi. 1996. Interleukin 6 induces the expression of vascular endothelial growth factor. *J.Biol.Chem.* 271:736-741.

225. Fenton, R. R., S. Molesworth-Kenyon, J. E. Oakes, and R. N. Lausch. 2002. Linkage of IL-6 with neutrophil chemoattractant expression in virus-induced ocular inflammation. *Invest Ophthalmol.Vis.Sci.* 43:737-743.

226. Gubler, U., A. O. Chua, D. S. Schoenhaut, C. M. Dwyer, W. McComas, R. Motyka, N. Nabavi, A. G. Wolitzky, P. M. Quinn, P. C. Familletti, and . 1991. Coexpression of two distinct genes is required to generate secreted bioactive cytotoxic lymphocyte maturation factor. *Proc.Natl.Acad.Sci.U.S.A* 88:4143-4147.

227. Bennett, C. L. and B. E. Clausen. 2007. DC ablation in mice: promises, pitfalls, and challenges. *Trends Immunol.* 28:525-531.

228. Chinnery, H. R., T. Humphries, A. Clare, A. E. Dixon, K. Howes, C. B. Moran, D. Scott, M. Zakrzewski, E. Pearlman, and P. G. McMenamin. 2008. Turnover of bone marrow-derived cells in the irradiated mouse cornea. *Immunol.* 125:541-548.

229. Probst, H. C., K. Tschannen, B. Odermatt, R. Schwendener, R. M. Zinkernagel, and B. M. Van Den. 2005. Histological analysis of CD11c-DTR/GFP mice after in vivo depletion of dendritic cells. *Clin.Exp.Immunol* 141:398-404.

230. Hochweller, K., J. Striegler, G. J. Hammerling, and N. Garbi. 2008. A novel CD11c.DTR transgenic mouse for depletion of dendritic cells reveals their requirement for homeostatic proliferation of natural killer cells. *Eur.J.Immunol.* 38:2776-2783.

231. Hochweller, K., J. Striegler, G. J. Hammerling, and N. Garbi. 2008. A novel CD11c.DTR transgenic mouse for depletion of dendritic cells reveals their requirement for homeostatic proliferation of natural killer cells. *Eur.J.Immunol.* 38:2776-2783.

232. Asbell, P. A. and T. Kamenar. 1987. The response of Langerhans cells in the cornea to herpetic keratitis. *Curr.Eye Res.* 6:179-182.

233. Kassim, S. H., N. K. Rajasagi, B. W. Ritz, S. B. Pruett, E. M. Gardner, R. Chervenak, and S. R. Jennings. 2009. Dendritic cells are required for optimal activation of natural killer functions following primary infection with herpes simplex virus type 1. *J.Virol.* 83:3175-3186.

234. Vollstedt, S., M. O'Keeffe, B. Ryf, B. Glanzmann, H. Hochrein, and M. Suter. 2006. The long-term but not the short-term antiviral effect of IFN-alpha depends on Flt3 ligand and pDC. *Eur.J Immunol* 36:1231-1240.

235. Colonna, M., G. Trinchieri, and Y. J. Liu. 2004. Plasmacytoid dendritic cells in immunity. *Nature Immunology* 5:1219-1226.

236. Lund, J. M., M. M. Linehan, N. Iijima, and A. Iwasaki. 2006. Cutting Edge: Plasmacytoid dendritic cells provide innate immune protection against mucosal viral infection in situ. *J Immunol* 177:7510-7514.

237. Dunn, P. L. and R. J. North. 1991. Early gamma interferon production by natural killer cells is important in defense against murine listeriosis. *Infect.Immun.* 59:2892-2900.

238. MacMicking, J., Q. W. Xie, and C. Nathan. 1997. Nitric oxide and macrophage function. *Annu.Rev.Immunol.* 15:323-350.

239. Hendricks, R. L., M. Janowicz, and T. M. Tumpey. 1992. Critical role of corneal Langerhans cells in the CD4- but not CD8-mediated immunopathology in herpes simplex virus-1-infected mouse corneas. *J Immunol* 148:2522-2529.

240. Lee, H. K., M. Zamora, M. M. Linehan, N. Iijima, D. Gonzalez, A. Haberman, and A. Iwasaki. 2009. Differential roles of migratory and resident DCs in T cell priming after mucosal or skin HSV-1 infection. *J.Exp.Med.* 206:359-370.

241. Zhao, X., E. Deak, K. Soderberg, M. Linehan, D. Spezzano, J. Zhu, D. M. Knipe, and A. Iwasaki. 2003. Vaginal submucosal dendritic cells, but not Langerhans cells, induce protective Th1 responses to herpes simplex virus-2. *J.Exp.Med.* 197:153-162.

242. Zitvogel, L. 2002. Dendritic and natural killer cells cooperate in the control/switch of innate immunity. *J.Exp.Med.* 195:F9-F14.

243. Candinas, D., S. Belliveau, N. Koyamada, T. Miyatake, P. Hechenleitner, W. Mark, F. H. Bach, and W. W. Hancock. 1996. T cell independence of macrophage and natural killer cell infiltration, cytokine production, and endothelial activation during delayed xenograft rejection. *Transplantation* 62:1920-1927.

244. Conlan, J. W. and R. J. North. 1994. Neutrophils are essential for early anti-listeria defense in the liver, but not in the spleen or peritoneal cavity, as revealed by a granulocyte-depleting monoclonal antibody. ***J.Exp.Med.*** 179:259-268.

245. Tang, Q., W. Chen, and R. L. Hendricks. 1997. Proinflammatory functions of IL-2 in herpes simplex virus corneal infection. *J Immunol* 158:1275-1283.

246. Carr, D. J., J. Ash, T. E. Lane, and W. A. Kuziel. 2006. Abnormal immune response of CCR5-deficient mice to ocular infection with herpes simplex virus type 1. ***J.Gen.Virol.*** 87:489-499.

247. Romagnani, P., L. Lasagni, F. Annunziato, M. Serio, and S. Romagnani. 2004. CXC chemokines: the regulatory link between inflammation and angiogenesis. *Trends Immunol* 25:201-209.

248. Luster, A. D. 2002. The role of chemokines in linking innate and adaptive immunity. ***Curr.Opin.Immunol.*** 14:129-135.

249. Pape, K. A., D. M. Catron, A. A. Itano, and M. K. Jenkins. 2007. The humoral immune response is initiated in lymph nodes by B cells that acquire soluble antigen directly in the follicles. ***Immunity.*** 26:491-502.

250. Lepisto, A. J., G. M. Frank, and R. L. Hendricks. 2007. How herpes simplex virus type 1 rescinds corneal privilege. ***Chem.Immunol Allergy*** 92:203-212.